FINAL REPORT

MARS LANDER/ROVER VEHICLE DEVELOPMENT

An Advanced Space Design Project

for

USRA and NASA/OAST

SPRING 1987

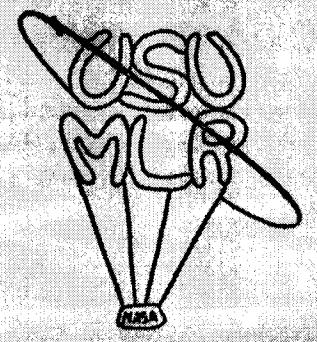

UTAH STATE UNIVERSITY

Logan, Utah

FOREWORD

This Final Report, along with its companion Interim Reports from Fall and Winter Quarters, present the results of the first year of research under the auspices of the Universities Space Research Association (USRA) Advanced Space Design Project at Utah State University (USU). However, innovative research efforts of this type have been conducted at USU for quite some time. The first Get Away Special payload to fly into space aboard the space shuttle was developed and built at USU, as were several subsequent payloads. This tradition of solid research and accomplishment has been continued in the work summarized in these documents.

The students involved varied from quarter to quarter as their schedules permitted (see listing at front of each report), although several participated throughout. Each quarter, however, the team was comprised of individuals from several disciplines, ranging from Mechanical Engineering to Biology, which undoubtedly strengthened the design process.

It deserves mention that this design course has resulted in the authoring and presentation of three papers at conferences: AIAA Region VI Student Conference (May 1987), The Case For Mars III Conference (July 1987), and the AIAA Lighter-Than-Air Conference (August 1987). Final design results were presented to the Utah Section of the AIAA, related articles appeared in three Utah newspapers, and a local radio station and the Salt Lake City CBS Television affiliate broadcasted stories on the course.

On behalf the design team members, I wish to express gratitude to USRA and NASA/OAST for funding, to Mr. Jim Burke of Jet Propulsion Laboratory for excellent and expeditious technical support, and to Dr. Frank J. Redd and Dr. L. Rex Megill for their excellent guidance throughout the year in this endeavor.

Raymond J. LeVesque, II
Graduate Teaching Assistant/Editor
USU/MLR Advanced Design Course

Spring 1987 Design Team

Environment

Jim Siplon

Landing Site Selection

Ted Holtz

Balloon System Development

Grant Williams

Balloon Deployment

Ground-based: Jim Cantrell
On-Descent: John Higham

Optics & Communications

Steven Brown

Payload Power Supply

Marie-Paule Cellier

Payload

Oscar Monje
Perry Voyer

Course Leader/Systems Engineer/Editor

Raymond J. LeVesque, II

Winter 1987 Design Team

Environment & Trajectory

Roger Hart
Ted Holtz
*Russ Laher
Jim Siplon

Payload Subsystem

John Atkinson
*Oscar Monje

Ground Systems

Steven Brown
*Jim Cantrell
Marie-Paule Cellier
Neal Oman

Balloon System

John Higham
S. Ali Siahpush
*Grant Williams

Course Leader/Systems Engineer/Editor

Raymond J. LeVesque, II

*Denotes Team Leader

Fall 1986 Design Team

Payload Sizing

*Lane Bostrom
Mark Hatfield
Brad Hunting
Arun Nanisetti
Larry Stocking
Perry Voyer

Soft Landing

John Atkinson
Layne Cook
John Higham
Mark Ketchum
John Maloney
S. Ali Siahpush
*Grant Williams

Trajectory & Environment

Marcha Fox
Roger Hart
*Russ Laher
Ian Monson
Jim Siplon

Rover

Steven Brown
Jim Cantrell
Marie-Paule Cellier
Neal Oman
Linda Palo
*Steve Wassom

Course Leader/Systems Engineer/Editor

Raymond J. LeVesque, II

* Denotes Team Leader

FINAL REPORT

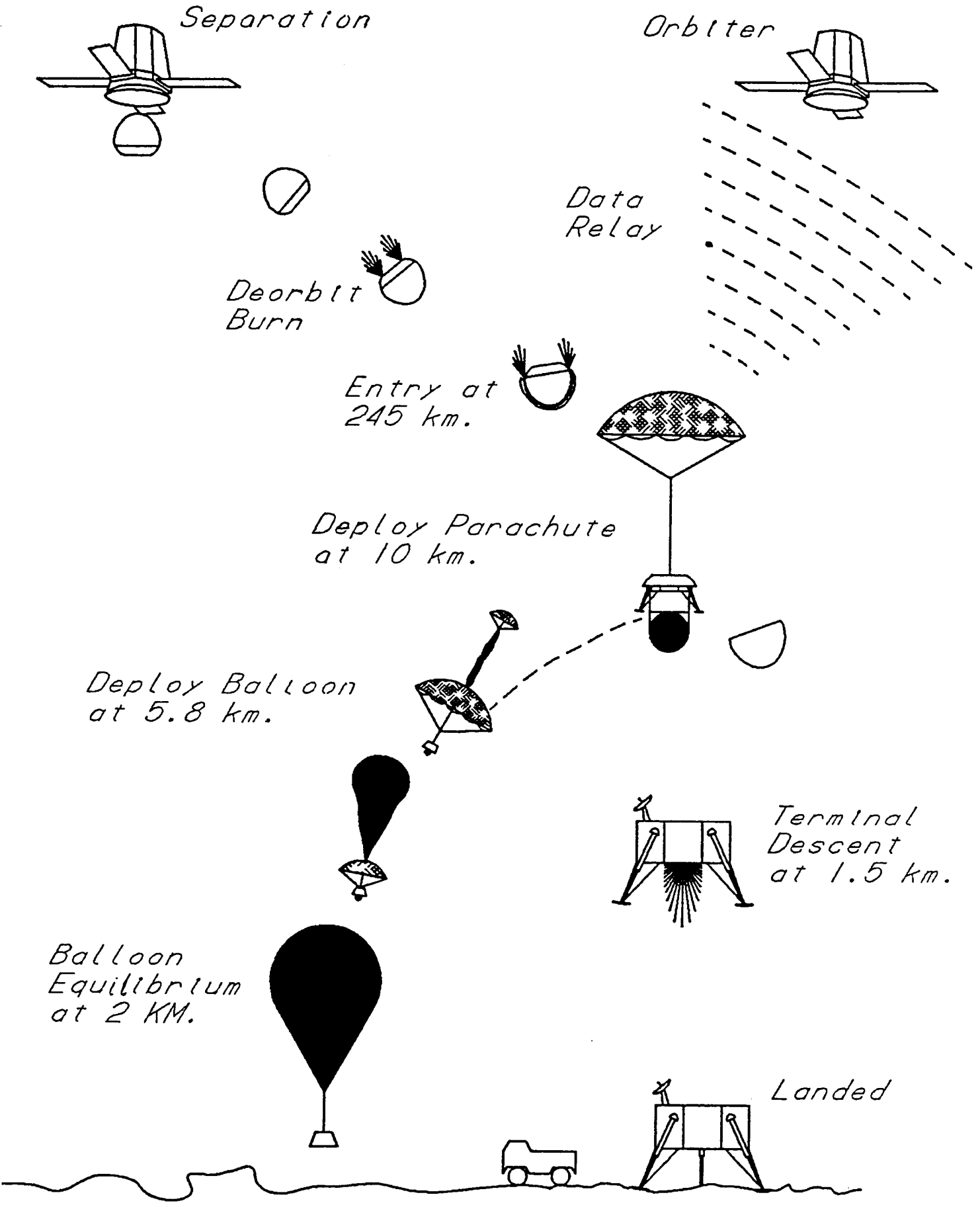
Separation
Orbiter
Data
Relay
Deorbit
Burn
Entry at
245 km.
Deploy Parachute
at 10 km.
Deploy Balloon
at 5.8 km.
Terminal
Descent
at 1.5 km.
Balloon
Equilibrium
at 2 KM.
Landed

1.0 Introduction

1.1 Report Objective

Development of the Mars Lander/Rover (MLR) spanned three academic quarters, representing distinct design phases. The first Interim Report presents the initial configurational decisions reached concerning major vehicle components. Next, the selected vehicle design was analyzed in greater detail, resulting in the modular, multi-vehicular system consisting of a mothership lander, a short-range sample acquisition rover (SAR) which supports the analysis faclities aboard the mothership, and an aerial payload, or balloon rover (BR), which provides high-resolution imaging of the surface, atmospheric characterization at a variety of altitudes and locations, and, eventually, a secondary, long-term data acquisition facility on the Martian surface. Details of this development are presented in the Winter Interim Report.

This Final Report is the third of the three-volume set. It contains the results of studies on one particular part of the MLR system: the Balloon Rover. This component vehicle was selected for further research and design during the Spring Quarter because of the lack of technical literature on this subject as compared to surface rover technology, an area of on-going research in both government and private research groups.

Another reason for this closer study of the Balloon Rover is that it provided an excellent opportunity to experience, in the design course, development of a system on a more well-defined level than in the previous two quarters. As evident in various parts of this Final Report, an important lesson demonstrated during this process was that design challenges tend to increase in number and complexity as the level of refinement increases, making design group interaction and evaluation even more important to the success of a project.

1.2 Operational Scenario

The baseline for this project has been derived from various sources, most notably the National Commission on Space Report. This information, combined with the decision that delivering the payload to Mars orbit would not be considered within the scope of this study, resulted in the following overall mass constraint. It was assumed that future launch vehicles would be capable of delivering 5000 kg to the surface of Mars(from National Commission on Space Report). Further, it was decided that this mass would be made up of five separate landing vehicles. Each of these vehicles consists of a landership (termed the mothership), a local sample acquisition rover, and an airborne balloon rover. This system was selected from a group of candidates (see Winter Interim Report) as the most feasible and effective method of accomplishing the goal of wide-scale characterization of Mars. Additionally, the number of these lander vehicles can be tailored, in a modular fashion, to match realized future launch capabilities.

1.3 Organization of Report

The report is divided into sections pertaining to the various aspects of the Balloon Rover development. Each is presented as a complete sub-element of this document, and consequently, may be read in a different order, if desired. References are found at the end of each section, and supporting appendices are located in a separate section at the end of the document. Appendix numbering corresponds to the respective sections of the text.

2.0 Environment & Landing Site Selection -- Jim Siplon & Ted Holtz

2.1 Environment

The global environment of Mars, its extremes, and specific landing site selection made up the primary focus of our research this quarter. Environmental constraints are critical to all hardware design, especially for the balloon rover vehicle. Environmental factors studied in detail include incident solar flux, wind speed and direction, temperature extremes, atmospheric pressure, airborne particulates, and terrain. This section details these areas, and their potential impact on the balloon rover.

2.1.1 Solar Flux

Mars receives between 36% and 52% of the solar radiation received by the earth. These bounding values occur at aphelion and perihelion, respectively. These figures translate into 400 W/m^2 and 600 W/m^2 perpendicular to the sun, decreasing as the cosine of the angle of the sun. The atmosphere of Mars reflects approximately 20% of the incoming light, but allows 100 times the cosmic radiation that strikes the earth's surface to strike the surface of Mars. Instruments must be shielded accordingly to prevent damage. The feasibility of using solar panels is directly affected by the radiation flux, both in terms of power output and degradation due to exposure(see Sec. 6.1 Solar Panels). In general, materials must be chosen carefully so that lifetime is maximized.

2.1.2 Winds

On the average, winds blow constantly from 0 to 10 m/s with gusts up to 25 and even 35 m/s on occasion. Winds up to 20 or 30 m/s were observed by Viking to occur every 3.3 days. Global wind storms occur every 2 Earth years during the Martian southern summer, with wind speeds as high as 75 m/s. These winds hurl particles of dust into the air and can last for weeks. Winds 20 to 30 km aloft range between 100 and 120 m/s. As a means for comparison, a 100 m/s wind on Mars has the same force as a 10 m/s wind on Earth due to the relative densities of the atmospheres. Winds are obviously important in the balloon deployment and cruise phases, as well as the life of the balloon rover. Airborne particles resulting from dust storms drastically change atmospheric temperatures and available solar flux at Mars' surface. All of these factors, and specifically wind direction and speed at each site, will be critical to the landing site selection process.

2.1.3 Atmospheric Pressure

Pressure appears to be largely altitude- and temperature-dependent on Mars. Viking data shows 7 mb at a location 1 km below the planetary datum and 7.8 mb at 2 km below the datum. These figures vary 20% to 25%, due to seasonal temperature fluctuations, in a quasi-sinusoidal fashion. This variation is shown in Figure 2.1. Altitude is an important factor in site selection as a 1 km change in altitude can mean a 1 to 2 mb change in pressure and a corresponding drop in density. This is significant in determining balloon rover cruising altitude and ultimately the balloon life, depending upon the local geography. See Figure 2.2.

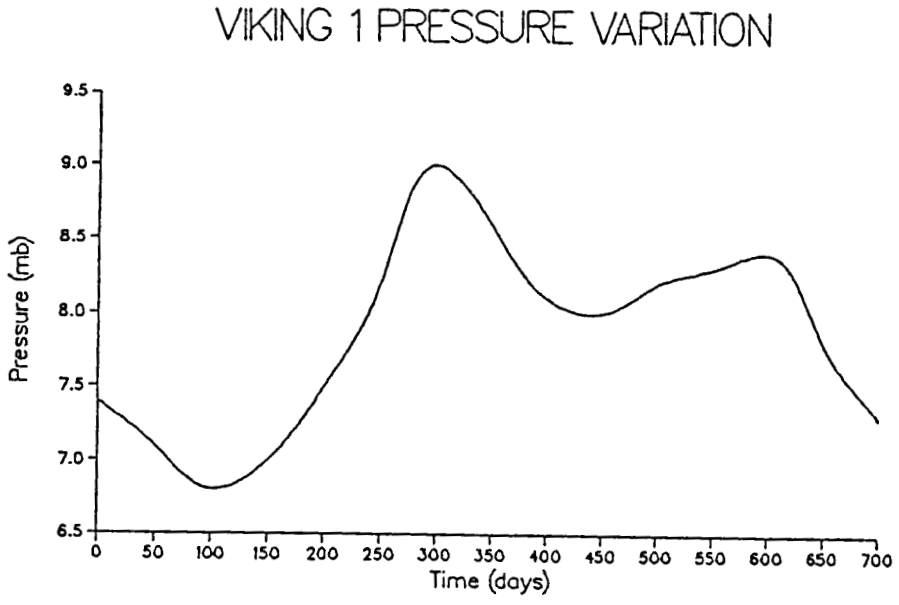

Figure 2.1

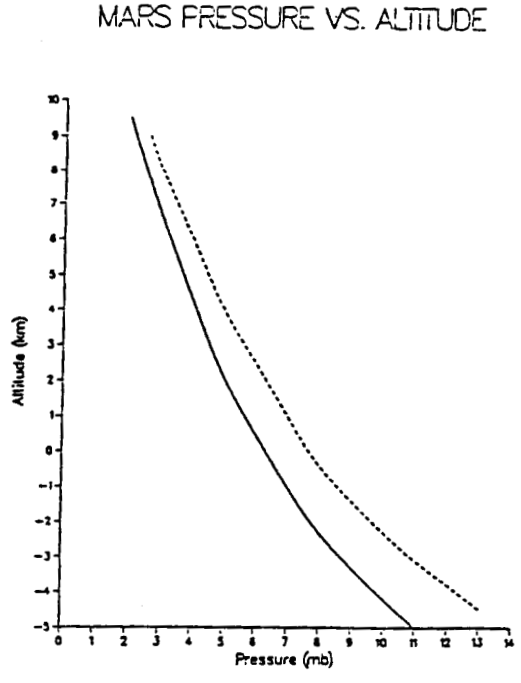

Figure 2.2

2.1.4 Temperature

Temperature ranges at the equator vary from 180 to 250 K and from 145 to 180 K in the polar regions. The low temperature at the poles results in the condensation of CO_2 into solid form, which is the predominant constituent of the polar caps. Daily temperature variations are as great as 80 K between sunrise and noon. These ΔT's could have an immense impact on the brittleness of balloon materials. There is also as much as a 50 K difference between the temperature at the surface and 1 to 2 meters above it. Temperatures vary mainly with altitude and latitude.

2.1.5 Summary

All of the above environmental factors were observed to be altitude related as well as a function of atmospheric density. The selected sites, which are presented in the following section, constitute a compromise between geographic location, and thus scientific interest, and altitude. The altitude requirement is driven mainly by the descent system parachute sizing.

2.2 Landing Sites

A total of five landing sites were selected for the baseline MLR mission. These are described and shown on this and the next three pages.

1. Capri Chasma (48° W 14° S) This site is near the eastern mouth of Valles Marineris, having walls that rise to between 2 and 4 km on either side, about 300 km away. The canyon is approximately 200 km wide and 4500 km long, which is roughly the span of the United States, east to west. The site altitude is 0 km, in other words, it is at the altitude of the planetary datum. The anticipated pressure is 6-7.5 mb. Winds are nominally out of the northeast and will be accelerated through the canyon due to a venturi effect.

2. Olympus Mons (152° W 17° N) This area consists of plains and ancient volcanic lava flows located 1500 km due west of the largest known volcano in the solar system, at an altitude of 0 kilometers. Pressures are expected to be 6-7.5 mb.

3. Hellas Planitia (304° W 40° S) This large crater in the southern hemisphere is felt to have been formed by either a large meteor or comet impact. Since the site is four kilometers below the datum, pressures between 10 and 12.5 mb are expected.

4. Apollinaris Patera (190° W 5°S) This site has volcanic constructs, plains, knobby terrain, and heavily cratered uplands. As with the first two sites, this location is at an altitude of 0 with respect to the planetary datum, indicating a probable pressure of 6-7.5 mb.

See Figure 2.3 for these four sights.

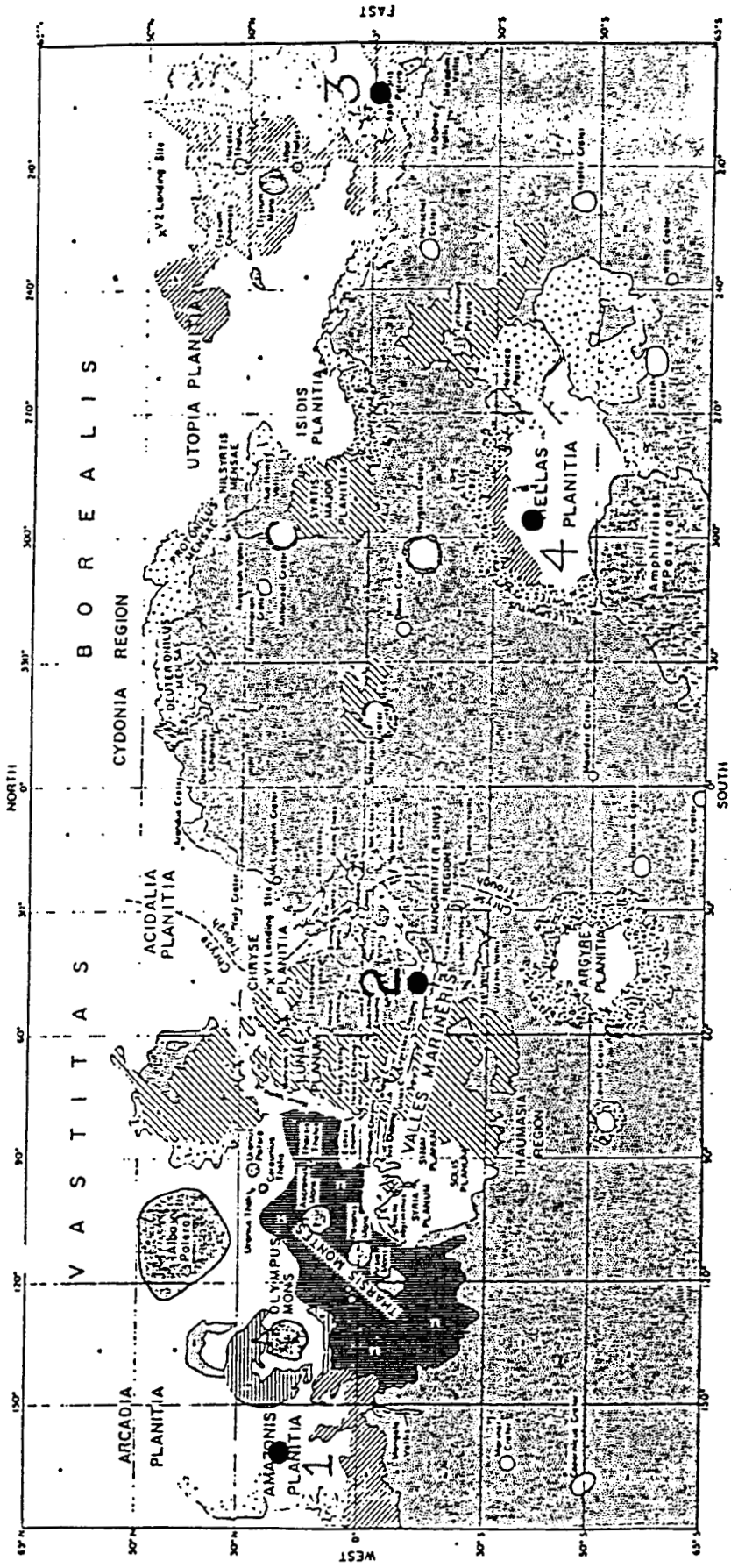

Figure 2.3

5. North Pole Region (18° W 70° N) This site was selected because of its low altitude and the chance of discovering water on Mars. Its altitude is 3 km below the datum, suggesting typical pressures of 8.5 to 10.5 mb. Long balloon life is anticipated here because everything north of 50° is below the datum. This region has terrain such that the balloon rover, cruising at its nominal altitude, would have a flight corridor 2000km wide by 8000km long. Possible missions in this area range from multiple balloon rovers to specialized surface rovers designed to deal with the ice in winter. A major problem anticipated is the fact that, as winter approaches, carbon dioxide precipitates from the atmosphere onto the surface, covering surface rovers under meters of snow. This site is indicated on the figure below.

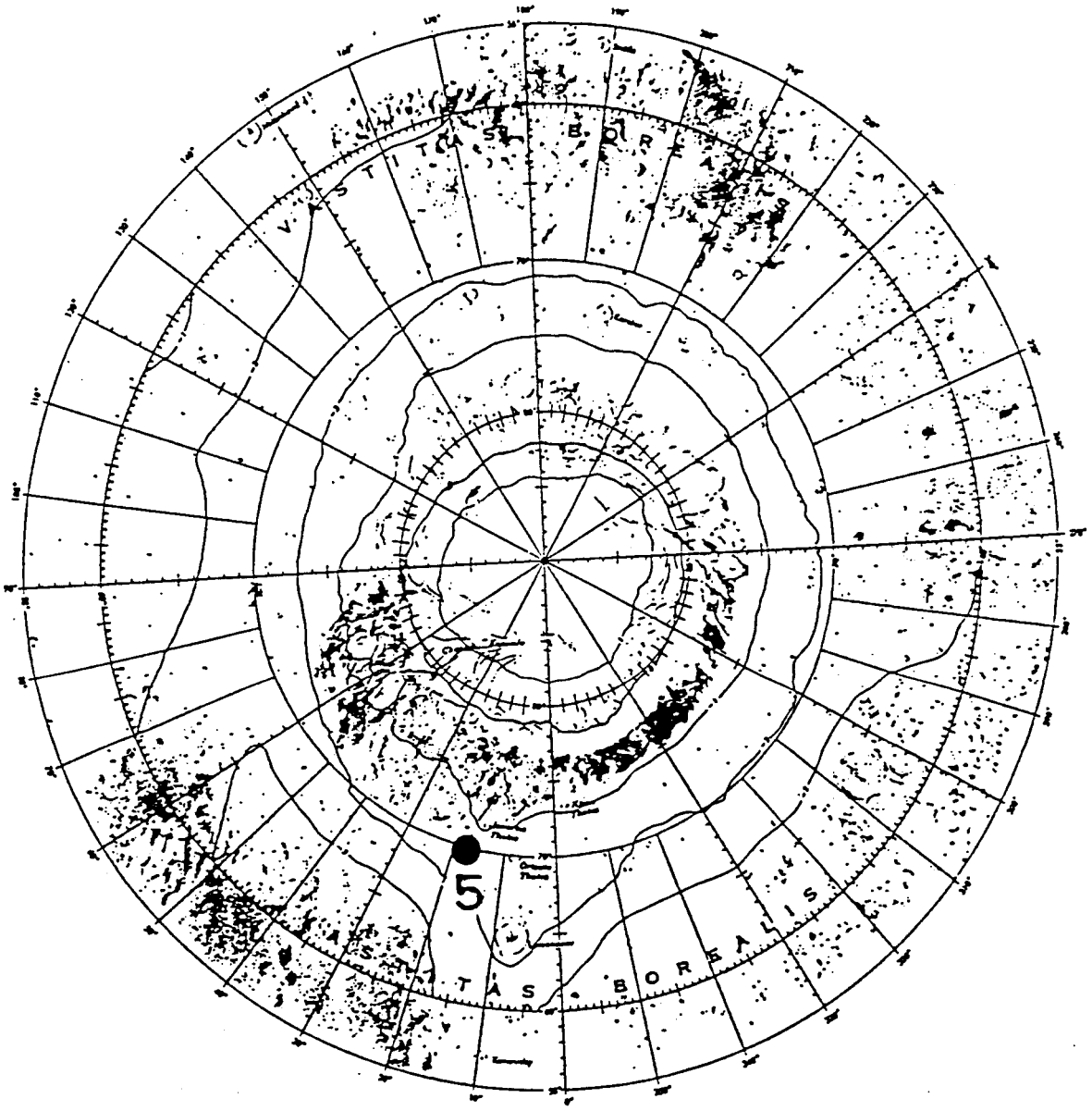

NORTH POLE

Figure 2.4

REFERENCES

NASA/JPL, "Viking-Mars: Anatomy of Success," Mission Status Bulletin, No. 46, October 31, 1978.

Corliss, W. R., "The Viking Mission to Mars," NASA-SP334, Scientific and Technical Information Office, NASA, Washington, D.C., 1974.

JPL Report No. 715-23, Jet Propulsion Laboratory, Pasadena, California, 1980.

Carr, M. H., "The Surface of Mars," Yale University, 1980.

Baker, V. R., "The Channels of Mars," University of Texas, 1982.

Solar System Exploration Committee of the NASA Advisory Council, Planetary Exploration Through Year 2000: An Augmented Program, part 2 of a report, Washington, D.C., 1986, pp. 58 - 101.

3.0 Balloon System Development -- Grant Williams

In conjunction with the MLR group's focus on the balloon rover, a more complete evaluation of the balloon design was needed. As our knowledge of the atmospheric properties at the various landing sites and of balloon dynamics improved, I determined the proper balloon size/payload tradeoffs, and predicted pressure and volume variations, as well as select a suitable balloon fabric.

3.1 Balloon Environmental Considerations

Since the balloon will be filled with hydrogen and sealed prior to deployment, it will act as a super-pressure balloon. A positive pressure difference develops between the inside of the balloon fabric and the surrounding atmosphere; this ΔP varies directly with the temperature of the balloon gas. As long as the volume remains constant, the balloon will float along a constant density plane in the atmosphere.

In order to effectively determine balloon performance, a reliable atmospheric model had to be used. From Ref. 1, pressure and temperature models were obtained based on Viking Lander data. Using these models with the Ideal Gas Law, a density profile was obtained at each Viking site. As can be seen in Figure 3.1, both models predicted density levels significantly higher than the isothermal model used in last quarter's study.

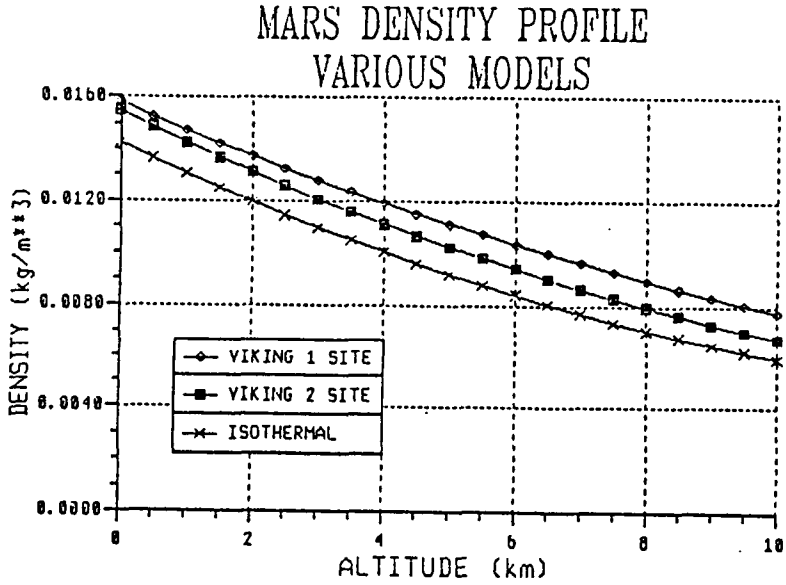

Figure 3.1 Mars Density Profile

Examination of Martian surface conditions revealed that the Viking 2 site lies two km below the Martian datum, and therefore, has a higher density at the surface than many of the designated landing sites. Noting the variation in altitude at the five sites chosen, it was decided to determine a baseline design, using that same balloon radius for all of the rovers. Another option is to tailor each balloon to the atmospheric conditions at each site, but this concept was not consistent with our desire to make the five rovers as uniform as possible, and thus was rejected.

Besides variations with location, local daily variations in density also were determined. At night, the local density increases slightly over its daytime value due to atmospheric cooling. To account for this density change, the temperature model and the pressure scale height were multiplied by 180/220, the ratio of mean nighttime temperature to mean daytime temperature. The resulting density profile is shown in Figure 3.2.

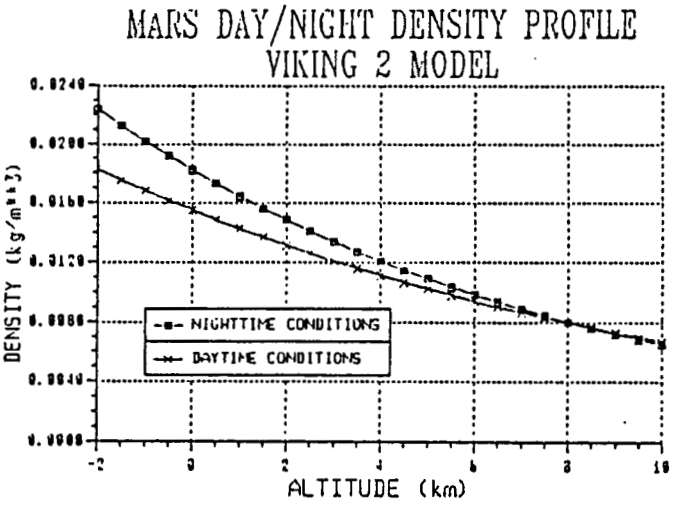

Figure 3.2 Day/Night Density Profile

Equally important to balloon design were the expected temperature extremes of the balloon. As will be shown in the next section, the balloon temperature directly affects the pressure inside the balloon envelope. To determine the maximum-daytime/minimum-nighttime temperature extremes, the balloon was modeled as an isothermal body. The resulting steady-state heat balance, Eqn (1), offsets solar flux and ground radiation inputs with balloon surface radiation.

$$\alpha_b Q_m/2 + \varepsilon_g \alpha_b \sigma (T_g^4 - T_b^4)/2 = \varepsilon_b \sigma T_b^4 \qquad (1)$$

where

α_b = balloon surface absorbtivity
Q_m = Martian solar flux (560 W/m2)
ε_g = ground emissivity
T_g = ground temperature (300 K daytime/150 K nighttime)
T_b = balloon temperature
ε_b = balloon emissivity
σ = Stefan-Boltzman constant

Assuming surface absorbtivity and emissivity values of 0.015 and 0.30, respectively, (typical values for Mylar, from Ref. 3, page 123), the maximum and minimum temperatures of the balloon were found to be 290 K and 136 K, respectively. For design purposes, the temperature range was set at 300 K to 130 K.

3.2 Balloon Design Results

Using a computer program based on Archimedes Principal (as described in last quarter's report, Ref. 4), I developed a profile of cruising altitude vs. balloon radius for different payload sizes, as shown in Fig. 3.3. This and a supporting program are shown in Appendices 3.1 and 3.2.

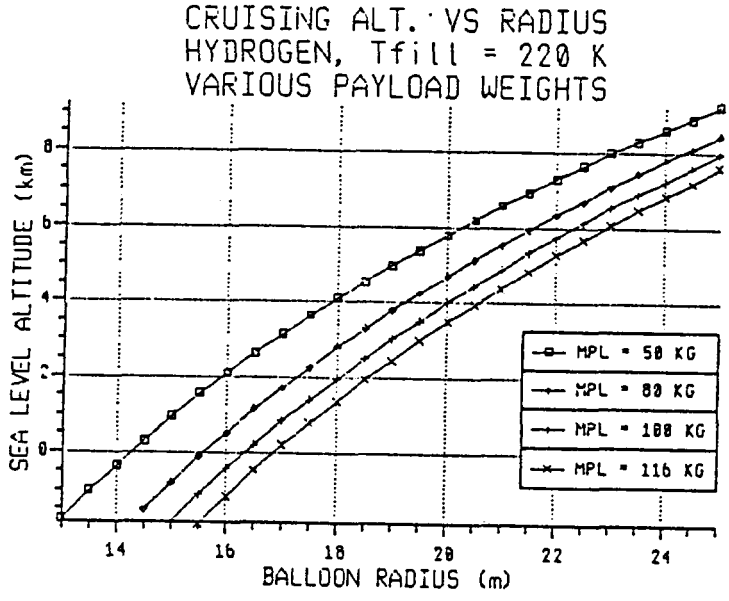

Figure 3.3 Balloon Cruising Altitude vs. Radius

From this figure, a 19 m radius balloon was selected, which will lift 116 kg of payload to an altitude of 2.5 km above the Martian datum. This "payload" refers to all mass other than the balloon fabric and gas, including the scientific payload, power supply, and tethering. The local cruising altitude depends upon the altitude of the specific landing site, and varies from 2.5 to 4.5 km. The total system mass approaches 370 kg, requiring 70 kg from the mass budget's Management Reserve. The class decided to dip into the reserve rather than downsize the payload to meet the system mass requirement of 300 kg because we would have lost a significant portion of the valuable scientific capabilities of the mission. Consequently, the mass budget was changed so that the Balloon Rover now has 400 kg.

The fabric chosen for the balloon has to endure severe environmental conditions that include large temperature extremes, prolonged exposure to UV radiation and significant pressure-induced stress. The study examined four fabrics commonly used in super-pressure balloon applications: Mylar, Polyethylene, FEP-Flourocarbon, and a Mylar/Rip-Stop Nylon laminate.[3] Each material was evaluated based on data from Ref. 3, pg 77 and Ref. 5, pg 25.

As described in the previous section, the balloon fabric temperature could get as cold as 130 K. Both Polyethylene and the Mylar/Nylon laminate become brittle below 190 K, and could fail under even optimistic nighttime temperatures. FEP and Mylar have much lower minimum temperatures, 53 K and 83 K, respectively. Since FEP is much denser, but only about 1/10 as strong as Mylar, Mylar was chosen for the balloon fabric.

3.3 Balloon Pressure Effects

The internal pressure of the balloon varies directly with it's temperature; as the balloon heats during the day, it's pressure rises as well. The pressure difference (ΔP) between the inside of the balloon and the surrounding atmosphere places a stress on the fabric that can be expressed as:

$$\sigma = \Delta P r / 2t \qquad (2)$$

where

σ = induced stress (N/m^2)
ΔP = ambient-internal pressure difference (Pa)
r = balloon radius (m)
t = fabric thickness (m)

This equation was used to find the stress vs ΔP for various balloon sizes(Figure 3.4). The yield strength of Mylar was taken from tensile test data in Ref. 5. As can be seen in the figure, the maximum ΔP a 19 m radius balloon can take without yield is about 510 Pa.

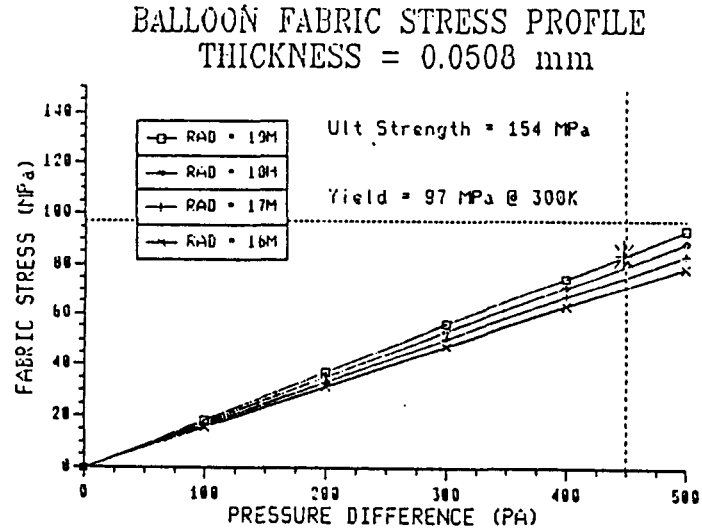

Figure 3.4 Balloon Stress vs. Pressure Difference

The pressure-induced fabric stress had to be considered when optimizing the amount of hydrogen to place in the balloon. If too much gas is placed in the balloon envelope, then the ΔP at 300 K will exceed the yield strength of the fabric. However, enough gas must be used so that, as the balloon cools at night, the balloon pressure remains above ambient, since further cooling after this point reduces the balloon volume, which adversely affects buoyancy.

The Ideal Gas Law was used to determine the ΔP resulting from a sealed balloon with a fixed amount of H_2 as it rises to its cruising altitude. The changes in both pressure and volume resulting from expected temperature fluctuations were also calculated by Ideal Gas Law, according to the equations shown below.

$$\delta P_b = mR/V_b \ \delta T \qquad (3)$$

$$\delta V_b = mR/P_b \ \delta T \qquad (4)$$

$$\delta P_b = \Delta P_o + \delta P_b \qquad (5)$$

where

P_b = balloon pressure
T = balloon temperature
V_b = balloon volume
m = mass of lifting gas
R = H_2 gas constant

By calculating the maximum ΔP at 300 K and the volume change at 130 K, the effect of daily large-scale temperature variations on balloon performance was determined for different amounts of lifting gas. Based on this procedure, the 19 m radius rover should be filled with 22 kg of H_2. At 300 K, a maximum ΔP of 423 Pa results, which is within acceptable limits, as seen in Fig 3.4. The balloon volume stays constant down to 169 K, then shrinks as much as 23% if the balloon temperature drops to 130 K. Based on a nighttime density profile, the balloon would then drop to an altitude of 1.0 km above the Martian datum.

3.4 Aerial Mission Duration

The balloon will remain aloft, day and night, until buoyancy is lost either through a tear in the balloon envelope, or through diffusion losses. Based upon diffusion rates given in Ref. 3 for H_2 through Mylar, diffusion losses do not significantly affect mission life. The possibility exists for tears in the fabric resulting from particle impingement. The balloon should therefore be launched during the Martian northern summer to avoid the hazard of dust storms.

The limiting factor in balloon lifetime is loss of fabric tensile strength due to prolonged UV radiation exposure. Based on data in Ref. 3, the tensile strength of Mylar is reduced by as much as 30% after 120 hours of exposure. Since the balloon will be exposed for approximately 12 hours each day, and with the tensile yield strength safety margin being around 20%, I estimated a balloon lifetime of 5 - 7 days. It should be noted, however, that there are coatings available which absorb UV radiation; these have the potential to significantly improve the lifetime of the balloon.

3.5 Areas of Further Study

The results of the Balloon Systems Design analysis indicate that a feasible Martian Balloon Rover can be developed with present-day technology. Some areas of analysis and design need to be researched in greater detail, however, before a final Balloon Rover design can be developed.

Further work is needed to better understand the surface characteristics of the balloon fabric, Mylar, and tailoring for optimum performance in the Martian environment. Significant variations in the balloon temperature range can be realized by changing the surface emissivity and absorbtivity of Mylar, possibly using thermal coatings. Coatings can possibly be used to absorb UV radiation, which would increase the rover's aerial mission duration. Some type of self-sealing system, such as used in modern automotive tires, would reduce the threat of particle impingement.

It should be noted that there is a great deal of research being conducted on improved balloon fabrics that would greatly enhance the capabilities of a Martian rover. High strength, lightweight fabrics are being developed by the Jet Propulsion Lab, among others.[2] Their extremely low fabric densities, 1/4 that of standard Mylar, would allow a substantial increase in payload capability, or a downsizing of the balloon used to lift the same payload.

REFERENCES

1. Kirk & Seiff, "Structure of the Atmosphere of Mars at Mid Latitude in Summer" from Scientific Results of the Viking Project reprinted from the Journal of Geophysical Research, American Geophysical Union. Washington D.C., 1977.

2. B. Murray, et al, "Mars Model Atmosphere" from Report of the CalTech Mars SURF; Balloons: A Promising Option for the Surface Exploration of Mars, California Institute of Technology, August 1986.

3. Davis, M.H. & S.M. Greenfield, The Physics of Balloons and Their Feasibility as Exploration Vehicles on Mars, R-421-JPL, Rand Corporation, September 1963.

4. Interim Report, Mars Lander/Rover Vehicle Development, An Advanced Space Design Project for USRA and NASA/OAST, Utah State University, Logan, Utah, Winter 1987.

5. Tests of Balloon Materials, NCAR Facilities Report FRB-1-64, November 1964.

4.0 Balloon Deployment

Two fundamentally different methods for deploying the balloon system were studied in order to determine their feasibility. These methods are: 1) to deploy the balloon out of the mothership once it has landed, and 2) to deploy the balloon during the initial descent from orbit. In this section, these options are developed and discussed, and the better of the two selected for the baseline design.

4.1 Ground Deployment -- Jim Cantrell

4.1.1 Fabric Storage and Deployment

Some of the issues governing the ground deployment scheme are: 1) the balloon fabric storage method, 2) the balloon lift during the filling period, and 3) the balloon's angular deflection (toward the ground) due to surface wind conditions. The balloon fabric needs to be stored in a fashion conducive to simple deployment, and the system must be able to lift itself out of the storage bay without damage to the fabric. These criteria were used to develop and evaluate the ground deployment system.

Requiring simple and controlled release and compact storage of the balloon fabric prior to deployment, the storage system shown in Figure 4.1 was created. View A shows the balloon in the deployed state. Note the creases which extend longitudinally around the perimeter of the balloon. These folds help the fabric to be drawn toward the central balloon axis in an orderly fashion when it is pulled lengthwise, as shown in view B. The fabric is then rolled, or twisted, like an umbrella, and encased with a thin membrane, which is shown in the cross-section, A-A. The major benefits to such a system are controlled deployment, and its ability to be coiled for storage.

While filling, the balloon does not have sufficient buoyancy to begin lifting even the fabric out of the storage bay until a critical volume is reached. This critical point corresponds to a critical radius defined by:

$$R_{cr} = \frac{\frac{3\,\rho_f\,T}{P}}{\frac{1}{R_{CO2}} - \frac{1}{R_{H2}}}$$

where:

R_{cr} = critical balloon radius (m)
ρ_f = fabric area density (kg/m^2)
T = ambient temperature (K)
P = ambient pressure (Pa)
R_{CO2} = CO_2 gas constant (188 N m/kg K)
R_{H2} = H_2 gas constant (4124 N m/kg K)

(This relation is derived in Appendix 4.2)

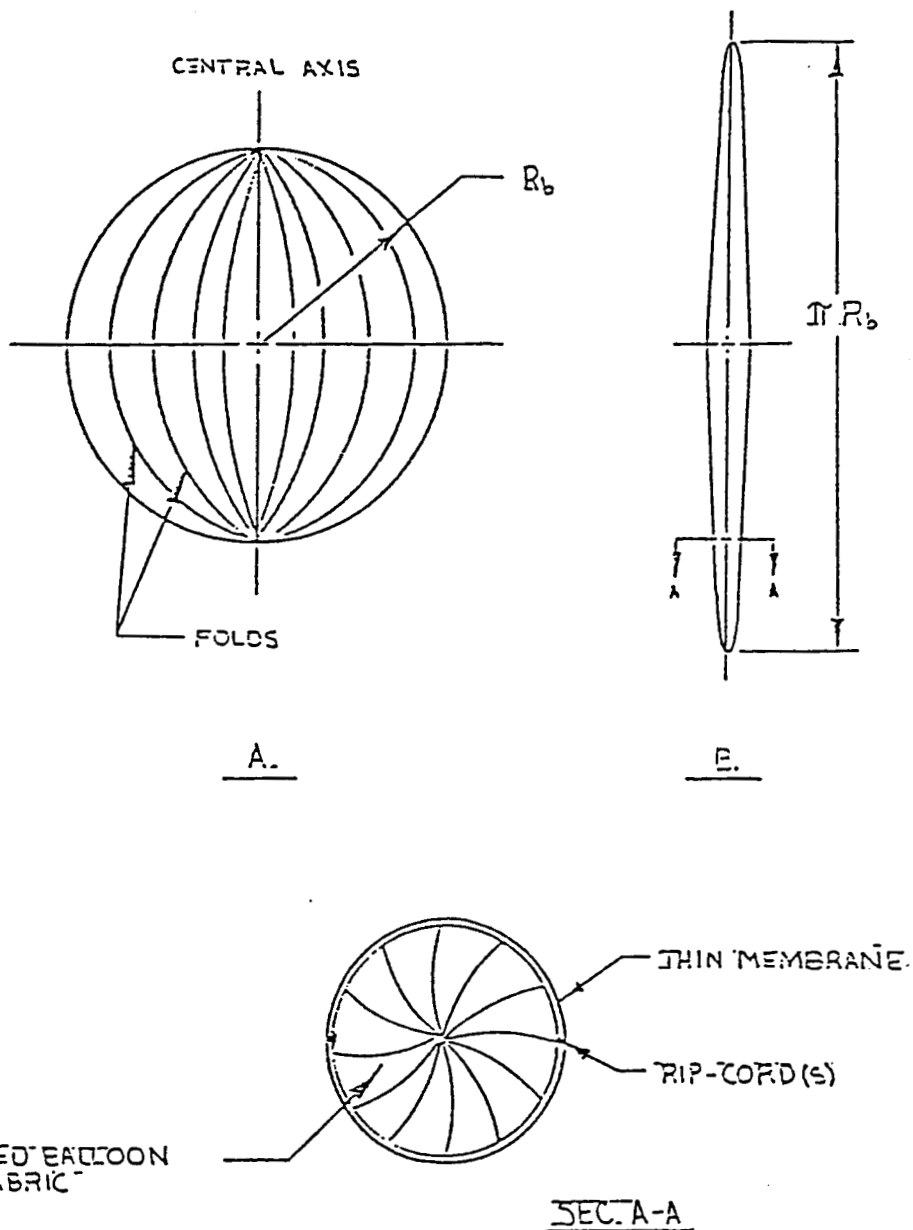

FIGURE 1 — A) BALLOON FOLDING.
B) BALLOON STORAGE

Figure 4.1

Using a fabric density of 0.0502 kg/m^2, an ambient pressure of 600 Pa and temperature of 220 K, the critical radius is 10 meters. This figure is much too large to expect the balloon to lift itself out of the deployment bay.

The need for some form of a lifting mechanism to deploy a length of the balloon is obvious. Several possibilities include the use of a mechanical arm, or a drogue balloon. The mechanical arm has several major drawbacks, among which is the immediate danger of damage to the balloon fabric during the inflation phase. This, along with the mass penalty and complexity inherent in an arm make it less desirable than a passive system such as the drogue balloon. Figure 4.2 shows the deployment system using a drogue. The drogue has the advantage of low mass and simplicity as well as posing no obvious threat to the integrity of the balloon fabric.

The drogue balloon, being made of ultra-thin material, has a small critical radius and thus lifts itself out of the deployment bay. Use of an ultra-thin material does not compromise this balloon as its mission is relatively short-lived since it is not needed after the main balloon is deployed. The drogue's lift is sufficient to raise an amount of the main balloon such that its critical volume can be reached. Figure 4.3 shows, graphically, the relationship between net drogue lift and the amount of undeployed balloon length (see Appendix 4.2). The drogue lift requirements are quite reasonable for lengths of deployment less than 3 meters (< 1.5 kg). Using a lift of 1.5 kg, and a fabric area density of 10 g/m^2, a radius of 2.87 meters is required for the drogue balloon. This is a reasonable size that can be easily stored and deployed.

The overall deployment scheme proceeds as follows. The drogue balloon (2.87m) fills with hydrogen and begins to rise out of the bay, lifting the undeployed balloon material. An equilibrium point is reached and filling of the main balloon commences. Once the critical radius is reached, the main balloon begins to lift itself, deploying more of the fabric by tearing away the protective sheath via the ripcords, like peeling a banana. This allows the lift to control the rate of fabric deployment. The top of the balloon rises according to:

$$y = \frac{-F/g + L_d + V*t*\rho_{CO2} - mdot*t}{2\,\pi\,R_b\,\rho_f} + l_i$$

where:

y = total height above the lander (m)
l_i = initial deployment length (m)
F = ripcord tension (N)
L_d = net drogue lift (kg)
ρ_{CO2} = atmospheric density (kg/m^3)
$mdot$ = mass flow rate into the balloon (kg/s)
t = time since begin of fill (sec)
R_b = balloon radius (m)
ρ_f = fabric area density (kg/m^2)

$$V = \frac{mdot*R_{H2}*T_{amb}}{P_{amb}}$$

(list continues on page 21)

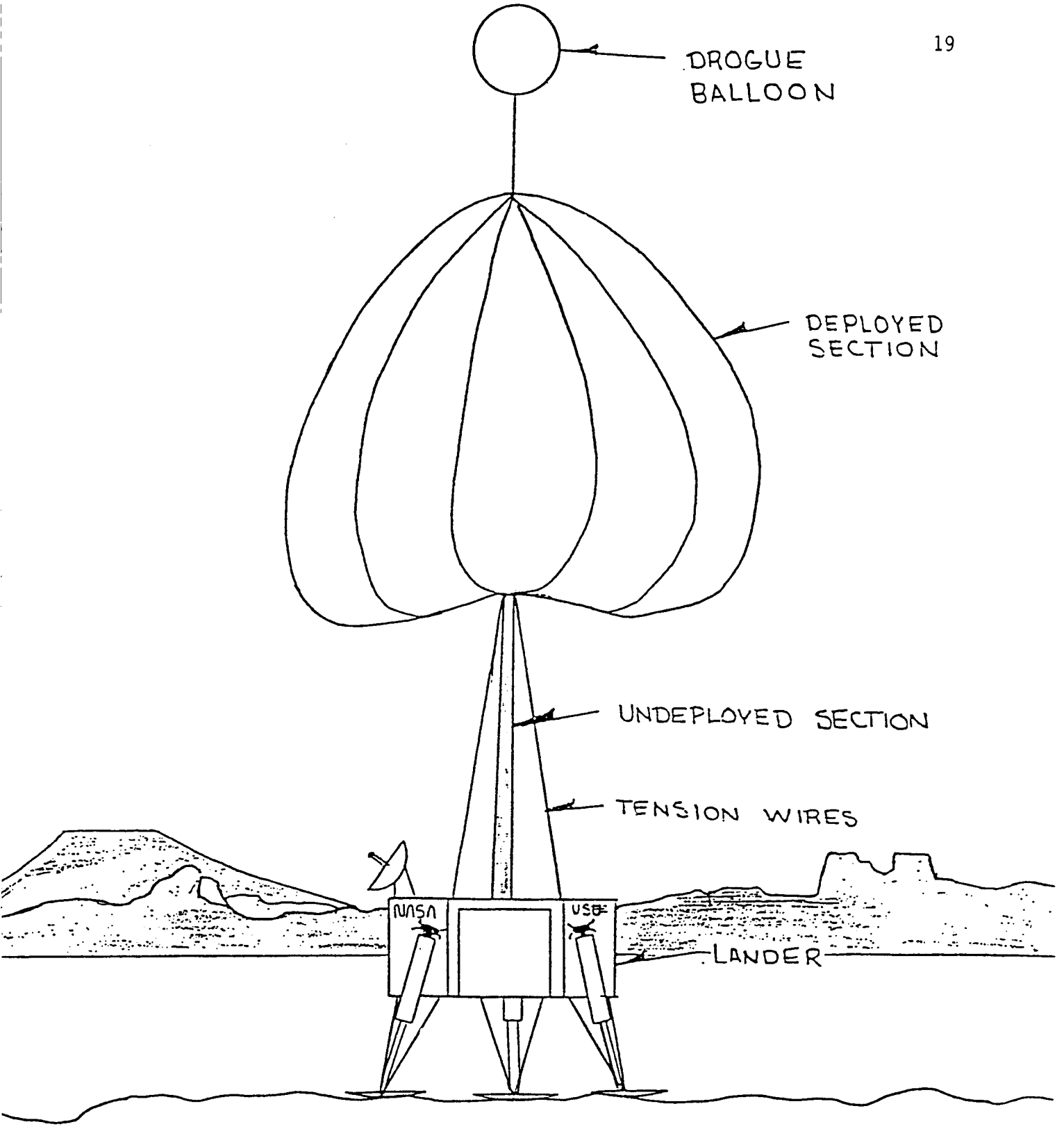
DROGUE
BALLOON
DEPLOYED
SECTION
UNDEPLOYED SECTION
TENSION WIRES
NASA
USSR
LANDER

Figure 4.2

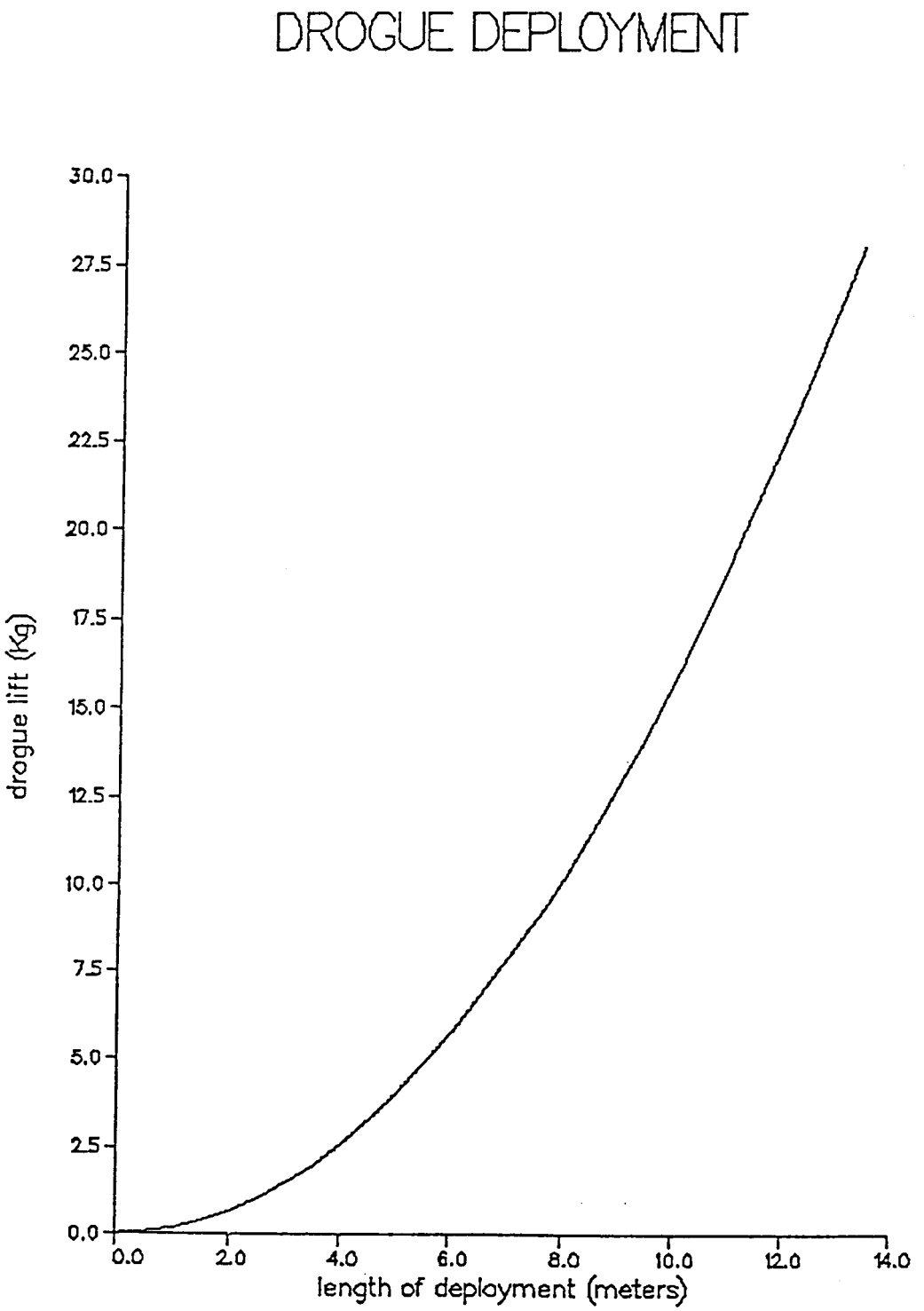
DROGUE DEPLOYMENT
drogue lift (Kg)
30.0
27.5
25.0
22.5
20.0
17.5
15.0
12.5
10.0
7.5
5.0
2.5
0.0
0.0
2.0
4.0
6.0
8.0
10.0
12.0
14.0
length of deployment (meters)

Figure 4.3

R_{H2} = hydrogen gas constant (4124 N m/kg K)
T_{amb} = ambient temperature (K)
P_{amb} = ambient pressure (Pa)
(Derived in Appendix 4.3)

From this relationship, Figure 4.4 was derived. Various mass flow rates were used in order to compare the behavior of the balloon during deployment. A slight dipping is seen during the initial phases of the deployment due to the non-linear release of the fabric, but it is not significant. It is also apparent from this figure that a ground deployment scheme is not mass flow intensive as even very small flow rates exhibit no detrimental effects on the balloon deployment.

Balloon deflection due to surface winds are a limiting factor in the ground deployment scheme. Large deflections could result in damage to the balloon fabric, instability in the mothership/lander, and undesirable balloon fabric deployment. An equation describing the deflection is derived in Appendix 4.4:

$$\theta = \tan^{-1} \frac{L_d*(r_1 + r_2) + L_b*r_2 - m_d*g*r_2/2}{(F_b*r_2 + F_d*(r_1 + r_2))}$$

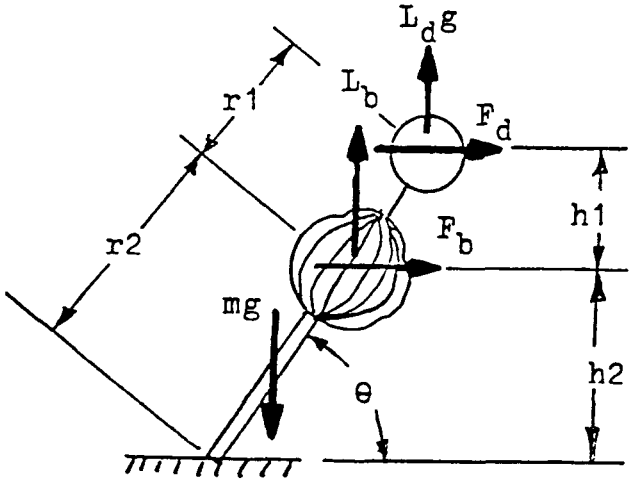

$$F_d = \frac{\pi}{2} r_d^2 * \rho CO2 \; V^2 \; C_D$$

$$F_b = \frac{\pi}{8} x^2 \; \rho CO2 \; V^2 \; C_D$$

Using this relationship, Figure 4.5 was developed. As can be seen, wind speeds above 15 m/s pose a threat to the balloon, but average surface winds of 5 m/s pose little danger. It must be noted that the deflection angles are most severe during a short transient period. Thus, it may be tolerable to launch the balloons in winds up to 15 m/s. It is interesting to note at this point that a wind condition of 30 m/s and a mass flow rate of 15 g/s grounded the balloon. This is due to the wind drag forces deploying the balloon fabric before enough lift is generated to support it. Considering the above results, it is apparent that winds do pose a problem for the overall ground deployment scheme and impose criteria concerning allowable launch conditions.

Balloon Deployment

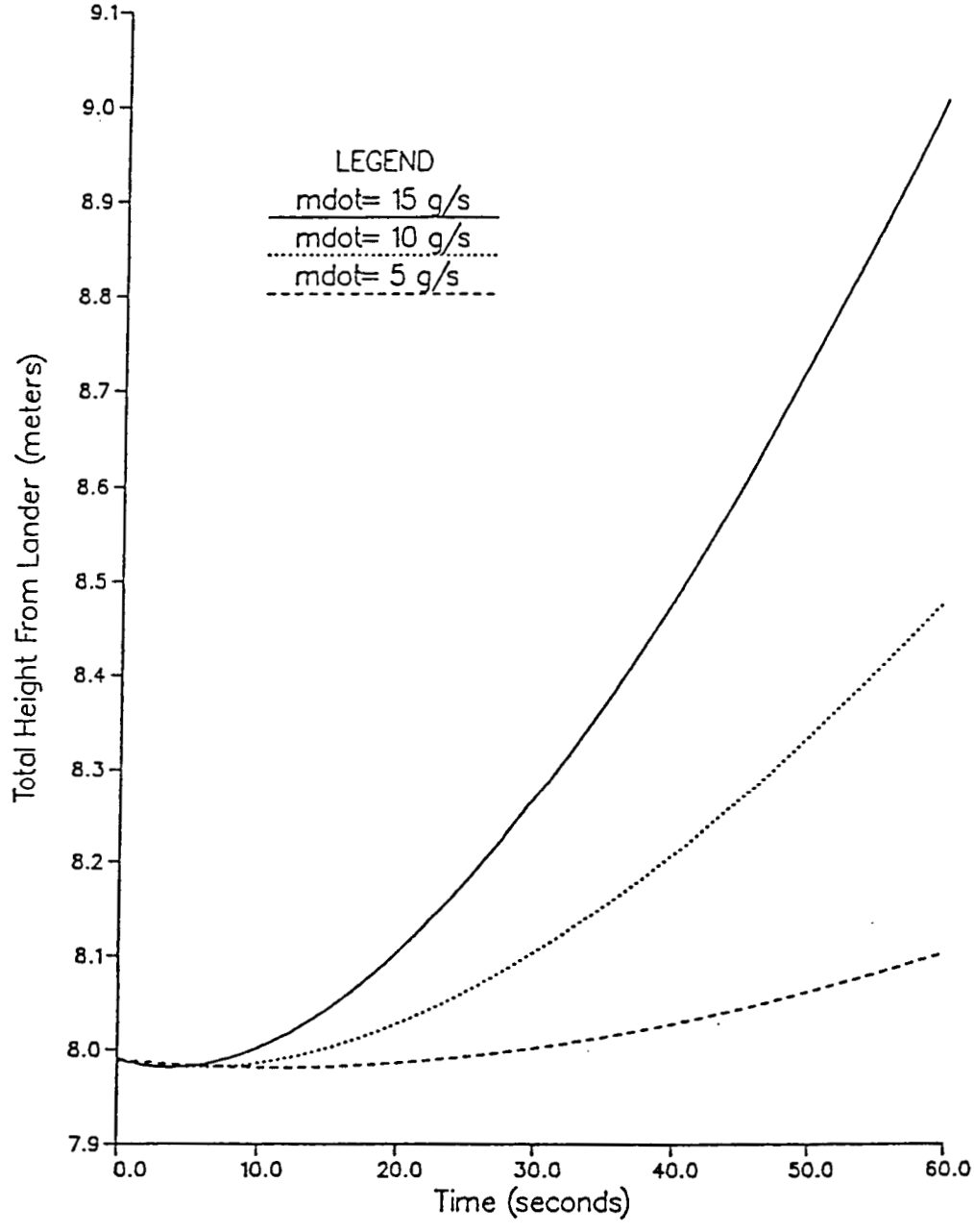

Figure 4.4

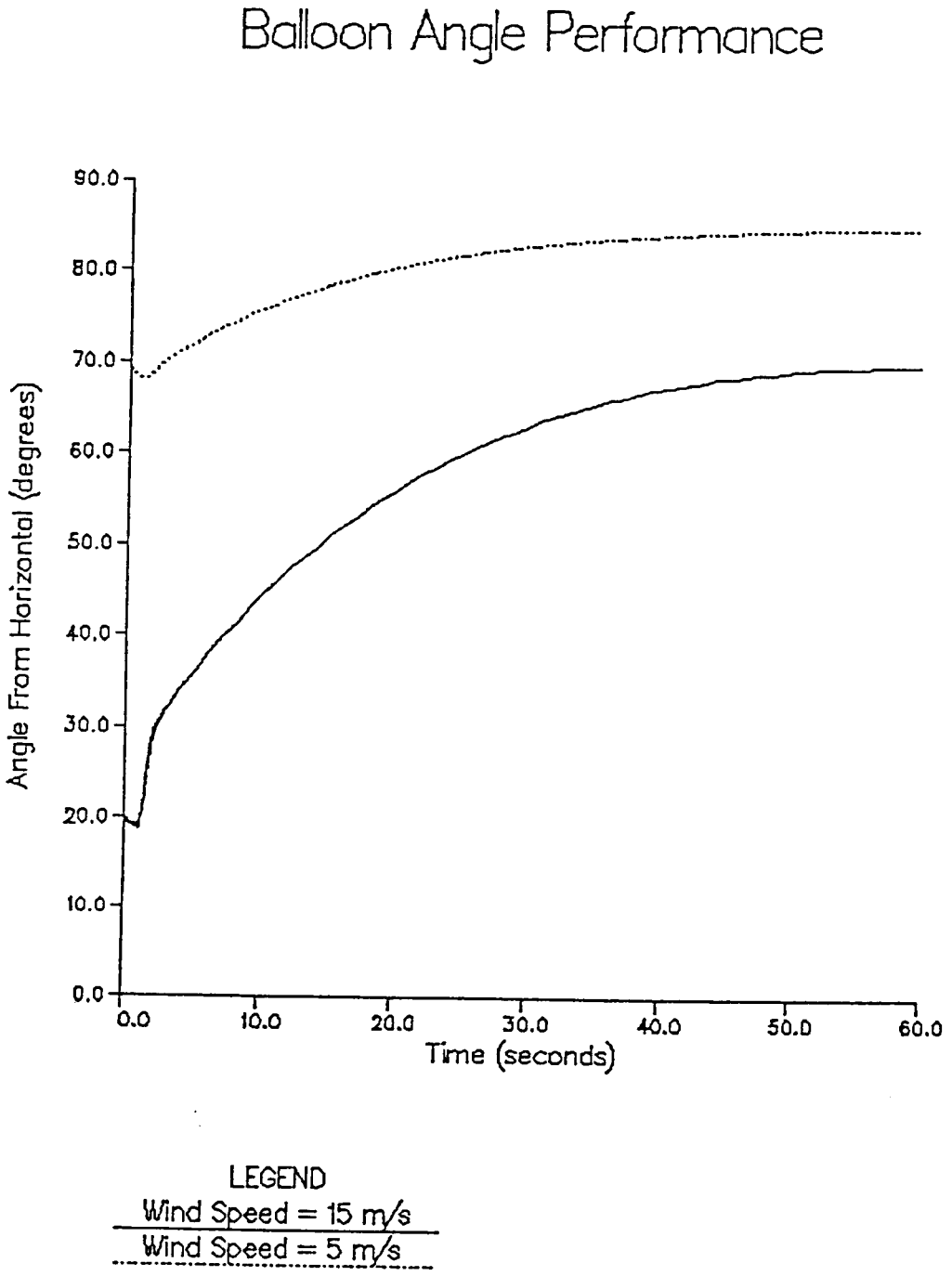
Balloon Angle Performance
90.0
80.0
70.0
60.0
50.0
40.0
30.0
20.0
10.0
0.0
Angle From Horizontal (degrees)
0.0
10.0
20.0
30.0
40.0
50.0
60.0
Time (seconds)
LEGEND
Wind Speed = 15 m/s
Wind Speed = 5 m/s

Figure 4.5

4.1.2 Hydrogen Storage

The storage of 22 kg of hydrogen in a small volume (< 1 m^3) for a long period of time (2 years) poses some very challenging design problems when the system mass is as critical as it is with this balloon rover. Three methods of storage were considered: 1)conventional high pressure storage, 2)cryogenic storage, and 3)solid storage. The problem with high pressure is the large mass associated with such systems, and liquid hydrogen must be maintained at an extremely low temperature (6.86 K).[1] Solid storage can be mass-intensive and also presents extraction problems. Due to the lack of literature on this method it was not pursued. High pressure was deemed the most feasible manner of storage in light of expected advances in lightweight structural materials.

The use of conventional metals for the pressure vessel result in an unacceptably high mass, mainly due to the storage pressures of up to 28 MPa. A sphere constructed of titanium requires 225kg. This mass is much too high. Alternative materials were sought in order to reduce this mass requirement. One possible class of materials are carbon fiber reinforced composites.

Composites offer good strength-to-weight ratios, as well as being actively researched and advanced at present. Despite this, diffusion of H_2 through the tank material is a very real concern, especially with a porous material such as a composite. This is an area of current research and for the purposes of this preliminary design, it was assumed that this problem will prove solvable.

Figure 4.6 shows the relationship between the geometric properties and the mass of a spherical tank composed of carbon fiber laminates. The figure is based on a quasi-isotropic ply angle lay-up: (45,90,-45,0), the Reidlich-Kwong equation of state for hydrogen, thin-wall pressure vessel analysis, and a single-ply failure criterion. For our application, the vessel has the following specifications:

dimensions	1.24 m dia., 1 m^3 volume
capacity	22 kg hydrogen
mass	80 kg (w/o hydrogen)
max. temperature	300 K
pressure	28 MPa

(see Appendix 4.9)

As can be seen in the figure, the use of composites offers substantial mass savings over conventional materials. As previously mentioned, further research needs to be conducted in order to assess problems of diffusion and the effects of repeated load cycling due to temperature and pressure fluctuations.

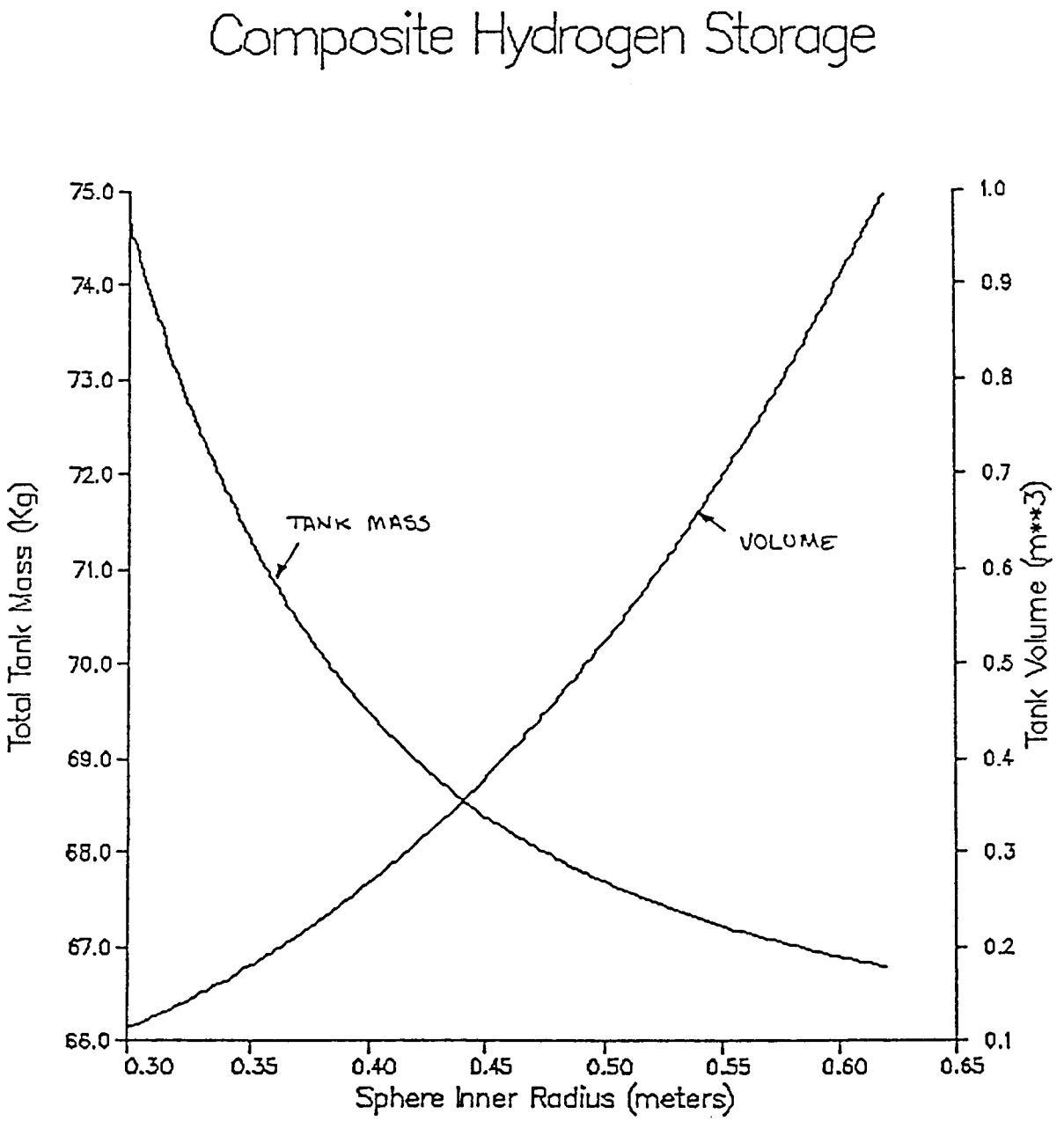
Composite Hydrogen Storage
Total Tank Mass (Kg)
Tank Volume (m**3)
TANK MASS
VOLUME
75.0
74.0
73.0
72.0
71.0
70.0
69.0
68.0
67.0
66.0
1.0
0.9
0.8
0.7
0.6
0.5
0.4
0.3
0.2
0.1
0.30
0.35
0.40
0.45
0.50
0.55
0.60
0.65
Sphere Inner Radius (meters)

Figure 4.6

4.2 Descent Deployment -- John Higham

4.2.1 Initial Designs

Three schemes for descent deployment were considered. The first is to leave the balloon rover attached to the lander, and to fill the balloon as the system descends. The second option is to land the entire MLR unit, then use a small rocket to launch the balloon rover into a parabolic trajectory and to begin filling the balloon when apogee is reached. The third idea is to separate the balloon and its payload, along with the necesssary inflation apparatus, from the lander when the lander is ready to deploy its parachute (~5800 meters). This last scheme is the one studied in the most detail for reasons that follow.

In order to fill the balloon while attached to the descending lander, it is necessary to have the balloon full and ready to detach prior to the firing of the lander retro-rockets. This may not be a problem, but filling the balloon behind a vehicle as large as the mothership (2 meter dia.) may be, due to the resultant turbulence. It was decided that avoidance of this potential would be prudent and thus, this design was not considered in great detail.

The motive for deploying the balloon as it reached the peak of a suborbital trajectory was that the velocity would be essentially zero at the point of deployment. This could be used to advantage by deploying a parachute sized to provide as much fill time as necessary. A major disadvantage is the obvious increase in mass of the landing systems and the balloon launch rocket. This deployment system, therefore, is viewed as a "last resort" option.

Deploying the balloon and its payload as it descends, separate from the mothership, proved to be the preferred method. In addition to providing sufficient fill time (depending upon parachute sizing), it also considerably decreases the landed mass. This, in turn, allows an increase in the payload mass for the surface operations. The remainder of this section is devoted to describing how the descent was modeled and the resulting solutions.

4.2.2 Descent Modeling

It was decided to separate the balloon payload from the lander just prior to when the lander deploys its parachute. This translates into an altitude of 5800 meters and a velocity of 250 m/s. Next I proceeded to develop a Free Body Diagram of the balloon rover system in order to model its motion. The following differential equation resulted (See Appendix 4.6 for the derivation):

$$\frac{d^2x}{dt^2} + G - \frac{F_B + F_P}{M} = 0$$

where

F_B = Balloon lift force

F_P = Balloon/parachute drag force

G = Gravity force on Mars

M = System mass

x = Distance above the surface of Mars

This equation was calculated in a computer program that allowed variation of parameters such as fill time, drag coefficients, and parachute size. Results from several cases were compared to define possible descent scenarios. The following table presents pertinent data on the parachute which is arguably the best choice. Of special interest are the maximum deceleration, balloon fill time, and cruising altitude.

Parachute size: 300 m^2

Time (sec)	Altitude (m)	Velocity (m/s)	
0	5800	-235	
1	5604	-165.3	Maximum deceleration
~			
300	705	-9.4	Balloon is full
~			
310	656.59	-0.644	
311	656.29	0.033	Balloon begins to rise
~			
877	2693.22	0.008	
878	2693.22	-0.005	Cruising altitude
~			
900	2690.11	-0.272	Small oscillations about cruising altitude

Graphical representation of the results of this computer analysis is shown in Figures 4.7 through 4.12. A listing of the program code is included in Appendix 4.7.

4.2.3 Filling the Balloon

One of the major questions that needs to be answered is what a reasonable fill time is. In order to answer this question we first need to know the gas storage method. As was discussed in Section 4.1.2, the high pressure option appears best, especially for descent deployment, which will require fairly rapid inflation. To calculate the mass flow rate into the balloon, ideal gas conditions were assumed. Even though the storage pressure for the hydrogen is quite a bit above the critical pressure for hydrogen, it turns out that this assumption is valid (see Appendix 4.8 for details).

For Figures 4.7 - 4.12, the following data apply,

Initial velocity	250 m/s
Descent angle	20°
Initial altitude	5800 m
Radius of balloon	19.5 m
Total payload mass	363 kg
Mass of hydrogen gas	22 kg
Mass of H_2 storage tank	80 kg
Parachute deployment time	15 sec
Parachute C_D	1.0

Additional parameters apply to each figure, as noted.

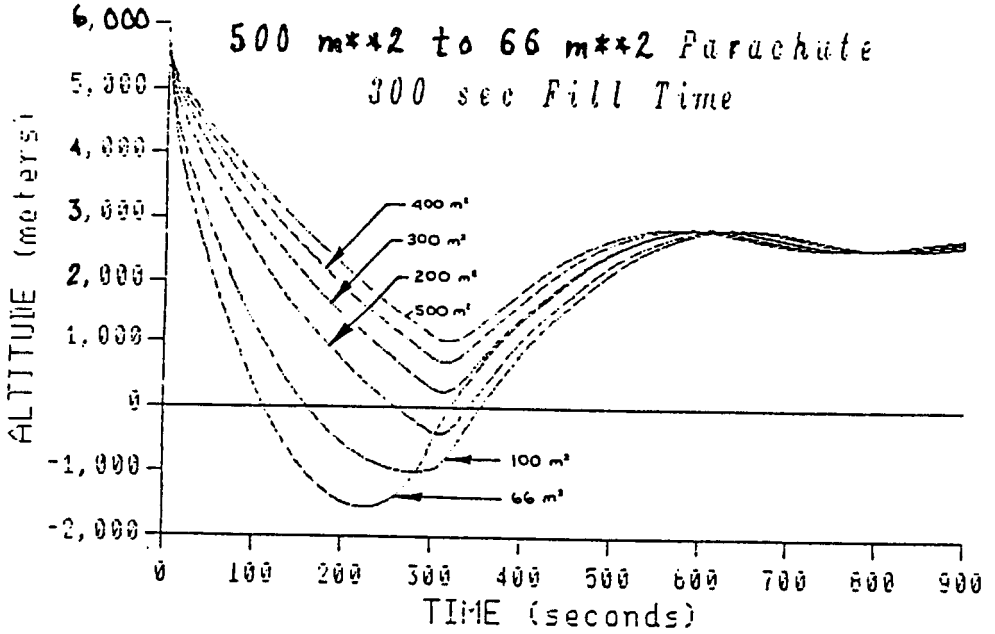

Balloon C_D: As filling -- 0.01, Filled -- 0.1
Parachute detaches when balloon is full

Figure 4.7

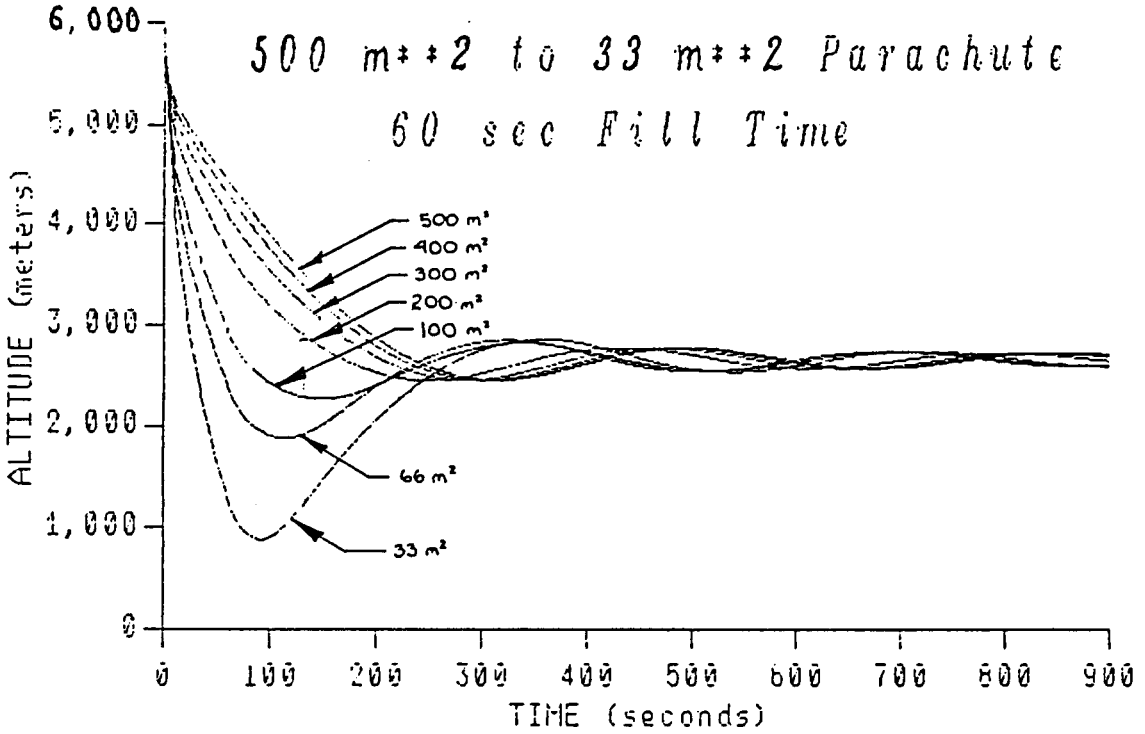

Balloon C_D: As filling -- 0.01, Filled -- 0.1
Parachute detaches when balloon is full

Figure 4.8

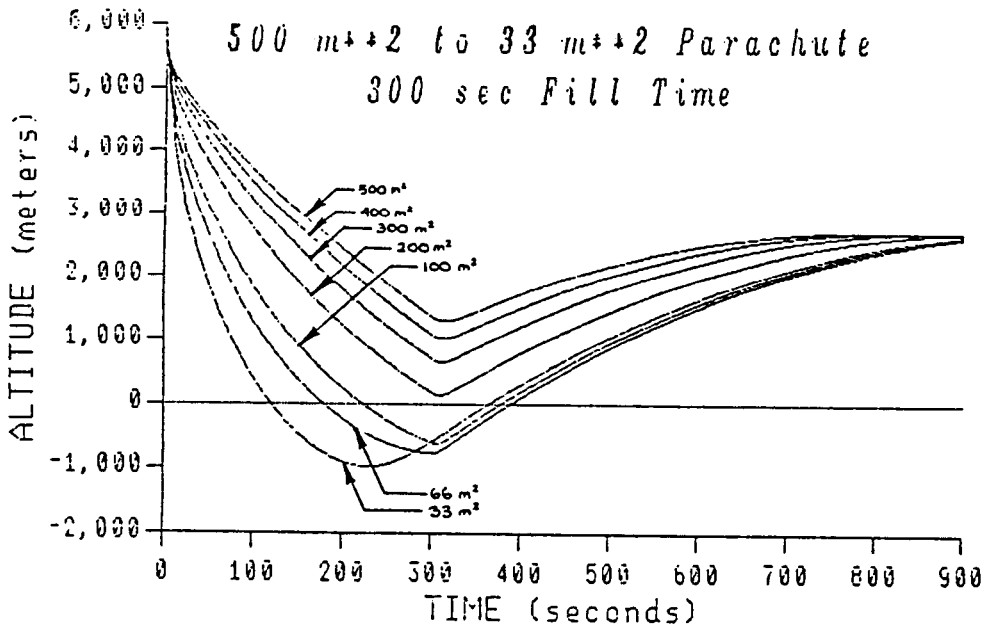

Balloon C_D: As filling -- 0.1, Filled -- 0.5
Parachute detaches when balloon is full

Figure 4.9

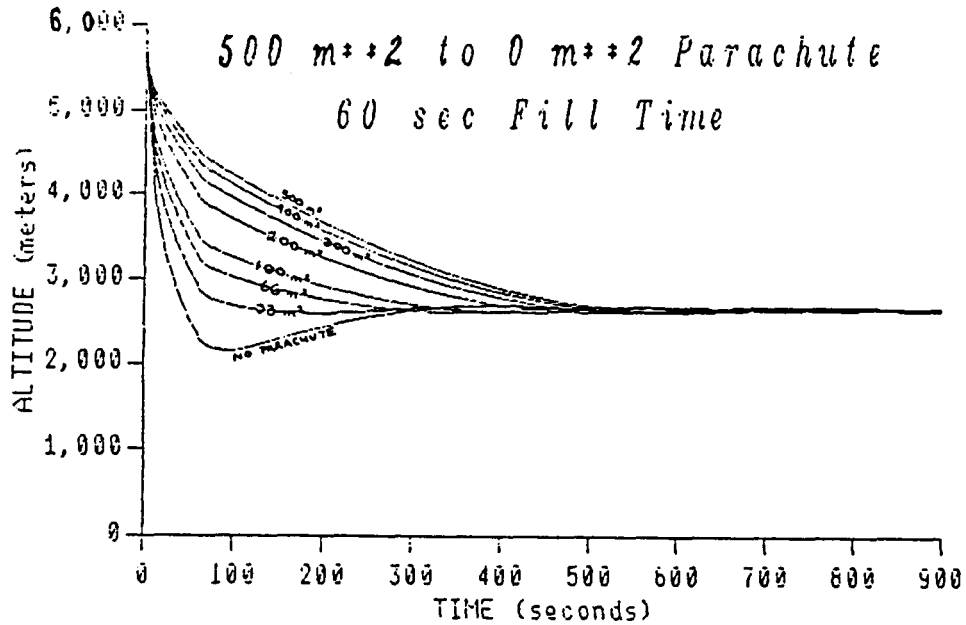

Balloon C_D: As filling -- 0.1, Filled -- 0.5
Parachute detaches when balloon is full

Figure 4.10

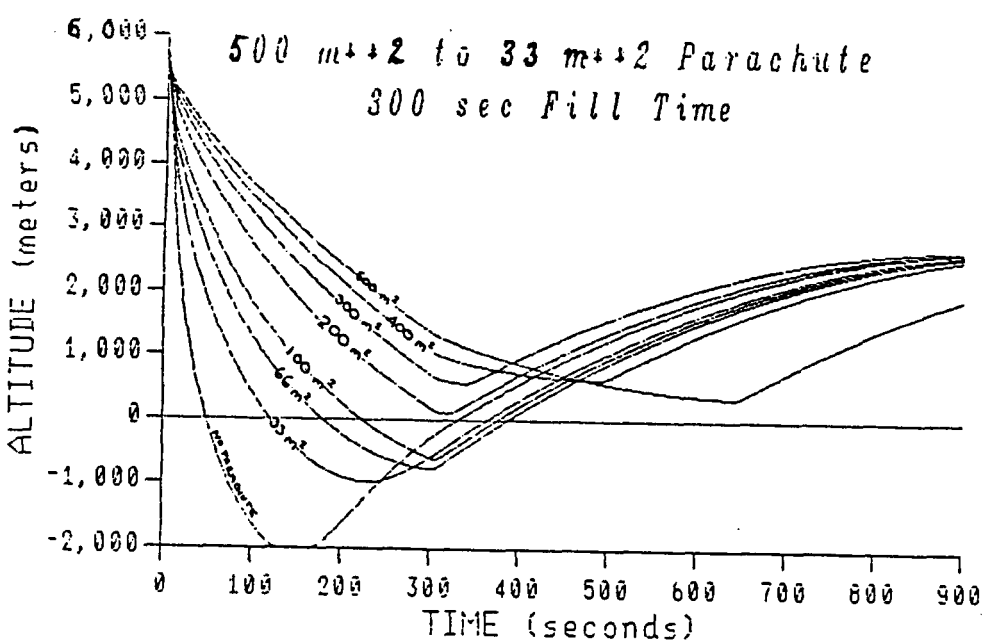

Balloon C_D: As filling -- 0.1, Filled -- 0.5
Parachute detaches when balloon begins to rise

Figure 4.11

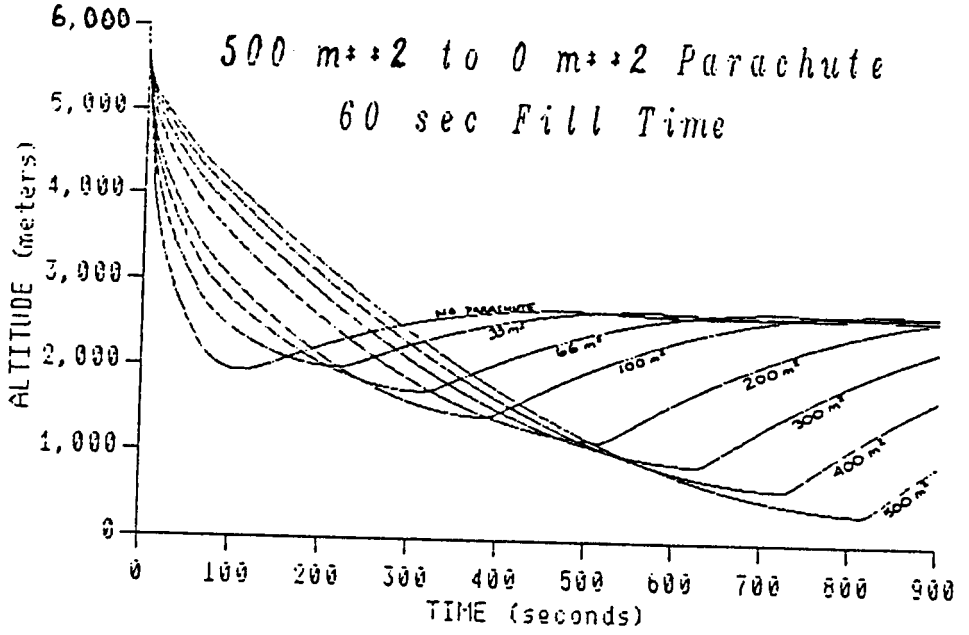

Balloon C_D: As filling -- 0.1, Filled -- 0.5
Parachute detaches when balloon begins to rise

Figure 4.12

Using this assumption, it was found that for a 15 meter, 25.4 mm diameter fill tube, it takes approximately 23 seconds for the balloon to fill. This may, in fact, prove to be too fast, since the hydrogen coming out of the nozzle will have an initial velocity of 247 m/s and a mass flow rate of 3 kg/s. This is potentially hazardous to the fabric of the balloon. For this reason, fill times of up to 300 seconds (5 minutes) were considered. Further study is necessary to determine how rapidly the balloon can safely be filled. For additional mass flow considerations see Appendix 4.8.

A quick glance at Figures 4.9 through 4.12 indicates that the parachute is needed only until the balloon is full. If the parachute remains attached any longer than this it weighs down the balloon, not allowing it to rise. Of the cases presented above, it is believed that Figures 4.9 and 4.10 are the best models, with Fig. 4.9 being the most realistic, as the case in Fig. 4.10 has too rapid a fill time (see Appendix 4.8).

Graphs of velocity as a function of time were generated by the computer program, but the various cases were so close that it was very difficult to gain much information from these plots. Velocity profiles are important in determining expected decelerations. An abridged table of two worst-case situations are presented on the following page. This data shows the deceleration which takes place during the first ten seconds of balloon rover deployment when parachutes of 100 m^2 and 500 m^2, respectively, are employed.

Parachute Size = 100 m^2

Time (sec)	Altitude (meters)	Velocity (m/s)
0	5800.00	-234.923
1	5575.40	-214.968
2	5374.72	-187.788
3	5200.38	-162.305
4	5049.25	-141.103
5	4917.07	-124.138
6	4799.99	-110.666
7	4694.95	-99.911
8	4599.96	-91.237
9	4512.00	-84.158
10	4430.87	-78.312

Parachute Size = 500 m^2

Time (sec)	Altitude (meters)	Velocity (m/s)
0	5800.00	-234.923
1	5621.07	-139.861
2	5513.01	-85.652
3	5442.47	-59.081
4	5391.21	-45.015
5	5350.67	-36.848
6	5316.57	-31.774
7	5286.58	-28.463
8	5259.32	-26.219
9	5233.93	-24.653
10	5209.88	-23.532

The highest deceleration experienced with the 100 m^2 parachute is on the order of 3 Earth g's, whereas the larger parachute produces loading as high as 10 g's. This should be a major consideration in the eventual selection of a mission parchute because undoubtedly there will be payload components which limit the loading which the system can be subjected to.

4.3 Conclusions

After considering the advantages and problems associated with the ground-based and the descent deployment schemes, we decided that airborne deployment is preferred. This method avoids the potential problem of contact between the fabric and the Martian surface. However, turbulent air flow around the inflating balloon may cause damage to the fabric. This concern is best addressed by experimentation as was employed in the development of the Viking descent parachute. A major point in favor of descent deployment is that it increases the mass which can be used for the mothership and SAR, thus allowing more scientific payload.

REFERENCES

Flammer, G., et al, Fundamental Principles and Applications of Fluid Mechanics, Utah State University, 1986.

Klein, G., Planetary Spacecraft Systems Technology, Final Report 1986, Ocotber 30, 1986.

White, Frank M., Heat Transfer, Addison-Wesley, 1984.

5.0 Optics and Communictaions -- Steven Brown

5.1 Optical Requirements of Balloon Rover

One of the main objectives of the balloon rover is to obtain high resolution photographs of the surface of Mars. Some of the considerations are:

1. Minimum resolution requirements
2. Minimum area of coverage per photograph
3. Required lens focal lengths
4. Type of photographs
   a) black and white or color
   b) spectral response: infrared, visible, ultraviolet.

The resolution obtained is directly proportional to the number of photo-sensors in the device and inversely proportional to the area which is to be covered by each image. As the coverage area increases the area which is sensed by each pixel (photo-sensor) also increases, resulting in a lower resolution. This can be corrected by increasing the number of pixels per photograph. Another factor which must considered is the focal length required to obtain a particular resolution.

The area covered by a square array photo-detector is related to the resolution by the following equation:

$$R^2 = \frac{A}{N_p}$$

Where R is the resolution, A is the area covered and N_p is the number of pixels in the square array.

Assuming that a resolution of 0.5m is wanted for an area of .25km^2 would require a square array of 1000 pixels on a side. Since detectors are usually manufactured in powers of two, the detector array size needed would have 1024 pixels on a side. See Figure 5.1.

The resolution is also a function of focal length and distance to the object being photographed. This relationship is as follows:

$$R = \frac{dh}{f}$$

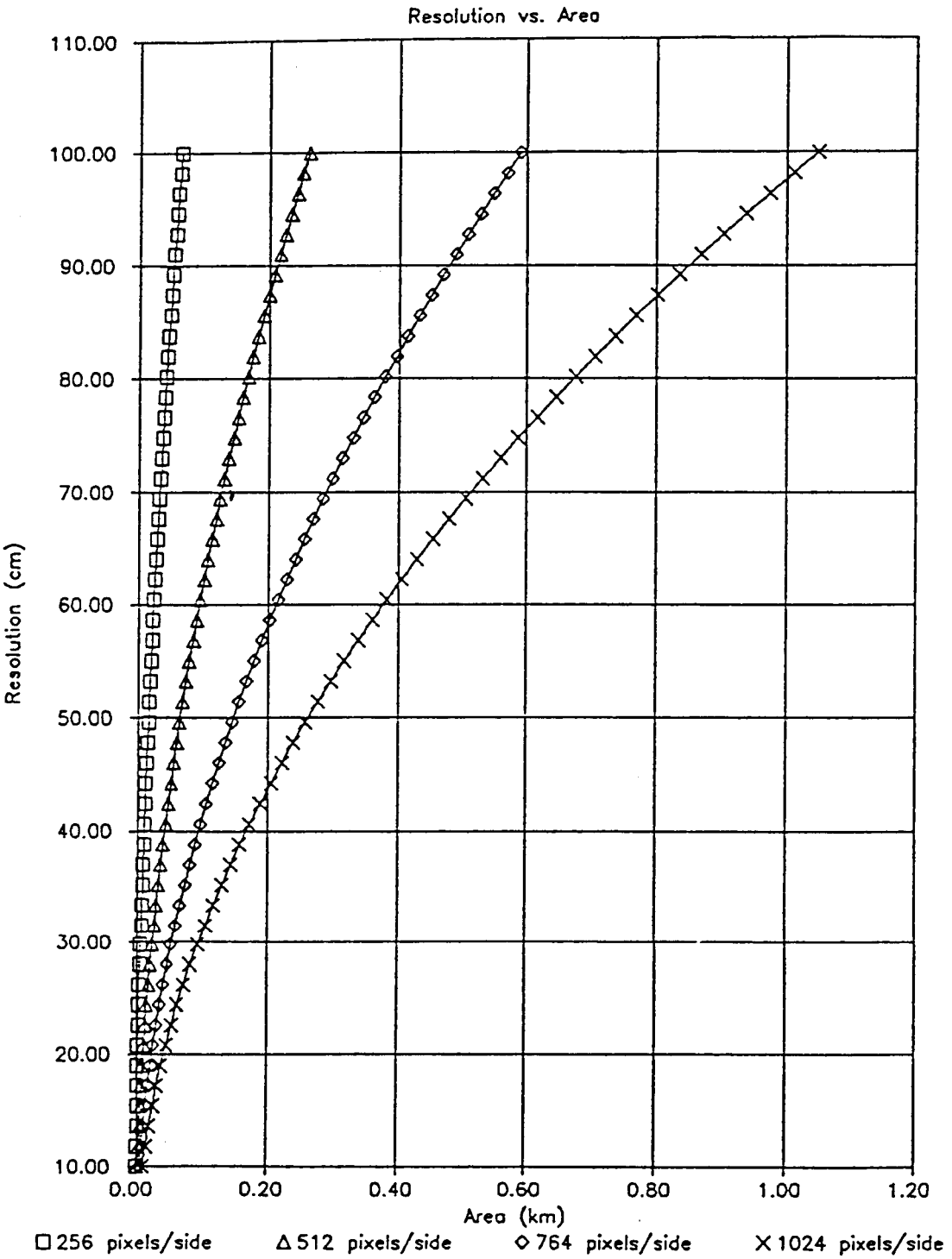
Resolution vs. Area
110.00
100.00
90.00
80.00
70.00
60.00
50.00
40.00
30.00
20.00
10.00
Resolution (cm)
0.00
0.20
0.40
0.60
0.80
1.00
1.20
Area (km)
□ 256 pixels/side
Δ 512 pixels/side
◇ 764 pixels/side
X 1024 pixels/side

Figure 5.1

Where R is the resolution, d is the center to center distance between pixels on the photo-sensing array, h is the height from the surface to the camera, and f is the focal length of the lens. The relation of resolution vs. focal length at different heights above the surface for a 40 μm center to center pixel spacing is shown in Figure 5.2.

At a maximum height of 4.5 km above the surface, a 50 cm resolution would require at least a 360 mm focal length. This would allow an area of 0.25 km^2 to be covered per photograph, using a photo detector with 1024 pixels per side, in a square array with 40 μm center to center spacing. If the resolution were increased to 40 cm then a 450 mm focal length would have to be used and the area covered per photograph would be approximately 0.17km^2, using the same photo detector.

As the distance between the balloon and the surface varies with changes in atmospheric density and surface elevation it will be necessary to adjust the focus of the lens. It may be useful to allow simultaneous adjustment of the resolution and photographic area by using zoom lenses on the cameras. Although the time delay in communication between the rover and ground control on Earth would require an automatic focus and zoom system, this would not prevent ground-based operators from commanding the camera system to increase or decrease the resolution to get higher quality pictures or to increase the field of view at the expense of resolution. A lens system which could zoom between 100 mm to 400 mm focal length would allow a very wide range of possibilities of resolution vs. field of view over a wide range of altitudes. At 2.5 km above the surface this system would allow changes in resolution between 100 cm and approximately 25 cm with covered areas ranging between 0.25 km^2 and greater than 1 km^2. These figures are assuming the same photo detector as above, that is 1024^2 pixels in a square array spaced 40 μm, center to center. This type of system is flexible enough to cover all of the proposed landing sites defined in Section 2.2. By mounting the camera and lenses inside the payload and using a periscope type system one camera could be used to take downward pictures while the balloon rover is hanging from the balloon and the same camera could take pictures after the payload has landed. Or, two cameras could be used, one for aerial photographs, mounted in the bottom of the payload, and another, mounted in the top of the payload, to be used after the payload had landed. The aerial camera is jettisoned just prior to landing.

To obtain color photographs requires photographing the same area with different color filters and then combining the composite picture into a color photograph. This requirement increases the complexity of the camera system. The incoming image is split up by prisms and directed through three filters and onto three separate photo detectors. When the information from the three photo detectors is recombined, the resulting photograph is in color. The information obtained by the use of color imaging makes this option worth considering as part of the payload.

Since the balloon will only be able to transmit pictures while the orbiter is overhead, the acquisition of pictures during darkness is also an important consideration. The use of infrared-sensitive photo detectors allows more efficient use of available transmission time.

Because infrared and visible wavelength sensing covers the requirement of obtaining high resolution photographs of the surface of Mars, ultraviolet sensing was not considered in this study, but may be an area for further study.

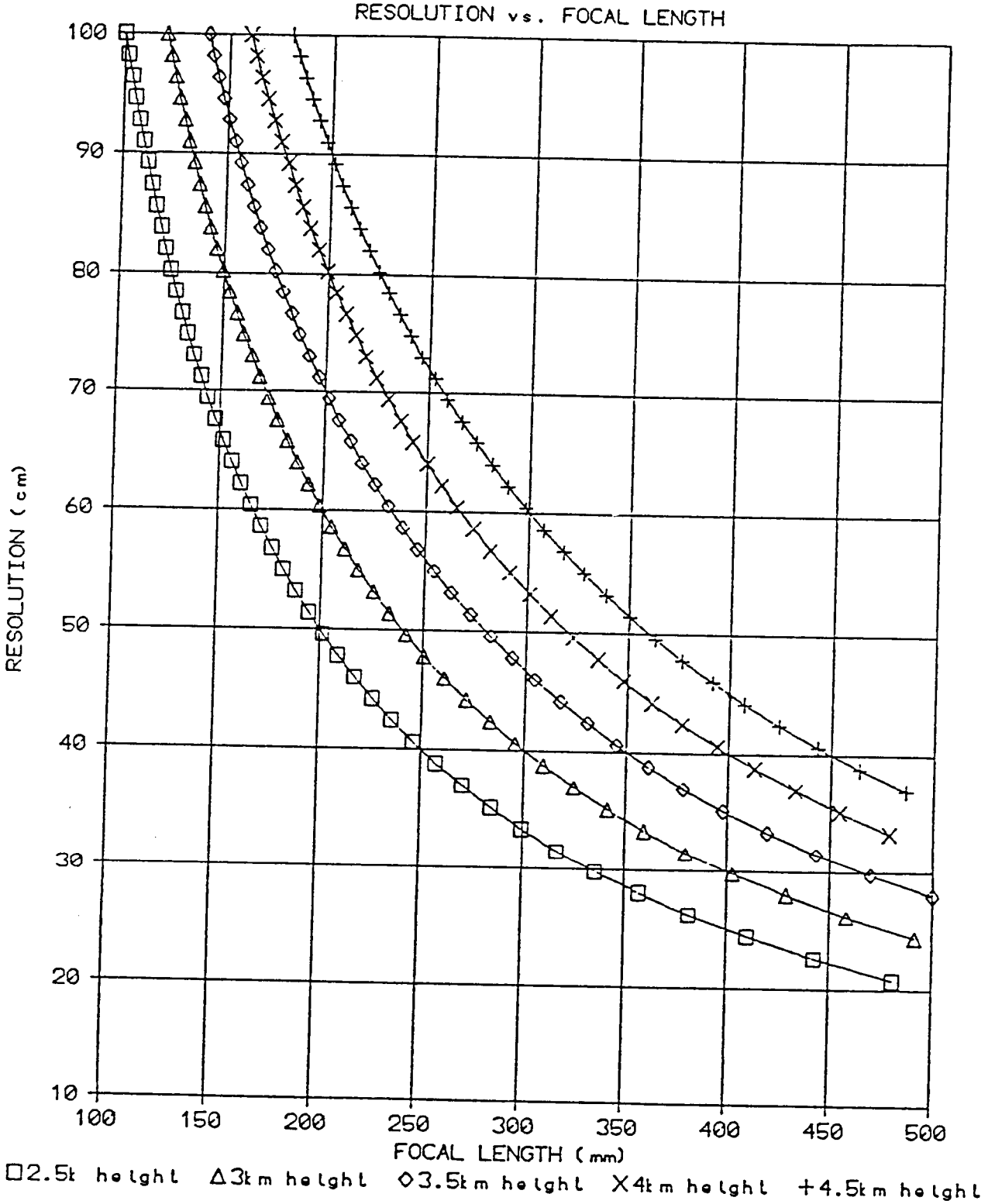
RESOLUTION vs. FOCAL LENGTH
RESOLUTION (cm)
100
90
80
70
60
50
40
30
20
10
100
150
200
250
300
350
400
450
500
FOCAL LENGTH (mm)
□2.5km height
Δ3km height
◇3.5km height
X4km height
+4.5km height

Figure 5.2

5.2 Communications Requirements

The main objective of this study as far as the communications are concerned is to determine some of the basic requirements and to make preliminary suggestions for the communication system.

The considerations of the communications systems are as follows:

1) Transmission speed

2) Power requirements

3) Mass

4) Physical size

5) Tracking

Since space and power are at a premium on the balloon rover, the orbiter will be used as a relay link in sending data back to earth. This reduces the amount of power required to send data and it also allows the use of a smaller antenna on the balloon payload.

Transmission speed is critical because of the bandwidth required to transmit video pictures. One effect of high frequencies is that it allows the use of smaller antennas. High frequency waves are, however, attenuated by water vapor. The lack of water vapor in the atmosphere of Mars is another factor in favor of high frequency usage. By using frequencies in the range of 30GHz the balloon rover will be able to transmit high resolution video images using a small antenna, probably in the form of a microstrip array. This could be integrated into the top of the payload.

Because the orbiter will be moving overhead in relation to the balloon and the balloon itself has no guidance system, telemetry between the balloon and the orbiter is a problem which must be considered. One possible solution to this problem is to use a tracking system which tracks the orbiter while overhead and then guides the transmission beam toward the orbiter. Guidance can be either mechanical, by physically pointing the antenna towards the orbiter, or electronic by using phased arrays which can be directed electronically without physically moving the antenna. The advantage of a guided system is that with a narrow directed beam the gain is much higher and thus the power requirements are lower. Another solution to this problem is to use a lower gain, wide beam antenna which would not require tracking of the orbiter. This has the benefit of simplicity but the increased power consumption may outweigh this advantage. The orbiter could send out a periodic signal and when the balloon received this signal it would begin to transmit data. It would continue to transmit until it lost the signal from the orbiter, waiting until the next overhead pass. By using the signal sent from the orbiter as a beacon, the balloon transmitter could direct the radio beam toward the orbiter. Data from the rest of the scientific payload (other than imaging) could be stored while the orbiter was not in range and transmitted as soon as it came back within range. Either the high gain, narrow beam antenna or the low gain, wide beam radiation pattern could be implemented with a microstrip array antenna. Another possible antenna configuration considered was a phased array antenna suspended below the

payload. This configuration would have a physical advantage in that it would have a tendency to damp oscillations of the balloon rover system. This stabilizing effect could be very helpful in quickly shifting winds. Unfortunately, this antenna would be very vulnerable to collission and would be useless once the payload landed. a parabolic dish type antenna was also considered, but the microstrip array presents significant mass and volume advantages.

The possibility of interference from the balloon itself was also considered. This would be an important consideration if the balloon material was such as would affect the signal. This could greatly reduce the time during which the balloon rover and orbiter could communicate. One possible solution is to direct the beam at an angle which would miss the balloon above (See Figure 5.3). The hanging phased array design would lend itself very well to this configuration. Although the communication time would still be reduced, the gain could be increased on the antenna because of the small angle, while the power requirements would remain about the same. In this case also, the microstrip antenna could be designed to produce the necessary transmission pattern and, though it would not have the stabilizing effect of the hanging phased array antenna, it would still be functional after the payload has landed. Although balloon interference was considered, it was decided that the balloon material would probably not interfere. Even so, it is a consideration which must be kept in mind as the balloon material is chosen.

The main purpose of this study was to decide which type of antenna system seems best suited to the balloon rover. Because the microstrip array type antenna is suitable for all the needed applications of the rover, it is the design which should be investigated further. A more in-depth study of the actual power requirements, the frequencies used and the resulting antenna design needed to fill these requirements is in order but is outside of the scope of this preliminary design.

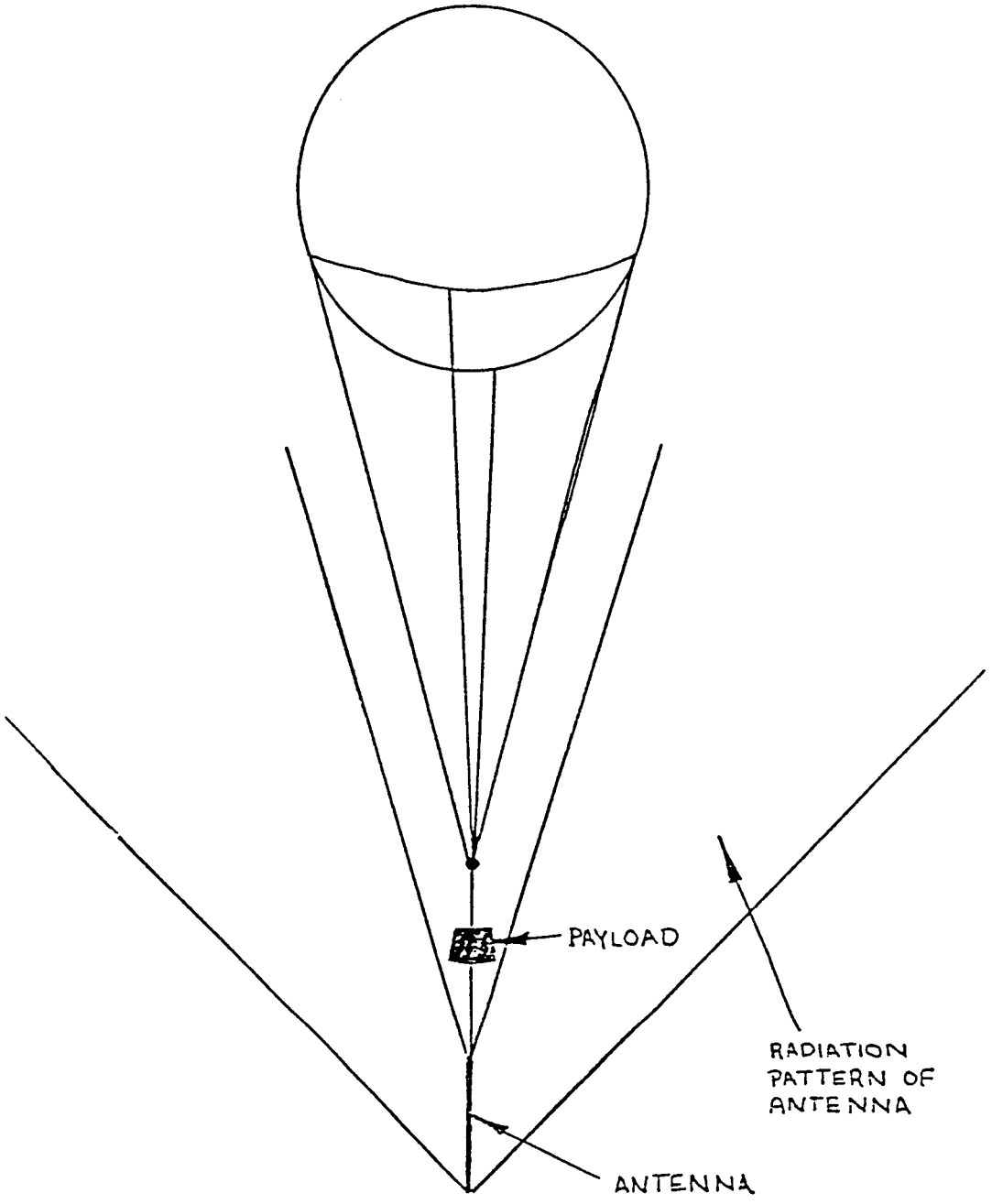

Figure 5.3

REFERENCES

Gruenberg, Elliot L., Handbook of Telemetry & Remote Control, McGraw-Hill Book Company.

Driscoll, Walter G., Editor, Handbook of Optics, McGraw-Hill Book Co., 1978, pp. 2-56, 2-57.

Tsipis, Costa, "Arms Control Pacts Can be Verified," Discover Magazine, April 1987, p. 87.

Rudge, A.W., Milne, K., Olver, A.D., Knight, P., The Handbook of Antenna Design, Peter Peregrinus Ltd., 1982.

Stutzman, Warren L., Thiele, Gary A., Antenna Theory and Design, John Wiley & Sons, Inc., 1981.

Pozar, David Ph.D., Antenna Design Using Personal Computers, Artech House, Inc., 1985.

6.0 Payload Power Supply -- Marie-Paule Cellier

Considering the power needed by the payload operations, and the fact that it is desirable that this instrumentation work 24 hours a day, a power source is needed that is able to supply a continuous 85 W of power (nominal payload power requirement). A priori, two solutions come to mind:

1. Solar panels

2. Radioisotope thermoelectric generator (RTG)

6.1 Solar Panels

6.1.1 Solar Cells

The design of a solar panel depends mainly upon the selection of solar cells and the arrangement of those cells into arrays. First, considering that the solar flux is predominantly blue and ultraviolet, we should choose photovoltaic cells especially sensitive to this part of the spectrum. The optimum response occurs when $h\nu = Eg$ (energy gap). Options presently available, or expected in the near future, include conventional silicon (typical efficiency: 10.6%), violet cells with a Ta-205 coating (efficiency: 14.5%), black cells (efficiency: 15.5%), and gallium arsenide (GaAs) cells, which are relatively efficient (21%) but expensive.

Next, we must take into account the possible damaging effects of ionization and atomic displacement which resulted in a degradation of 15% in the Viking Orbiter solar array power output (ultraviolet, proton, and neutron damage). On Mars, solar flares are of greater concern than on the earth due to the thinner Martian atmosphere. The weakness of the magnetic field around Mars reduces the potential for damage due to trapped electrons (this causes the auroral activity at the Earth's poles), but it does not screen out much cosmic radiation. Solar cell thickness is important in the prevention of long-wavelength absorption. Thin cells (< 0.3 mm) will reject wavelengths > 0.6 μm. The effects of temperature are important, as is, therefore infrared absorption, because of variations in both short-circuit current and open-ciruit voltage. Finally, the angle of incidence of the solar flux upon the cells must be considered as it can have a large impact on cell performance.

The radiation environment existent on Mars requires protection of the photovoltaic cells. Intense ultraviolet radiation quickly darkens most transparent glasses and all transparent plastics. Thus, filters are often incorporated into the covers, which are cemented directly to the cells. The selected cover is glass doped with Ceria, which prevents clouding of the glass during UV and charged particulate radiation.

Considering these criteria, GaAs cells appear to be the best-suited to our application. Allowing for proton degradation, the worst case with GaAs is still better than the best silicon cell case.

6.1.2 Solar Arrays

A solar array is a network of cells connected in series to provide the desired voltage and in parallel to provide the desired current. The resulting mass of the solar array, less supporting and connecting structures, is 9.89 kg/m^2. Assuming a lightweight support structure, thus creating a best case, the solar array system is assumed to have an area density of 10 kg/m^2.

Two types of photovoltaic collectors could be used: flat plate, and concentrator systems. However, the efficiency of solar collectors is directly related to the solar inclination with respect to the array surface. Even if the balloon rover stays perpendicular to the surface of Mars, a tracking system will be necessary in order to follow the sun. The problem with such a control system is that it requires additional mass and complexity. Moreover, any torque applied to the payload will cause it to spin. Solar concentrators alleviate this problem to some extent through the use of optical devices which increase the intensity of solar flux on a smaller number of cells. Present-day passive designs of this type allow misalignment errors of up to 1 degree with less than 5% loss in performance. They employ either a reflective cone or a conical glass lens.

As described in Section 2.0 of this report, five landing sites were selected. Considering the solar flux on the atmosphere of Mars as 36% to 52% of that incident upon the atmosphere of the earth, with 20% of that being reflected back into space, the available solar energy at the surface ranges from 392 W/m^2 to 566 W/m^2. This quantity varies with the cosine of latitude, requiring separate analysis of each landing site. The latitudes of these sites vary from 14° South to 70° North, where there may be periods of total darkness for several weeks. This drawback was a major factor in the selection of the final power system.

6.1.3 Batteries

In order to provide power in times of no sunlight, a solar energy system requires rechargeable batteries. At present, four types of batteries are popular for use in spacecraft:

1. Silver-Zinc (Ag-Zn) 110 to 132 W-h/kg; low cycle life
2. Nickel-Cadmium (Ni-Cad) 22 to 26 W-h/kg; components suffer from aging and temperature degradation
3. Nickel-Hydrogen (Ni-H_2) 40 to 50 W-h/kg
4. Lithium ($LiTiS_2$) 120 to 145 W-h/kg; high performance, but unstable and potentially explosive

Recent research at JPL, among other places, has yielded promising data concerning lithium batteries. Based on these advances and forecasted improvements in lithium battery technology, it was decided that these would be baselined for use in the design solar energy system, for purposes of comparison with the alternative power supply, the RTG.

6.1.4 Array Placement

Assuming that the balloon is a sphere of 38 m diameter, and the payload is a cube 0.5 m on a side, two possible configurations were investigated:

1. On the sides of the payload canister

2. On top of the balloon

If the solar array(s) is placed on the side(s) of the payload, it has the advantages of relatively simple deployment and proximity to the payload. Several disadvantages exist for this configuration, though. Especially in light of it's size, the balloon's shadow may cause significant reductions in power production. This could be partially remedied by increasing the tether length. However, as is presented in Appendix 6, to have much effect, this would require an absurdly long, and consequently, heavy tether. Further, when the sun is overhead, the array will be completely in shadow, regardless of the tether length.

Placing the solar cells on top of the balloon eliminates the problem of shadowing, but sun angle will still affect the power production, especially when the sun is low in the sky. This possibility was not explored extensively due to the inherent problems involved in the deployment of an ultra-thin-fabric balloon with such relatively massive objects on top of it (or on it's sides for that matter). This arrangement would also be prone to inducing fabric failure near the solar cells due to stress concentration.

A final point which represents a major drawback for a solar-powered system, regardless of design and configuration is that, during the frigid Martian nights, solar panels provide no means for heating the payload components, other than electrical resistance heating which would greatly increase the array and battery sizing requirements.

6.1.5 Solar Array/Battery System Summary

To meet the power requirement of 85 W using GaAs solar cells with $LiTiS_2$ batteries requires a system weight of at least 18.8 kg. Batteries (70% depth of discharge, 9 hours of darkness) represent 8.7 kg of this, with the balance being the solar array and support structure. This analysis assumes an average sun inclination angle of 40° and no tracking system. For purposes of comparison, this translates into an efficiency of 4.5 W/kg. This is a very optimistic best case for several reasons, not the least of which are that at high latitudes, during part of the year, there will be total darkness for a period of weeks, and that the balloon's own shadow significantly decreases the system efficiency. Balloon-top cells not only present deployment difficulties, but also are lost, along with the balloon, once the payload lands, leaving the system powerless; payload-mounted panels may also be seriously damaged upon landing.

6.2 Radioisotope Thermoelectric Generator

A radioisotope thermoelectric generator (RTG) was also investigated as a potential power supply for the balloon rover payload. Devices of this type have been used quite successfully in the Viking missions, as well as several

Options:

1)

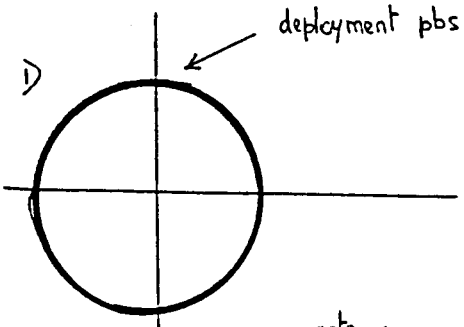

deployment pbs

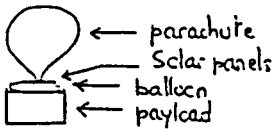

2)

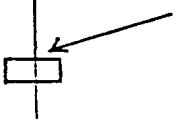

antenna.
the solar panels can't be on the top of the payload.

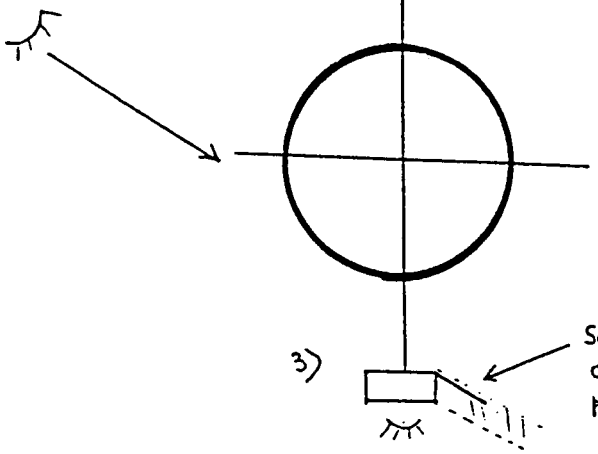

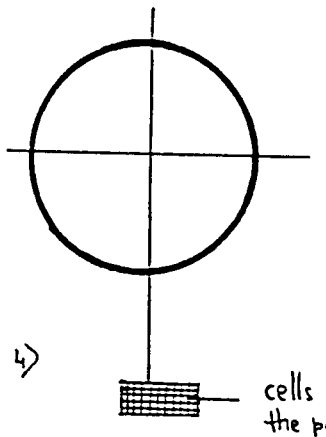

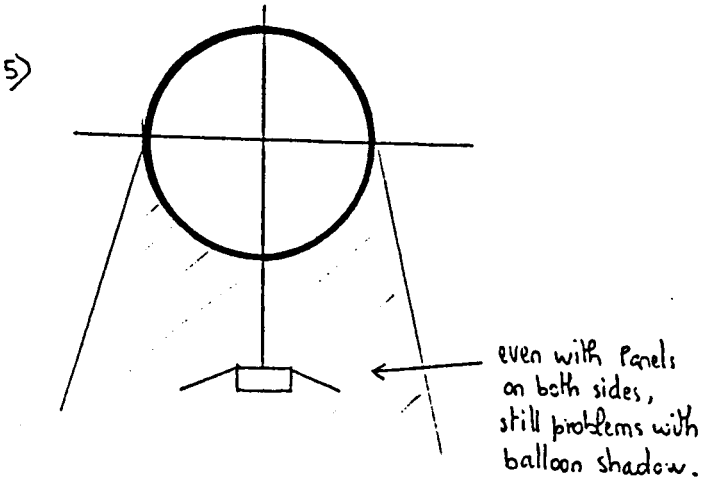

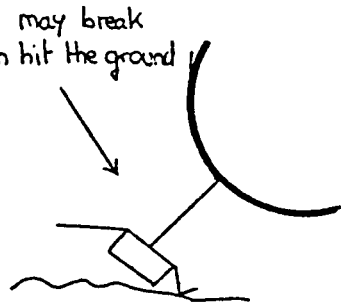

other interplanetary spacecraft. A major advantage of RTG's is that in addition to providing electrical energy to the payload, thermal energy is also available to maintain acceptable operating temperatures for the payload instruments in the often-icy Martian environment. Another advantage to an RTG system is continuity of power. RTG's produce relatively constant power over the course of their useful lifetime (which may exceed 2 years), unlike the cyclical power profile of solar arrays. This introduces a major mass savings as batteries are unnecessary. The predominant disadvantage associated with RTG's is the radiation hazard. Extensive experience with these sytems, however, demonstrates that this need not be a controlling consideration.

6.3 Conclusion

Comparing solar array/battery and RTG systems on a mass efficiency basis, the following chart was produced.

System	Efficiency (W/kg)	
Solar Array	18.84	(70% depth of discharge)
Solar Array	16.89	(90% depth of discharge)
RTG	17.36	

Here we see that the system efficiencies are comparable, but, even with relatively high solar cell efficiencies (> 25%), the problems of configuration and payload thermal control remain. Additionally, in order for the balloon rover to perform a long-term secondary mission once landed, it must have a reliable power source. RTG's have proven to be well-suited to such applications, and would be capable of withstanding landing loads with far less damage than is probable with solar cells. Consequently, the power supply selected for the balloon rover is an RTG-based system.

REFERENCES

Agraval, Brij, "Design of Geosynchronous Spacecraft," Prentice-Hall.

Corliss, W. R., "The Viking Mission to Mars," NASA-SP334, Scientific and Technical Information Office, NASA, Washington, D.C., 1974.

Electronics and Power, "Batteries for Memory Protection," February 1986.

Gabano, J. P., Lithium Batteries, Academic Press.

Green, Martin A., Solar Cells, Prentice-Hall.

General Electric Nickel Cadmium Batteries Catalog

Klein, G., Planetary Spacecraft Systems Technology, Final Report 1986, Jet Propulsion Laboratory, October 30, 1986.

Meinel, Applied Solar Energy, Addison-Wesley.

NASA Contractor Reports 3361 - 3148

NASA Tech Briefs, October 1986, January 1987, March 1987.

Neville, Richard C., Solar Cells, Elsevier.

Research and Development, "MOCVD Research Produces Solar Cell Efficiency Record," February 1986.

7.0 Balloon Rover Payload -- Oscar Monje & Perry Voyer

7.1 Mission Objectives

The scientific mission of the USU/MLR is centered around the task of obtaining a detailed characterization of Mars. The overall scenario consists of deorbiting five separate, 1000 kg Lander/Rover modules at different sites(see Section 2.2). Each Lander/Rover will contain three different subsystems: a sample acquisition rover (SAR); a mothership lander with a soil sample analysis laboratory, meteorological sensors, imaging, and communications systems; and a balloon rover (BR).

The purpose of this section is to develop the scientific payload of the balloon rover, keeping in mind that this subsystem vehicle has been allotted 40% of the total module mass (400kg -modified from Winter Quarter). Due to the extremely thin Martian atmosphere, it is prudent, from the standpoint of balloon size, to design the subsystem to cruise at an altitude low enough to provide reasonable lift yet high enough to avoid surface obstacles. The need to accommodate the large mass of the balloon fabric, tethering, and support structures, places a substantial limitation on the scientific payload mass. The function of the balloon rover is the characterization of the lower Martian atmosphere and high-resolution aerial photography of the planet's surface. Completion of these tasks is sufficient justification for the mass expenditure associated with the balloon rovers.

The design problems encountered were solved by using technology extrapolated to the 1990's. The scientific instruments described below can be thought of as modular components whose arrangement can be tailored to suit different scientific missions. Thus, the overall arrangement of scientific components can be varied so as to allow the exploration of different Martian sites.

7.1.2 Scientific Objectives

The information gathered by such a balloon rover subsystem can be used to accomplish the following objectives:

1) Characterize the terrain morphology and climate of various candidate sites to be considered for the establishment of a Martian base.

2) Provide high-resolution aerial photographs of large regions of the planet, thus allowing the delineation of hazard free paths to be followed by large surface semi-autonomous rovers (i.e., a Mars sample return mission).

3) Measure seasonal climatic and seismic information at sites where the balloon rover lands, so that climatological and geological models can be developed.

4) Determine the composition and structure of the lower atmosphere of Mars so as to allow the development of empirical atmospheric models.

7.1.3 Scientific Instrumentation

The previously mentioned mission requirements can be met by selecting the appropriate instrument for site-specific studies from the following instrumentation:

1) Meteorology Devices:
Various transducers (i.e., temperature, pressure, density, wind speed and direction, and solar flux sensors) can be arranged with a data acquisition/relay system to characterize the local environment in flight and at the balloon landing site.

2) Atmospheric Composition:
The inclusion of an atmospheric mass spectrometer and various volatile detectors (i.e., water or CO_2) in the scientific payload permits the monitoring of seasonal variations in general and/or specific atmospheric components. Furthermore, a cross-section of the lower atmosphere can be studied during the aerial mission of the balloon rover.

3) Aerial/Ground Photography:
High-resolution, stereoscopic, multi-spectral cameras are recommended for a number of reasons. First, an airborne imaging payload permits the acquisition of photographs of the planet surface and of major geologic features over which the balloon flies. Second, a ground-based camera fixture allows the relay of 3-dimensional images chronicling soil and frost deposition in the immediate vicinity of the payload landing site.

4) Communication Devices:
The need to relay large amounts of data to Earth demands a communication network capable of sustaining high data transmission rates. These requirements also demand pre-transmission data analysis and compression. The antenna to be used aboard the balloon rover is a micro-strip phased array antenna. These lightweight devices consume little power, operate at high transmission rates, and do not require mechanical pointing or tracking devices(see also Section 5.2).

5) Radar Altimeter and Rotation Sensor:
This package allows determination of the BR position with respect to altitude and true North. Combined with aerial images and atmospheric data, this information is essential in constructing lower atmosphere composition profiles and surface maps.

6) Seismic Devices:
A seismometer can be included in the payload to record seismic events. These could be created by seismic thumpers ejected near the balloon landing site prior to landing.

7.2 Operations

7.2.1 Aerial Mission

The balloon rover, having no intrinsic guidance system, travels in a random fashion. The distance the balloon is expected to travel is based upon the average wind velocities and directions at the cruising altitude: 400-500 km/day. The flight duration depends upon balloon gas diffusion and environmental hazards such as airborne particles and balloon fabric degradation by UV radiation. The duration of the flight has been estimated to be 5 -7 days based on balloon fabric characteristics(see Section 3.0). The flight time will be dedicated to atmosphere composition characterization and high resolution imaging of the planet's surface.

7.2.1.1 Atmospheric Composition and Structure

The purpose of the atmospheric analysis is to identify the composition of the Martian atmosphere and to determine constituent abundance. The composition of the atmosphere is studied by sampling the Martian air at intervals, and analyzing these samples with a mass spectrometer and/or volatile detectors. The position at which each sample is taken is referenced by the use of a fiber optic rotation sensor (FORS) and a radar altimeter. In this fashion, atmospheric data can be correlated with planetary location. Measurement of wind speed and direction is a complex measurement while in flight, and is mainly investigated during the landed balloon rover mission.

7.2.1.2 Aerial Photography

The aerial photography mission is baselined as using lightweight CCD cameras on a stereoscopic mount, allowing reconstruction of 3-dimensional images. Various camera arrangements are discussed in Section 7.4.4. These arrangements involve trade-offs between camera simplicity and pointing ability during flight. Although it is desirable to be able to control the direction in which the cameras point (assuming a random flight pattern), motion of the cameras during flight introduces prohibitive complexity.

Depending on the balloon rover's ability to uplink data to the orbiter, the airborne imaging can proceed continuously for the duration of the mission. The image information may be processed prior to transmission (data compression) by computers in the payload. For further information concerning the requirements of the imaging and communications systems see Section 5.0 of this report.

7.2.3 Landed Mission

Since the payload will eventually land, a pressure bladder/shell landing system was incorporated into the balloon payload in order to allow the payload to survive the landing. (See pressure bladder development in Winter Interim Report, Appendices 4.1-4.4.) Once landed, the balloon is disconnected from the payload and the system becomes a stationary meteorological and imaging platform. A survivable balloon landing can be insured by the use of controlled

descent mechanisms in the balloon fabric which will cause a gradual drop in altitude (see Section 3.0). The landed payload will still be capable of measuring meteorological data such as pressure, air temperature, wind speed and velocity, and water content at the balloon landing site, as well as imaging. The location of this landing site cannot be predicted because the balloon flies at the mercy of the wind currents. Therefore, this will be a random site on the planet.

The meteorological instruments will characterize the environment near the surface, and provide atmospheric dynamics data on timescales ranging from seconds to several months. The seismology mission will obtain information pertaining to the structure, composition and dynamics of the interior of the planet. The amplitude and source of seismic activity can be determined, as well as information on the level, location, and nature of tectonic activity on Mars. A seismic study of the site can be carried out by deploying a battery powered siesmic thumper during the descent phase of the balloon, and then monitoring the ground vibrations with a seismometer contained within the payload.

The duration of the landed mission can be quite long because the RTG power source has a long lifetime(~2 years). Thus, seismic and meteorological data, as well as ground photographs of the site can be transmitted for several years.

7.3 Instrument Arrangement Considerations

There are several general constraints imposed by the position of various instruments:

1) Temperature sensors should be shaded so as to keep the sensor in thermal balance with the atmosphere, not radiative balance.

2) The altimeter should be positioned where it is always facing the ground (i.e., on the bottom of the structure).

3) Air intakes should be provided for the atmospheric mass spectrometer, volatile detectors and pressure sensors.

4) The RTG and other heavy instruments should be arranged in a fashion conducive to stable landing dynamics.

5) Solar panels and antennas should be positioned for protection and to optimize operation.

6) A gimbal system should be used to tether the balloon to the payload so as to avoid tangling or spinning.

7) The cameras should be placed so as to function both during flight and when grounded.

8) Temperature-sensitive instrumentation must be insulated from the RTG and from the Martian weather extremes. Thus, a major design consideration should be payload thermal control.

7.4 Balloon Payload Instrumentation Configurations

The scientific payload will have a mass of 62 kg, occupying a cylindrical payload canister assembly 0.75 meter tall and 0.75 meter in diameter. The canister and its lander shell will be made of composite materials in order to reduce the system mass. Placement of the various instruments within the payload canister must be done with care in order to accommodate the various requirements of the individual instruments. Air intake and outlet lines must be placed so that atmospheric samples are not contaminated by sample outlet ports. A breakdown of the balloon rover system mass is shown in Appendix 7.1, along with possible camera arrangements.

The microstrip phased array antenna and the meteorological transducers are placed on the surface of the canister for easy access to the atmosphere. The flight camera, located on the bottom of the payload in the center, is deployed once the balloon is filled and the hydrogen tank has been detached. Before landing, it will be jettisoned. At all times this camera is positioned such that it does not significantly alter the position of the center of mass. The ground camera will be deployed after landing. It will be capable of taking photographs of the surface in all directions. The altimeter will be sacrificed upon landing as it is, obviously, no longer necessary. See Figure 7.1.

Instrument sizes were extrapolated to the 1990's. They were assumed to be rectangular or cylindrical solids for purposes of positioning. The wiring and mechanical linkages were not included in the payload configuration drawings, although there is plenty of room for their inclusion. For a list of instrument sizes see Figure 7.2. We decided to use the payload configuration shown in Figure 7.3. It is small, meets our mass budget, and allows enough room for instrument manipulation and inclusion. It also lends itself well to temperature control because of the selected power source, which is discussed presently.

7.4.2 Radioisotope Thermoelectric Generator Insulation

The radioisotope thermoelectric generator (RTG) produces a significant amount of heat as a byproduct of electrical power generation. Two insulation configurations were considered. The first one consists an RTG with radial fins attached to its central core. These fins extend out of the canister and act as radiators. The second configuration considered has no fins, but instead, 5 cm of insulation around the RTG. Six insulated thermal shunts extract the heat from the top of the RTG core. A heat exhaust plate (radiator) is then used to dump this excess heat out of the payload(see Figure 7.3). In order to maintain a constant internal temperature, an active thermal control system is necessary (see Section 8.1).

7.4.3 Tethering

Three arrangements for tethering the payload to the balloon were considered. Balloon and payload motion can produce rotational and pendular oscillations in the system. These oscillations must be minimized for proper camera and instrument operation. Entanglement of the tethering lines was also investigated as a possible complication.

PAYLOAD CONFIGURATIONS

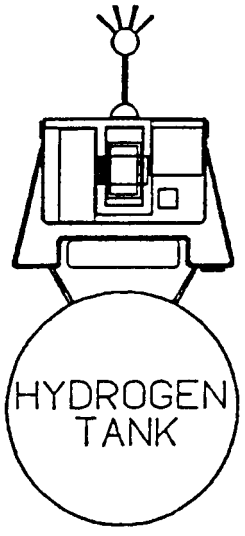

DESCENT

IN
FLIGHT

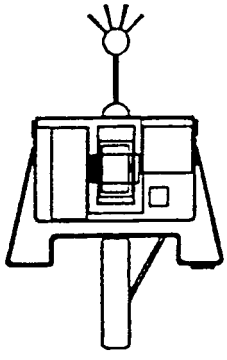

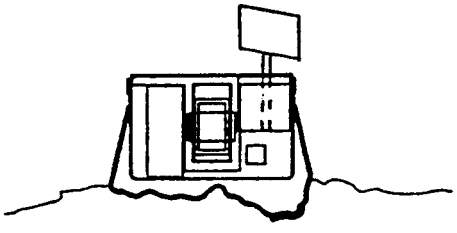

ON
MARTIAN
SURFACE

Figure 7.1

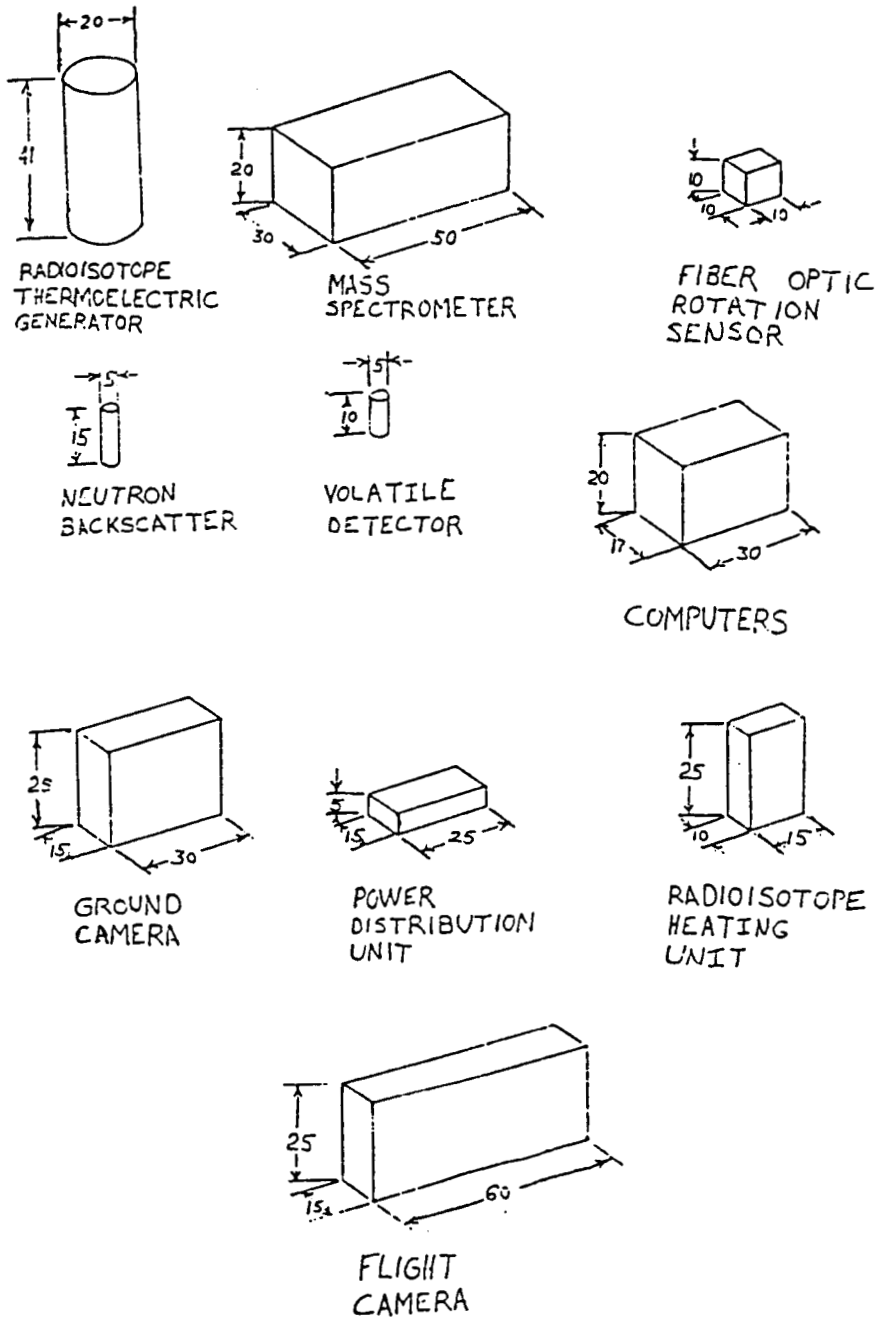

PAYLOAD INSTRUMENT SIZES

(ALL MEASUREMENTS IN CM)

Figure 7.2

PAYLOAD ASSEMBLY

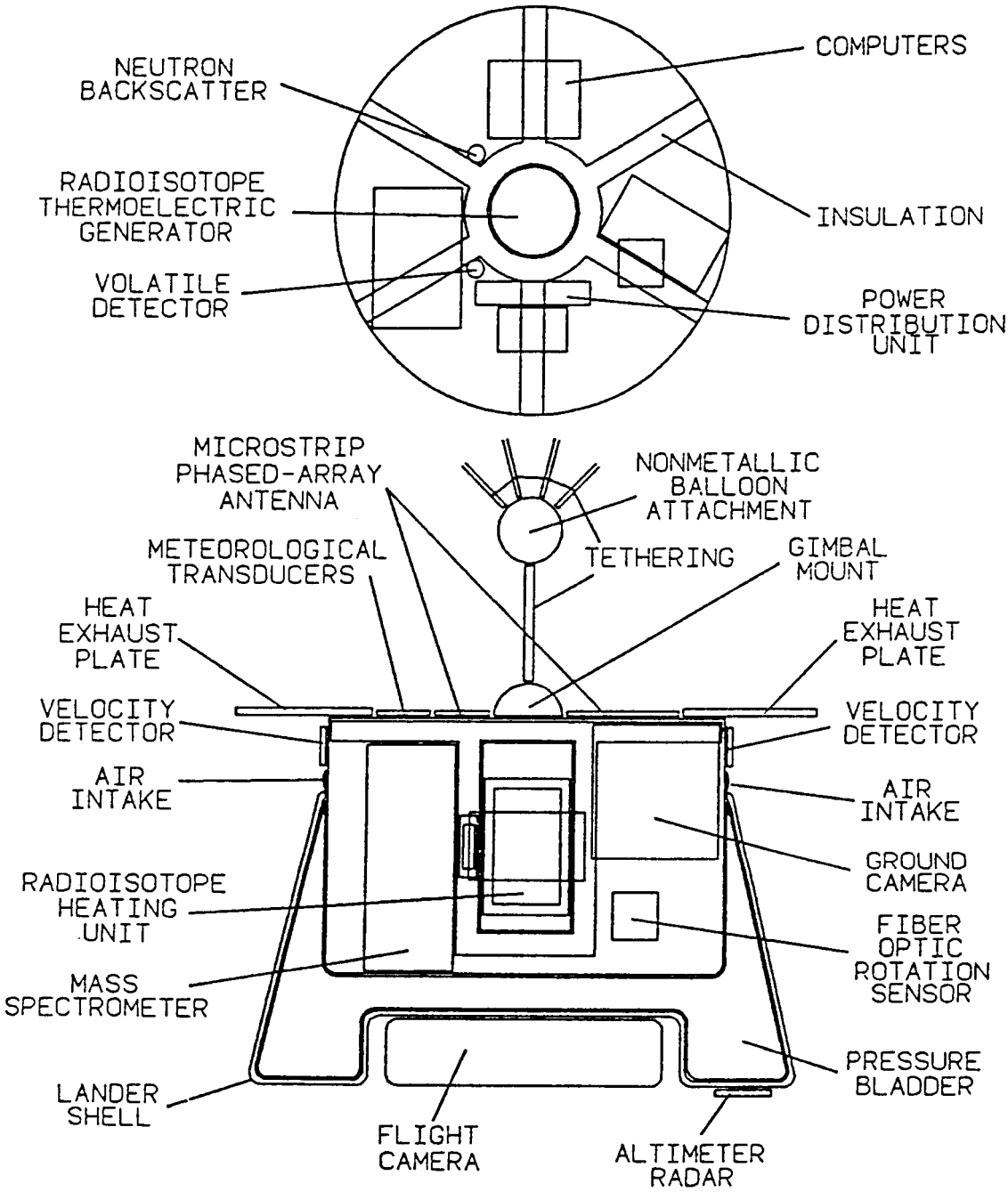

Figure 7.3

Because the microstrip phased array antenna is located on the top surface of the payload canister, all equipment above the payload must be nonmetallic, so as not to interfere with communications. The length of the tethering effects the oscillations. Short tether lengths could result in small pendular oscillations. The method of attachment, and tether length, can result in twisting of the tether lines.

In order to overcome these problems, several potential connection methods were examined, three of which are shown in Figure 7.4. Option 2 was chosen as the payload tethering arrangement. A composite rod is used, along with a composite gimbal attached to the payload canister. This prevents large payload motions without the antenna interference caused by metals devices. Details of this arrangement are shown in Figure 7.3, and derivations pertinent to this analysis are presented in Appendix 7.2.

7.4.4 Camera Arrangements

In order to meet the resolution specifications at a cruising altitude of 2.5 to 4.5 km, a focal length of up to 40 cm is required for the in-flight camera. The ground camera has a 10 cm focal length. These cameras require support electronics which add 20 cm to their length. Thus, the flight camera is 60 cm in length and the ground camera, 30 cm.

Three camera configurations were considered:

1) Active -This arrangement consists of two camera booms, each with a pair of cameras for stereoscopic imaging. This arrangement would provide the balloon rover with the ability to photograph in any direction. This option was discarded, however, because it is so mass intensive and because of the torques and oscillations which would be introduced by motion of the cameras.

2) Passive -This option consists of two pairs of cameras: one aerial and one for use on the ground. The aerial cameras would be fixed on the bottom of the balloon and take stereoscopic pictures of the terrain directly below the balloon rover's path. The ground camera pair remains stowed until the rover has landed. Note that the aerial camera pair is dropped prior to landing.

3) Periscope -This configuration uses a periscope device that brings the images to an internal camera through an optical system. This system was deemed too complex and demanding in terms of instrument survival.

All cameras employ CCD technology and zoom lenses to vary focal length. The spectral range includes visible to infrared so as to allow night-vision. These three options are depicted in Figure 7.5. It should be noted that each camera pair is a single unit; Option 1 has a total of four cameras in two units.

PAYLOAD TETHERING OPTIONS

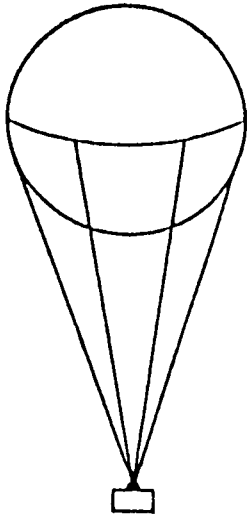

Option 1

Small Pendulum Oscillations
More Apt For Entanglement
Rigid Tethering

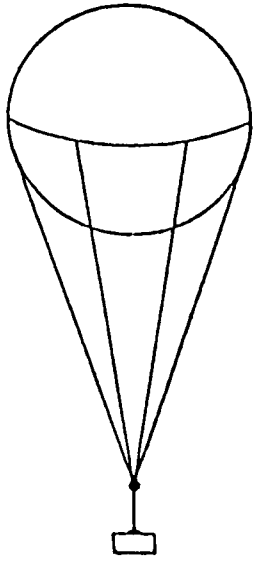

Option 2

Small Pendulum Oscillations
Gimbal Mountings
Independent Rotations

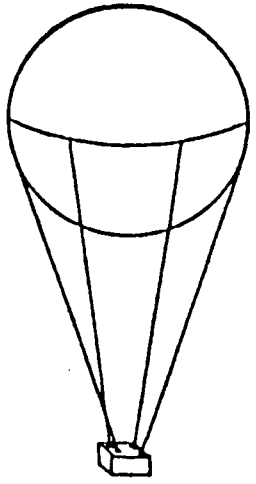

Option 3

Dependent Rotational Oscillations
More Surface Area for Tethering

Figure 7.4

CAMERA ARRANGEMENTS

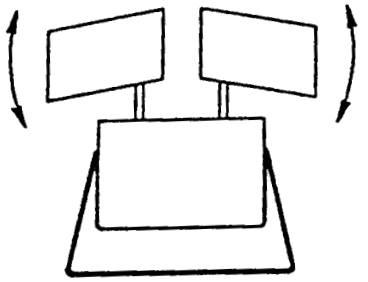

OPTION 1

60 CM CAMERA
LARGE ACTUATORS
TORQUE MOVEMENTS
ACTIVE SYSTEM

OPTION 2

30 CM GROUND CAMERA
60 CM FLIGHT CAMERA
FLIGHT CAMERA EJECTED
PASSIVE SYSTEM

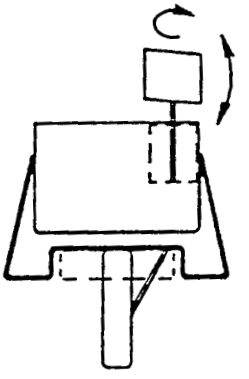

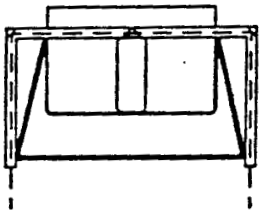

OPTION 3

ONE INTERNAL CAMERA
DUST FREE ENVIRONMENT
AIR TIGHT SEALS
NO REDUNDANCY
PASSIVE SYSTEM

Figure 7.5

From these considerations, Option 2 was chosen as the preferred camera arrangement. Reasons for this selection include simplicity of operation, lack of induced motion during flight, and compatibility with the remainder of the payload.

7.4.5 Balloon Payload Sizing

The following table shows a mass, power and volume breakdown of candidate balloon rover subsystems. The power estimates were based on peak power consumption (most instruments on at once) plus a 20 W safety margin. The mass estimates of the RTG unit were made using a projected 8W/kg power output to mass ratio. A detailed breakdown of payload power and mass requirements is presented in Appendix 7.1.

The balloon rover subsystems from Appendix 7.1 can be arranged and the masses added to give a mass budget for potential balloon rover configurations. Those shown below provide varying degrees of information about Mars. These configurations can be used to tailor payloads to specific mission needs at the selected sites or to develop a payload suitable for use at any of the sites, as was done here. We have chosen Option 4 as the balloon rover payload, noting that it satisfies the modified mass constraint of 400 kg. The resulting payload configuration is shown in Figures 7.1 and 7.3. (Appendices 7.1 and 7.2 provide additional background information).

Option #	Capabilities	Power (W)	Subsystem (kg)	Total Mass (kg)
Option 1	Imaging Power	85	45.4	99.4
Option 2	Imaging Meteorology Power	90	49.7	103.7
Option 3	Imaging Composition Power	105	57.7	111.7
Option 4	Imaging Meteorology Composition Power	110	62.0	116.0
Option 5	Imaging Meteorology Composition Power Seismometry	120	70.8	124.8

7.5 Conclusions

The balloon rover provides an efficient manner of characterizing the composition and structure of the lower Martian atmosphere while also providing high resolution (< 0.5 meter) aerial images of the Martian surface. It also provides a secondary meteorological station when landed. The resulting data would be important in planning future exploratory missions employing semi-autonomous surface rovers and, possibly, manned missions.

REFERENCES

NASA/JPL, "Viking-Mars: Anatomy of Success," Mission Status Bulletin, No. 46, October 31, 1978.

Corliss, W.R., "The Viking Mission to Mars," NASA-SP334, Scientific and Technical Information Office, NASA, Washington, D.C., 1974.

Blanchard, R.C. and G.D. Walberg, "Determination of the Hypersonic Continuum/Rarefied Flow Drag Coefficients of the Viking Lander Capsule I Aeroshell from Flight Data," NASA Technical Paper 1973, December, 1980.

Swanson, W.M., Fluid Mechanics, Holt, Reinhart, and Winston, New York, 1970.

JPL Report No. 715-23, Jet Propulsion Laboratory, Pasadena, California, 1980.

Carr, M.H., "The Surface of Mars," Yale University, 1980.

Baker, V.R., "The Channels of Mars," University of Texas, 1982.

8.0 Additional Considerations -- Jim Cantrell

These are some other areas of importance in the system development which impacted several parts of the payload, and thus warranted analysis. A summary of those investigations follows.

8.1 Payload Thermal Control

Often times, little attention is paid to the thermal control in designs of a preliminary nature. Such was the case in this design until we realized how much heat would be generated by the radioisotope thermoelectric generator (RTG) power system. This, combined with the small size of the payload and the negligible convective heat transfer in the Martian atmosphere, posed a non-trivial problem in the payload design. Normally, one might be tempted to think of the thermal control of a payload operating in a cold environment such as Mars (200 K) to be one of providing enough heat to the instruments to keep them operable. This is not the case with the selection of the RTG as the payload power source. There exists a large amount of waste heat due to inefficiencies in the power generation process. Left unchecked, this will overheat the payload, possibly causing critical failure. Two forms of heat transfer out of the payload considered were convection and radiation coupled with conduction. As mentioned above, due to the low density of the Martian atmosphere, free convection is negligible ($h = 0.25$; see Appendix 8.1). Thus, radiation heat transport is the main form of heat rejection. The general model for heat transport is shown below:

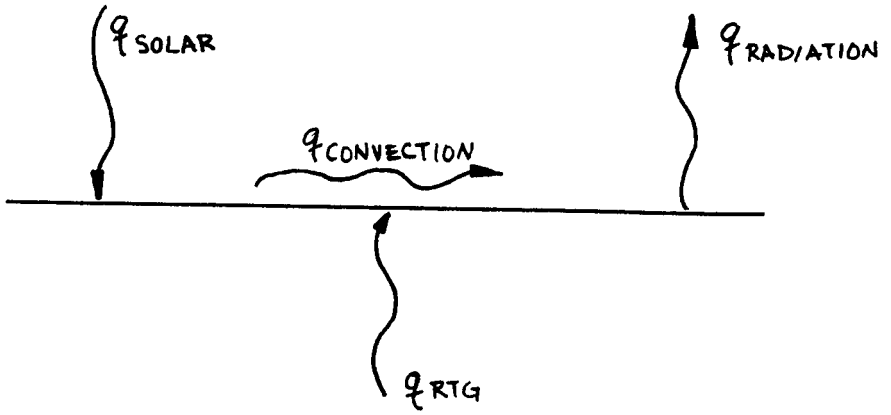

Here, a flat plate model is used with incident solar and background radiation balanced by outward radiation to deep space and convection off of the plate. Appendix 8.1 presents this model in detail. The general system configuration is shown in Figure 8.1. Aluminum conductors, which are insulated, carry heat from the RTG to an external radiation plate. Small amounts of heat flow out of the conductor lines via radiation and conduction within the payload, helping to balance heat flux through the walls of the payload. The conductor lines may also be "tapped" by an onboard control system to provide additional heat, if necessary, during night and in other cold conditions (i.e., polar regions) for the payload instruments.

The operating parameters are:

RTG heat flow	1000 W
RTG base temperature	171°C
Radiator operating temp. (daytime)	112°C
Radiator plate dimensions	1.25 m by 1 mm thick
Radiator plate area	0.91 m^2
Radiator plate emmissivity	0.8
Total radiator system mass (less RTG)	1.3 kg

(Equations and parameters are presented in Appendix 8.1)

It must be noted that this is a very preliminary study of the thermal control system and thus only offers one potential solution to the problem of excess RTG heat. Much more effort needs to devoted to this subject if a more in-depth design were to be contemplated.

8.2 Payload Tethering Structure

The balloon payload tethering structure was designed based on the need for overall low mass, wide load distribution over the balloon surface, and design simplicity. Mylar was chosen as the main tethering material because of its low density, high strength, flexibility, and general applicability in the operating environment. The design strength of the tethering system was based on a maximum loading equivalent to 2 Earth g's. The resulting configuration is shown in Figure 8.2. Thirty-two 50-mm wide Mylar straps support the payload and connect it to the cap on top of the balloon. The purpose of the cap is to distribute the load over the balloon and to protect the balloon envelope from UV radiation, which degrades the fabric strength. At the connection point between the payload and the tethering, a carbon-carbon composite gimbal and rod are employed in order to reduce payload oscillations and rotation (see Section 7.4.3: Payload Tethering). The overall system specifications are:

Maximum accel/deceleration:	19.62 m/s^2
Tether Straps	
Number	32
Dimensions	1 mil x 50 mm x 34.67 m
Material	Mylar
Total mass	1.5 kg
Tether Cap	
Dimensions	0.25 mil x 15 m x 38 m
Mass	20 kg
Tether Rod	
Dimensions	1 m x 2 mm dia.
Composition	Carbon-carbon laminate
Mass	1 kg

Further analysis is needed in order to fully evaluate the tethering system, such as implementation of a finite element model. This would greatly enhance understanding of the stresses in the balloon due to the tethering, which is a critical design consideration. Additionally, assessment of the dynamic stresses acting on the tethering and balloon fabric during both deployment and flight would be quite useful.

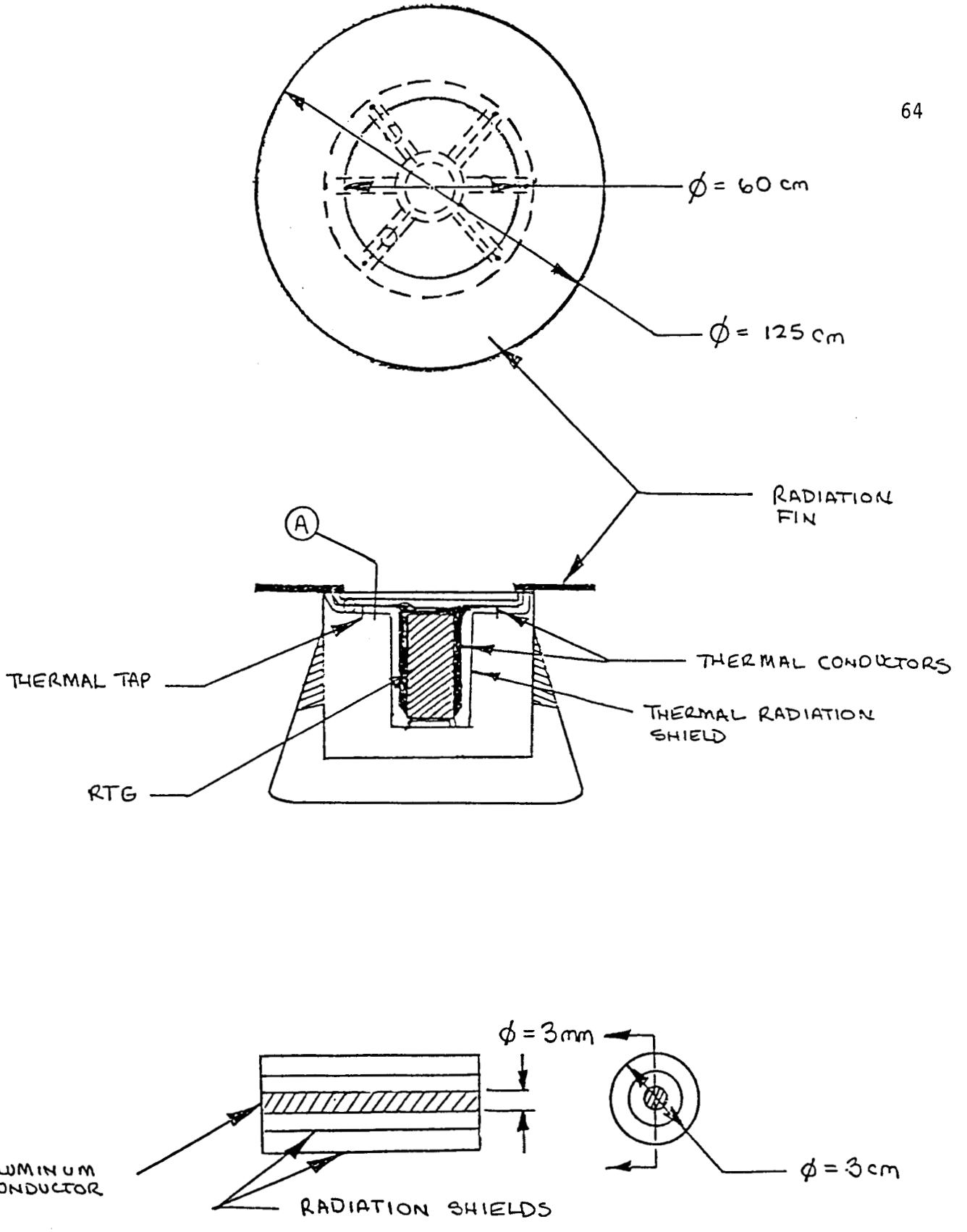

A. Thermal Conductor Cross Section

Figure 8.1 Thermal Control System

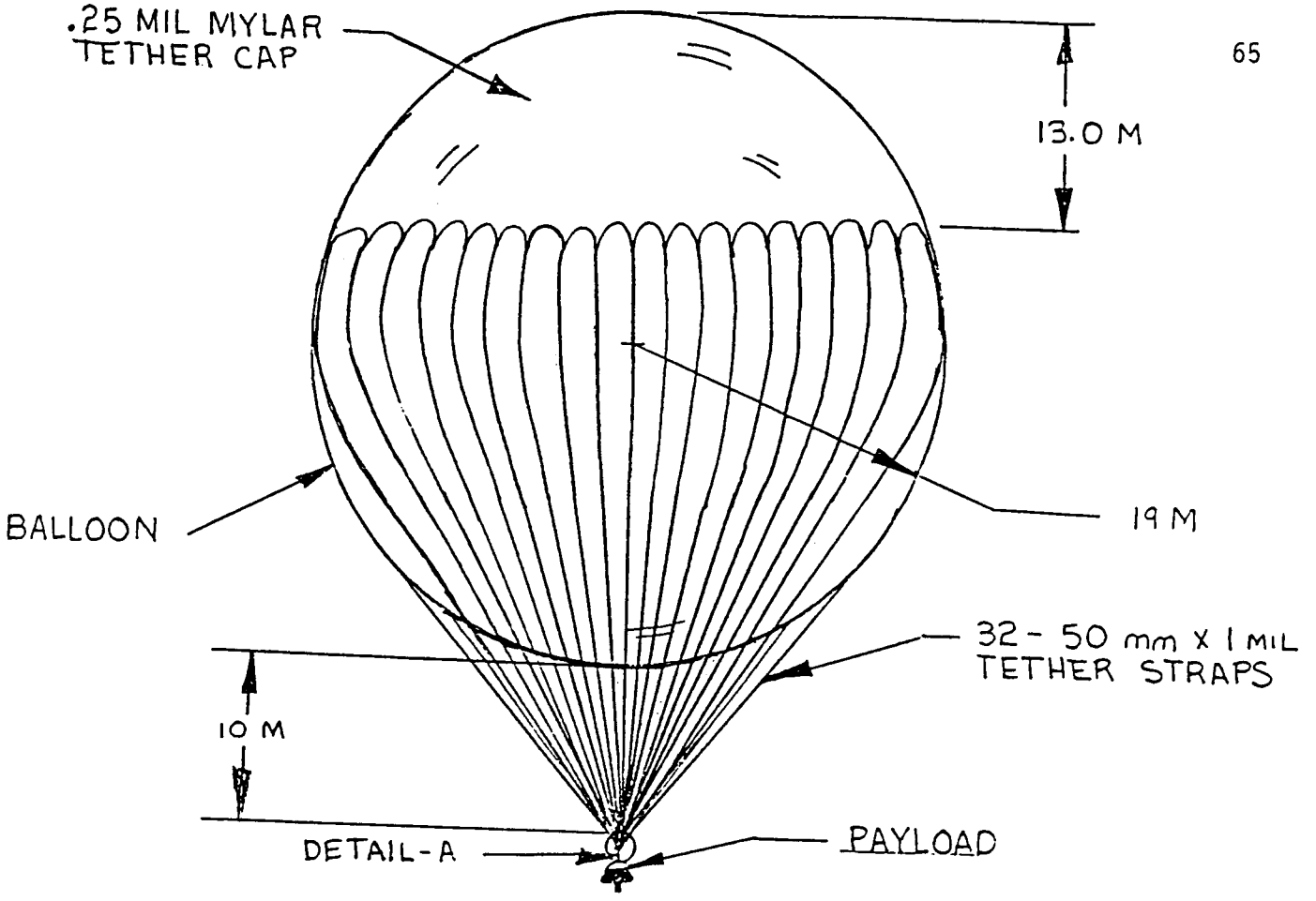

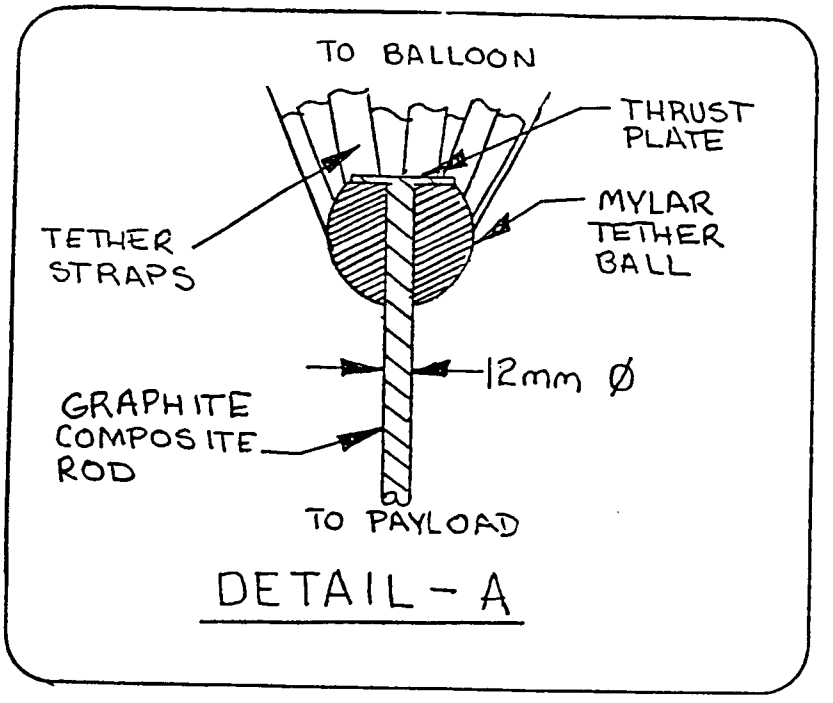

Figure 8.2 Payload Tethering System

9.0 Conclusions

During the Spring Quarter, the design of the Balloon Rover has changed in many ways. The process involved in this evolution has been quite illustrative of the way in which a project such as this would proceed in industry. This is a unique situation in the classroom and has proved to be very successful. The conclusions reached pertaining to various parts of this vehicle, while preliminary, represent significant progress in the development of such a rover. Especially in light of recent announcements by the Soviet Union, in relation to their plans to use balloon vehicles in the Martian atmosphere, we feel that our designs are well conceived, conservative and functional.

Together, the three reports generated during research on the Mars Lander/Rover project at Utah State University comprise a basis upon which future research efforts dealing with similar missions can be based. In this respect and many others, this course has been very effective and successful.

APPENDICES

Note: Appendix numbering corresponds to the referrant section. As such, the numbering appears discontinuous, but is employed for ease of reference to the appropriate sections within the report.

Appendix 3.1

Neutral Buoyancy Balloon Design Computer Program

```
**** TSO FOREGROUND HARDCOPY ****
DSNAME=STU222.FORTLIB.FORT                                    (BALI2    )
```



```
*
*
****** ************************************************************
*
*           BALLOON ANALYSIS PROGRAM FOR
*           MARS DESIGN PROJECT
*           BY DR. AL SAGEBRUSH
*           COPIED ON IBM BY GRANT WILLIAMS
*
*           MODIFIED ON 4/6/87 TO INCLUDE
*           VIKING ATMOSPHERIC DATA
*
****** ************************************************************
*
C         THIS PROGRAM CALCULATES THE LIFT FORCE FROM A BALLOON OF
C       VARYING RADII, IN TERMS OF THE ALLOWABLE PAYLOAD MASS, I.E.
C       HOW MUCH LIFT IS AVAILABLE AFTER ACCOUNTING FOR BALLOON FABRIC
C       MASS.  THE LIFT IS A FUNCTION OF THE BALLOON GAS CHOSEN, THE
C       GAS AND AMBIENT TEMPERATURES. THE AMBIENT PRESSURE. AND THE
C       CRUSING ALTITUDE CHOSEN, AS WELL AS THE BALLOON VOLUME.
*
****** **********************
*
      REAL MW, LIFT,DATAR(3,100),DATAPL(3,100),DATATL(3,100)
      INTEGER FLAG,CASE,NP(3),PLOT
      CHARACTER ANS*1, OUTPUT*8
*
100   FORMAT(' ',F4.1,5X,F6.0,5X,F6.0,5X,F6.0,5X,F6.1,5X,F5.3)
200   FORMAT(' ',F6.1,',',F6.1)
25    FORMAT('1',2(/),20X,10('*'),' BALLOON LIFT ANALYSIS ',10('*'),
     &       3(/))
30    FORMAT(' ','INPUT PARAMETERS: ',2(/))
35    FORMAT(' ',15X,'BALLOON MATERIAL DENSITY(KG/M**3):',4X,F6.1,(/),
     &           15X,' AMBIENT TEMPERATURE(K):',16X,F5.1,2(/),
     &           15X,' GAS TEMPERATURE(K):',20X,F5.1,(/),
     &           15X,' GAS MOLAR WEIGHT(G/MOLE):',14X,F5.1,(/),
     &           15X,' CRUSING ALTITUDE(KM):',18X,F5.1,2(/))
40    FORMAT(' ','BRAD',6X,'MFAB',6X,'MGAS',5X,'PL MAS',4X,'TOT MAS',
     &       4X,'RELPL',2(/))
45    FORMAT(' ',3(/),10X,10('*'),' NO LIFT AVAILABLE FOR PAYLOAD')
*
*
      WRITE(6,*)'ENTER THE NAME OF THE OUTPUT FILE (<=8 CHAR)'
      READ(5,'(A)') OUTPUT
*
      CALL CONECT(10,'STU222.'//OUTPUT//'2$','STA=UNK,CAR=YES$')
      OPEN(10)
      CALL CONECT(20,'STU222.BOUT$','STA=UNK,CAR=YES$')
      OPEN(20)
*
C     ENTER INPUT PARAMETERS
*
      CASE=1
99    WRITE(6,*)'ENTER THE BALLOON FABRIC DENSITY(G/M**2)'
      READ*, DENB
      WRITE(6,*)'ENTER MAX BALLOON RADIUS (M)'
      READ*, RMAX
      WRITE(6,*)'ENTER BALLOON PRESSURE DIFFERENTIAL'
```

```
      READ*, DP
      WRITE(6,*)'ENTER GAS TEMP.(K), MOLAR WGT'
      READ*, TB,MW
      WRITE(6,*)'ENTER CRUISING ALT. WRT/DATUM (KM)'
      READ*, ALT
      WRITE(6,*)'VIKING 1 DATA(1), OR VIKING 2 DATA(2)?'
      READ*, IVIK
*
      WRITE(10,25)
      WRITE(10,30)
      WRITE(10,35) DENB,TA,TB,MW,ALT
      WRITE(10,40)
*
C     CALCULATE GAS DENSITIES.  THE LIFT IS THEN CALCULATED BY FINDING
C     THE BUOYANT FORCE CAUSED BY THE DIFFERENCE IN DENSITIES INSIDE
C     AND OUTSIDE THE BALLOON, AS PREDICTED BY ARCHIMEDES PRINCIPLE,
C     FOR VARIOUS BALLOON RADII. NOTE THAT AN EQUILIBRIUM ALTITUDE IS
C     ASSUMED AS AN INPUT PARAMETER.  THE MINIMUM ALLOWABLE BALLOON
C     RADIUS IS ONE THAT PROVIDES ENOUGH LIFT FOR JUST THE WEIGHT OF
C     THE BALLOON FABRIC, WITHOUT ANY EXTERNAL PAYLOAD.
*
*
      FLAG=1
      RBAR=8314.
      PI=3.141592
*
C       IN THIS MODEL, THE AMBIENT PRESSURE AND TEMPERATURE ARE CALCU-
C     LATED USING EXPOTENTIAL MODELS BASED UPON VIKING DATA. THE DEN-
C     SITY IS THEN CALCULATED BY IDEAL GAS LAW
*
      IF(IVIK .EQ. 1) THEN
         ALT=ALT+1
         TA=237.5-3.7*ALT
         PA=762.*EXP(-(ALT/11.697+0.0002612*ALT*ALT))
      ELSE
         ALT=ALT+2
         TA=225.6-0.97*ALT
         PA=782.*EXP(-ALT/11.363)
      ENDIF
      DMAR=PA/(RBAR/44.)/TA
      P=PA+DP
      DGAS=P*MW/RBAR/TB
      I=1
      DO 10 R=.5,RMAX,.5
           BALMAS=4.*PI*R**2*DENB/1000.
           VOLUME=4.*PI*R**3/3
           GASMAS=VOLUME*DGAS
           PLMAS=VOLUME*(DMAR-DGAS)-BALMAS
           TOTMAS=PLMAS+BALMAS+GASMAS
           RELPL=PLMAS/TOTMAS
           IF(PLMAS .GE. 0) THEN
                FLAG=2
                DATAR(CASE,I)=R
                DATAPL(CASE,I)=PLMAS
                DATATL(CASE,I)=TOTMAS
                WRITE(10,100) R,BALMAS,GASMAS,PLMAS,TOTMAS,RELPL
                WRITE(6,100) R,BALMAS,GASMAS,PLMAS,TOTMAS,RELPL
                IF(I .GT. IMAX) IMAX=I
                I=I+1
           ENDIF
10    CONTINUE
```

```
         NP(CASE)=I-1
        IF(FLAG .EQ. 1) WRITE(10,45)
*
C       CASE COUNTER: ALLOWS EXECUTION OF UP TO THREE CASES WITH THE
C       RESULTS TO BE SENT TO THE SAME OUTPUT FILE
*
        IF(CASE .LT. 3) THEN
           WRITE(6,*)'ANOTHER RUN? (Y/N)'
           READ(5,'(A)') ANS
           IF(ANS .EQ. 'Y') THEN
              CASE=CASE+1
              GO TO 99
           ENDIF
        ENDIF
*
*
C       PRINTING OPTIONS
*
        WRITE(6,*)'CHOOSE OUTPUT PLOT TYPE'
        WRITE(6,*)
        WRITE(6,*)'      1. PLMASS,TLMASS VS R'
        WRITE(6,*)'      2. PLMASS VS R'
        WRITE(6,*)'      3. TLMASS VS R'
        WRITE(6,*)'      4. PLMASS VS TLMASS'
        WRITE(6,*)'      5. NO PLOT FILE'
        WRITE(6,*)
*
        READ*, PLOT
        IF (PLOT .EQ. 1) THEN
          DO 20 I=1,CASE
             DO 18 J=1,NP(I)
               WRITE(20,200)DATAR(I,J),DATAPL(I,J)
18           CONTINUE
             DO 19 J=1,NP(I)
               WRITE(20,200)DATAR(I,J),DATATL(I,J)
19           CONTINUE
20        CONTINUE
*
        ELSE IF (PLOT .EQ. 2) THEN
          DO 22 I=1,CASE
             DO 21 J=1,NP(I)
               WRITE(20,200)DATAR(I,J),DATAPL(I,J)
21           CONTINUE
22        CONTINUE
*
        ELSE IF (PLOT .EQ. 3) THEN
          DO 24 I=1,CASE
             DO 23 J=1,NP(I)
               WRITE(20,200)DATAR(I,J),DATATL(I,J)
23           CONTINUE
24        CONTINUE
*
        ELSE IF (PLOT .EQ. 4) THEN
          DO 26 I=1,CASE
             DO 27 J=1,NP(I)
               WRITE(20,200)DATATL(I,J),DATAPL(I,J)
27           CONTINUE
26        CONTINUE
        ENDIF
*
        CLOSE(10)
```

```
 CLOSE(20)
WRITE(6,*)'PLOT DATA STORED IN "STU222.BOUT"'
WRITE(6,*)'OUTPUT DATA STORED IN STU222.'.OUTPUT.'2'
STOP
END
```

Appendix 3.2

Ascent Pressure Profile for Analysis of

Superpressure Balloon Behavior

A Computer Model

```
**** TSO FOREGROUND HARDCOPY ****
DSNAME=STU222.FORTLIB.FORT                              (SPDRIV  )

*
****** ************************************************************
*
*                  DRIVER PROGRAM FOR CALCULATING ALTITUDE VS
*                  RADIUS FOR VARIOUS PAYLOAD WEIGHTS
*                  USES SUBROUTINE 'SPB'
*                  BY GRANT WILLIAMS
*
*                  MARS ROVER/LANDER DESIGN COURSE
*                  UTAH STATE UNIVERSITY
*
****** ************************************************************
*
*
C         THE FOLLOWING DRIVER PROGRAM COMPILES DATA OF CRUISING ALTI-
C       TUDE VS RADIUS FOR A HYDROGEN-FILLED SUPER PRESSURE BALLOON.
C       THE USER INPUTS DESIRED PAYLOAD MASS, AND ALLOWABLE RANGE OF
C       BALLOON RADII, WHICH THE DRIVER USES IN CONJUNCTION WITH 'SPB'
C       SUBROUTINE TO FIND CRUISING ALTITUDE FOR EACH R.
*
        REAL MPL,R,ALT,MG,MT,DP,TB
        CHARACTER*1 YN
*
        EXTERNAL SPB
*
        CALL CONECT(10,'STU222.SPDAT$','STA=UNK$')
        CALL CONECT(20,'STU222.SPOUT$','STA=UNK,CAR=YES$')
        OPEN(10)
        OPEN(20)
*
40      FORMAT('1',10X,10('*'),' SP BALLOON ALT. VS RADIUS ',10('*'),
     & 3(/),20X,'PAYLOAD MASS(KG):   ',F5.1,(/),
     &       20X,'BALLOON FILL TEMP: ',F5.1,2(/))
50      FORMAT(' ',3X,'RADIUS',3X,'ALTITUDE',3X,'DEL PRESSURE',3X,
     & 'GAS MASS',3X,'TOTAL MASS',(/))
100     FORMAT(' ',4X,F4.1,6X,F5.2,7X,F6.1,8X,F4.1,6X,F6.1)
110     FORMAT(' ',F5.1,'.',F5.2)
*
*
C       INPUT PARAMETERS
*
999     WRITE(6,*)'ENTER PAYLOAD MASS(KG)'
        READ*, MPL
        WRITE(6,*)'ENTER BALLOON FILL TEMPERATURE(K)'
        READ*, TB
        WRITE(6,*)'ENTER BALI RADIUS RANGE(M): RMIN, RMAX'
        READ*, RMIN,RMAX
*
        WRITE(6,40)MPL,TB
        WRITE(6,50)
        WRITE(20,40)MPL,TB
        WRITE(20,50)
*
C       LOOP THROUGH RADII, CALLING SPB FOR EACH R
*
        DO 10 R=RMIN,RMAX,0.5
            CALL SPB(R,MPL,TB,ALT,DP,MG,MT)
            WRITE(6,100)R,ALT-2,DP,MG,MT
```

```
            WRITE(20,100)R,ALT-2,DP,MG,MT
           WRITE(10,110)R,ALT-2
10      CONTINUE
        WRITE(6,*)'ANOTHER RUN? (Y/N)'
        READ(5,'(A)') YN
        IF(YN .EQ. 'Y') GO TO 999
        CLOSE(10)
        CLOSE(20)
        WRITE(6,*)'PLOT DATA IN "STU222.SPDAT"'
        WRITE(6,*)'DATA IN "STU222.SPOUT"'
        STOP
        END
*
*
****** ****************************************
*
        SUBROUTINE SPB(RMAX,MPL,TB,Z,DP,MG,MTOT)
*
****** ****************************************
*
C         THE FOLLOWING ROUTINE DETERMINES BALLOON FORCE AND INTERNAL
C       PRESSURE PROFILES FOR A SUPERPRESSURE(SP) BALLOON, ASSUMING A
C       FIXED AMOUNT OF LIFT GAS, AND A FIXED MAXIMUM VOLUME.
*
        REAL MG,MPL,MFAB,ML,MTOT
        REAL VB,VMAX,DFAB
        REAL PB,TB,DB,PM,TM,DM
        REAL Z,FB,DP
        REAL RB,RMAX,GMAR
        REAL RMAR,RHYG
*
*
C       DEFINE PROBLEM CONSTANTS, BASED UPON INPUT
*
        DFAB=50.8
        MG=5.
*
        VMAX=4*3.14159*RMAX**3/3.
        MFAB=DFAB*4*3.14159*RMAX*RMAX/1000.
        ML=MFAB+MPL
*
        RMAR=8314./44.
        RHYG=8314./2.
        GMAR=3.8
*
C       INITIALIZATION OF VARIABLES
*

           PM=782.
           TM=225.6
           DM=PM/RMAR/TM
*
899        VB=MG*RHYG*TB/PM
           IF(VB .LT. VMAX) THEN
              PB=PM
           ELSE
              VB=VMAX
              PB=MG*RHYG*TB/VB
           ENDIF
           DP=PB-PM
           FB=(DM*VB-MG-ML)*GMAR
```

```
*
C       CHECK FB TO MAKE SURE ENOUGH GAS HAS BEEN PLACED IN THE BALI
C       ENVELOPE
*
        IF(FB .LE. 0 .AND. VB .GE. VMAX) THEN
            Z=999.
            GO TO 888
        ELSE IF(FB .LE. 0) THEN
           MG=MG+0.25
           GO TO 899
        ENDIF
        Z=0.
*
C       ENTER ALTITUDE LOOP
*
898     IF(FB .GT. 0) THEN
           Z=Z+0.05
           PM=782*EXP(-Z/11.363)
           TM=225.6-.97*Z
           DM=PM/RMAR/TM
*
           VB=MG*RHYG*TB/PM
           IF(VB .LT. VMAX) THEN
              PB=PM
           ELSE
              VB=VMAX
              PB=MG*RHYG*TB/VB
           ENDIF
           DP=PB-PM
           FB=(DM*VB-MG-ML)*GMAR
           GO TO 898
        ENDIF
888     MTOT=MG+ML
        RETURN
        END
```

Appendix 4.1

Balloon Surface Area

SURFACE AREA ON BALLOON:

CONSIDER THE SPHERE IN THE X-Y PLANE:

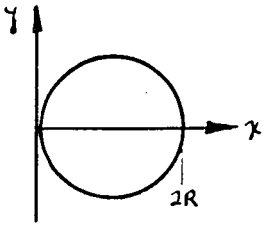

WHERE $Y=\sqrt{R^2-(X-R)^2} = \sqrt{2XR-X^2}$

THE SURFACE AREA BY REVOLUTION BECOMES:

using Bliss's Theorem: $SA(f)=2\pi\int_o^x f(x)\sqrt{1+(f'(x))^2}\,dx$

the surface area function becomes:

$$SA(x)= 2\pi\int_0^x (2XR-x^2)\sqrt{1+\frac{R^2-2Rx+x^2}{2xR-x^2}}\,dx$$

this then reduces to the basic integral:

$$SA(x)=2\pi\int_o^x R\,dx = 2\pi Rx\Big|_0^x = \boxed{2\pi Rx}$$

this has then a correlating mass as a function of x by relating the balloon fabric area density:

$$mass(x)=\boxed{2\pi Rx\,\rho_f}$$

ρ_f= area fabric density (Kg/m^2)

Appendix 4.2

Critical Radius Derivation

CRITICAL RADIUS DERIVATION:

consider a balloon system with the following properties:

ρ_f = area fabric density (Kg/m^2)
V = volume of the balloon (m^3)
ρ_a = atmosphere density (Kg/m^3)
ρ_b = balloon gas density (Kg/m^3)
R = balloon radius (m)

for equilibrium conditions:

net lift = weight of fabric

$$\text{net lift} = L_n = V(\rho_a - \rho_b) = 4\pi R^3(\rho_a - \rho_b)/3$$

$$\text{weight(mass) of fabric} = \rho_f 4\pi R^2$$

so solving the equation for, R and calling this R_{cr}, the minimum value for which lifting will occur:

$$R_{cr} = 3\rho_f/(\rho_a - \rho_b)$$

and substituting the equation densities by the perfect gas law:

$$R_{cr} = \frac{3\rho_f T}{p} \Bigg/ \left[\frac{1}{R_a} - \frac{1}{R_b}\right]$$

where:

p = atmosphere ambient pressure (Pa)
T = ambient atmosphere temperature (K)
R_a = gas constant for the atmosphere (NM/KgK)
R_b = gas constant for the balloon gas (NM/KgK)

Appendix 4.3

Ground Deployment Dynamics

DYNAMIC BEHAVIOR OF GROUND DEPLOYMENT SCHEME:

The following is a derivation of the governing relations for a ground deployed balloon system.

System Definition:

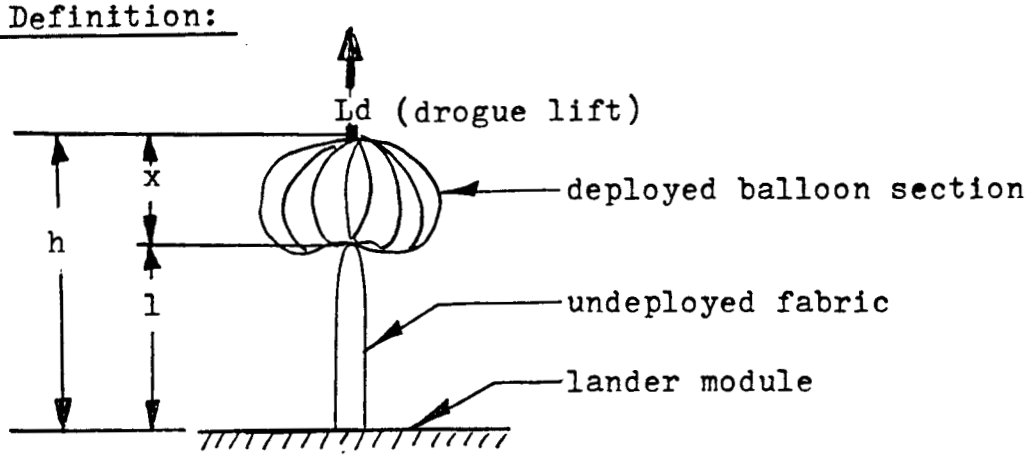

Coordinate Definitions:

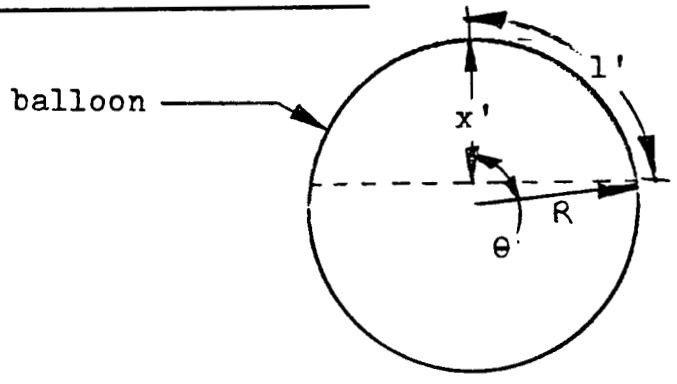

l': transformed axis for deployed section ($l' = \theta R$)
x': deployed section length
h : total height from lander
li: initial deployment height (determined by drogue lift)

Additional Relationships:

$$\theta = l'/R \qquad l' = R\cos^{-1}(1 - x'/R)$$

and by the perfect gas law: $$Vt = \frac{\dot{m}tRT}{p}$$

where:
- Vt = volume of balloon at time t (m^3)
- t = time after beginning of fill process (s)
- $\dot{m}$ = mass flow rate of gas into balloon (Kg/s)
- R = balloon gas constant (N*M/Kg)
- T = gas temperature (K)
- p = ambient atmosphere pressure (Pa)

Balloon Dynamics Con't.

F.B.D.

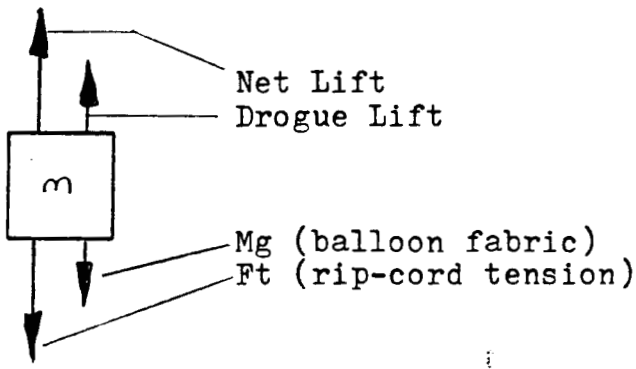

And from the free body diagram: (using steady state conditions)

$$2\pi R \rho_f g x' + F_t = L_d g + g(V_t \rho_a - \dot{m}t)$$

where:

ρ_f = fabric area density (Kg/m^2)
ρ_a = atmosphere density (Kg/m^3)
x' = total length of deployed balloon (m)
V_t = volume at time t (m^3)
g = martian gravity constant (3.73 m/s^2)
F_t = rip-cord tension (N)
L_d = drogue net lift (Kg)

here, some additional relationships derived from the aforementioned parameters are given:

$$l = R\cos^{-1}\left[\left(1 - \frac{L_d g - F_t}{2\pi R^2 \rho_f g}\right)\right] + \frac{R}{2}\cos^{-1}\left[\left(1 - \frac{(V_t \rho_a - \dot{m}t)}{(2\pi R^2 \rho_f)}\right)\right]$$

and h, the total height from the lander is defined:

$$h = x + l$$

where:

$$x = \frac{L_d g + g(V_t \rho_a - g\dot{m}t) - F_t}{2\pi R \rho_f g} - R(1-\cos(l/R))$$

where l,x,and h are shown in the system definition diagram

Appendix 4.4

Wind Effects on Ground Deployment

Wind effects on balloon performance

SYSTEM DEFINITION

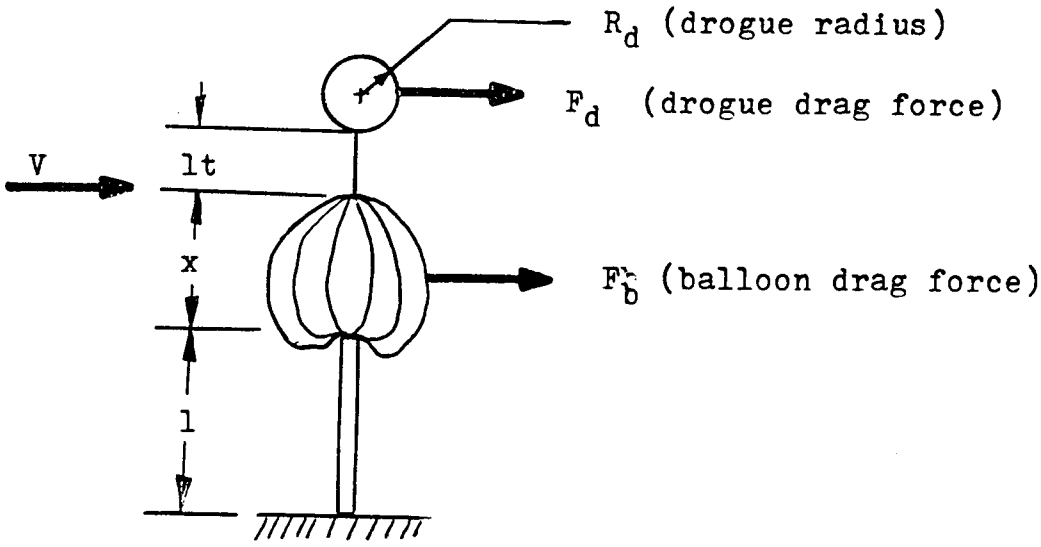

where:

Lt = tether length (2m)
x = deployed section of balloon (defined in previous appendix)
l = total undeployed balloon length (" " " ")

F_d = drag force on drogue (n)

F_b = drag force on balloon (N)

assumptions:

- deployed balloon section approximates a sphere
- tension of rip-cord does not contribute to deflection angle

additional parameters:

The Reynolds number for the two spheres , defined as $Re=VD/\nu$ where ν is based on the CO2 atmosphere @ 600 Pa and 220 K

system	Re range(5m/s to 25 m/s)
Drogue	4×10^4 - 2×10^5
balloon	3×10^3 - 1.5×10^6

Wind effects con't.

From reference 2 , figure 1 was obtained showing the relationship between Re and the coefficient of drag:

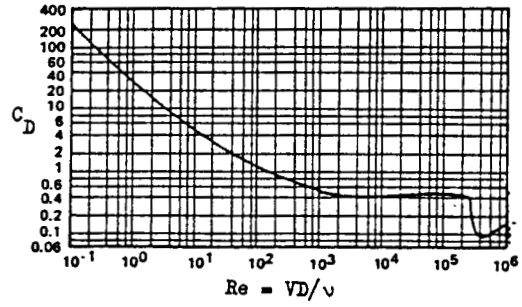

from this figure, it can be seen that the Cd for the range of Re for both the balloon and the drogue is approximately 0.5 and the drag force on each element is governed by:

$$F = Cd \frac{\pi}{2} R^2 \rho_a V^2$$

where:

F = drag force (N)
Cd= coefficient of drag (0.5)
R = element radius (m)
V = surface wind velocity (m/s)
ρ_a = ambient atmosphere density (Kg/m^3)

next consider the steady state free body diagram:

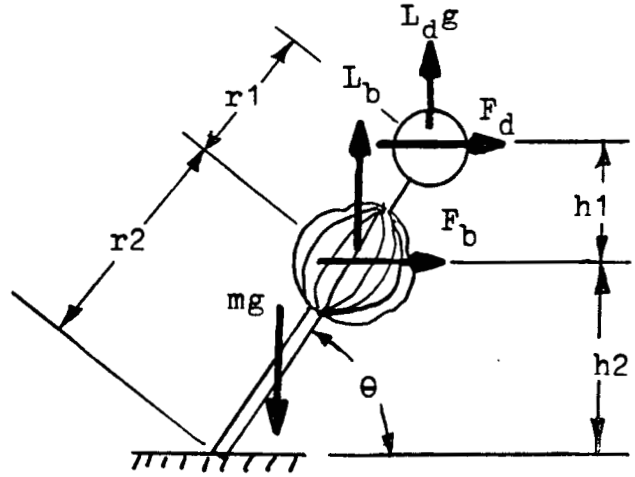

Figure 2

Wind effects con't.

where in figure 2 the angle θ becomes:

$(\Sigma M = 0)$

$$r1 = x/2 + lt + R_d$$
$$r2 = x/2 + l$$

(where x and l are defined in previous appendix)

$$L_d g \cos\theta\,(r1+r2) - Fb \sin\theta(r2) - F_d(r1+r2)\sin\theta - mgr2/2(\sin\theta) = 0$$

and solving for θ:

$$\theta = TAN^{-1}\left[\frac{Ld(r1+r2)g + Lb\cdot r2 - mg\cdot r2/2}{F_b r2 + Fd(r1+r2)}\right]$$

where:

m = deployed mass ($m=2\pi R^2 \rho_f (1- \cos[l/R])$)

```
ccccccccccccccccccccccccccccccccccccccccccccccccccccccccccccccccccccccc
c      program written by James Cantrell for Utah State University     c
c      Advanced Space Design program. It computes the transient states c
c      of the ground deployment scheme per derived parameters.         c
c      Included is the length deployed as well as the angular deflec-  c
c      tions.                                                          c
ccccccccccccccccccccccccccccccccccccccccccccccccccccccccccccccccccccccc

c      declare variables

       real rp,xp,ld,lp,lt,li,pi,rhof,rhoco2,mdot,Tco2,Th2,Rco2,Rh2,p,
     .      ldeployed,t,ml,mu,ms,tu,fb,fd,ft,r1,r2,ltether,v,rd,md,nue,
     .      mdd,cd

c     open output files for dissplа graphics

       open(unit=10, file='dyn.out',status='new')
       open(unit=20,file='dyn2.out',status='new')
       open(unit=30,file='dyn3.out',status='new')
       open(unit=60,file='the.out',status='new')
       open(unit=70,file='the2.out',status='new')
       open(unit=80,file='the3.out',status='new')

c      define operationalvariables

c      rhof=fabric  density : Ft=ripcord tension : p=ambient pressure
c      ld=drogue lift : rd=drogue radius

       pi=3.1415
       rhof=0.0508
       ld=2.5
       rp=16.0
       i=0
       p=600.0
       Rco2=188.9
       Tco2=220.0
       Rh2=4124.0
       Th2=250.0
       rhoco2=p/(Rco2*Tco2)
       Ft=5.0
       g=3.74
       xp=0.0
       ltether=4.0
       rd=5.0
       cd=0.5
       xtotal=0.0

c     user input parameters

       print*, 'enter upper time limit'
       read*,tu
       print*, 'wind velocity? (m/s)'
       read*, v

c     compute the initial length of fabric deployment

       li= rp*acos(1.0-(ld/(rhof*2.0*pi*(rp**2))))
```

```
c     vary mass flow rates and compute the resultng position

        do 150 mdot=.005,.015,.005

c     file parameters

                i=i+10
                j=i+50

c     vary time after flow begins

        do 100 t=0.0,tu,1.0

c               compute the system radiuses as defined in text
                r1=(xp/2.0+ltether+rd)
                r2=(xp/2.0+li)
c               compute wind drag forces
                fd=(pi/2.0)*(rd**2)*rhoco2*(v**2)*cd
                fb=(pi/8.0)*(xp**2)*rhoco2*(v**2)*cd
c               compute deployed mass
                md=2.0*pi*rp*rhof*g
c               compute instantaneous volume
                Vt=mdot*t*rh2*th2/p
c               transient balloon lift
                lb=g*(Vt*rhoco2-mdot*t)
                mdd=2.0*pi*rp*xtotal*rhof
c               second deployed mass parameter
                theta=(ld*g*(r1+r2)+(lb*r2)-g*mdd*li/2.0)/((fb*r2)+(fd*(r1+r2)))
                the= ATAN(theta)
c               compute total length deployed based on derivations in appendix
                xtotal=(((Ld*g)-Ft-(g*mdot*t)+(g*Vt*rhoco2))*(sin(the))+(fd+fb)
                        *cos(the))/md
                if(xtotal.gt.(2.0*rp))goto 100
                lt=rp*(acos(1.0-xtotal/rp))
                lp=lt-li
                xp=rp*(1.0-cos(lp/rp))
                ldeployed=li+xp
                the=the*180.0/pi

c               write output to files
                write(i,15) t,ldeployed
                write(j,15)t,the
15              format(1x,f12.4,1x,f12.4)

100     continue

150     continue


        end
```

Appendix 4.5

Payload Dynamic Response to Wind Impulses

PAYLOAD OSCILLATIONS DUE TO WIND IMPULSES

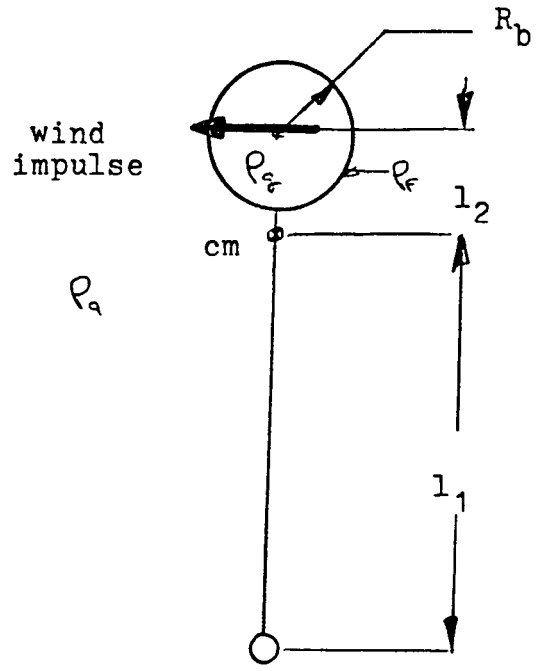

$$F_w = \frac{\pi}{2} \rho_a R_b^2 V^2 cd$$

ρ_a = atmosphere density
R_b = balloon radius
cd = coefficient of drag
F_w = wind impulse force
V_w = wind impulse velocity

assume: neglect damping in computations
neglect drag on payload
$l_1 + l_2$ = constant
link remains rigid

$$L_n = (4/3 \pi R_b^3)(\rho_a - \rho_b)g - \rho_f 4 \pi R_b^2$$

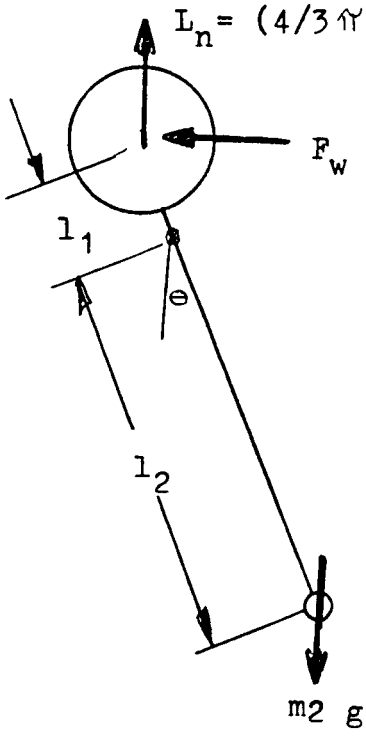

$$l_1 = m_2(R_b + l_1 + l_2)/(m1+m2)$$

writing the differential equation for the rotational motion:

$$I\ddot{\theta} = Ln l_1 \sin\theta + m_2 g\, l_2 \sin\theta + Fw\, l_1 \cos\theta$$

and by binomial expansion:

$$I\ddot{\theta} + (Ln\, l_1 + m_2 g l_2)\,\theta = Fw\, l_1$$

solving the D.E. :

$$\theta_t = \theta_h + \theta_p = c_1 \cos w_n t + c_2 \sin w_n t + Fw\, l_1/(I(L\, l_1 + m_2 g l_2))$$

solving for the initial conditions of:

$\theta(0)=0$ and $\dot{\theta}(\theta) = 0$

yields:

$$\theta(t) = \frac{Fw\, l_1}{I(Ll_1 + m_2 g l_2)} \left(1 - \cos w_n t\right)$$

$$\dot{\theta}(t) = \frac{Fw\, l_1\, w_n}{I(Ll_1 + m_2 g l_2)} \sin w_n t$$

$$w_n = \sqrt{\frac{L\, l_1 + m_2 g l_2}{I}}$$

$$\ddot{\theta}(t) = \frac{Fw\, l_1\, w_n^2}{I(Ll_1 + m_2 g l_2)} \cos w_n t$$

from this analysis, it was found that the effect of wind impulses on the payload and balloon is negligable for most range of tether lengths and impulses of up to 150 m/s. The conclusion is that for tether lengths in the range of 0-50m, and impulses of 0-150 m/s, the angular deflections are less than two degrees.

```
ccccccccccccccccccccccccccccccccccccccccccccccccccccccccccccccccccccc
c                                                                     c
c   PROGRAM WRITTEN BY JAMES CANTRELL FOR UTAH STATE UNIVERSITY       c
c   ADVANCED SPACE DESIGN PROJECT. PROGRAM IS USED TO COMPUTE         c
c   THE ANGULAR DEFLECTIONS OF THE AEROSTAT AND PAYLOAD FOR           c
c   DIFFERING WIND GUSTS.PROGRAM IS BASED ON THE EQUATIONS            c
c   DERIVED IN THE APPENDIX.                                          c
ccccccccccccccccccccccccccccccccccccccccccccccccccccccccccccccccccccc

c       declare variables

        implicit none
        real g,l1,l2,lt,lift,m1,m2,rhoco2,rb,cd,vw,fw,pi,vol,theta,tdot,tddot
     .       ,I,maxv,maxna,maxta,l,thetdd,thetd,v,volume,rhoh2,wn

        open(unit=10,file='de.out',status='new')

c       define operational parameters

        print*,'input maximum expected wind gust (m/s)'
        read*,v
        pi=3.1415
        cd=0.5
        rb=16.0
        rhoco2=600.0/(188.9*210.0)
        m1=(0.05)*pi*4.0*(rb**2)
        g=3.73

c       following equations based on previous derivations

        volume=4.0*pi*(rb**3)/3.0
        rhoh2=600.0/(4124.0*210.0)
        lift=((rhoco2-rhoh2)*volume*g)-(m1*g)
        m2=lift/g
        fw=(pi/2.0)*(rb**2)*rhoco2*(v**2)*cd

        write(15,*) '  Effect of Balloon Tether Length on Payload'
        write(15,*) '   '
        write(15,*) '   tether    max.      max.      max.     max.'
        write(15,*) '   length   theta      vel.       An       At '
        write(15,*) '     m       deg.      m/s       g''s     g''s  '
        write(15,*) '        '

c       vary tether lengths to obtain maximum thetas, velocities, accelerations


        do 20 lt=21.0,121.0,10.0

                l1=(m2*lt)/(m1+m2)-rb
                l2=lt-l1
                I=(m1*rb**2)/2.0+(m1*l1**2)+(m2*l2**2)
                wn=((lift*l1+m2*g*l2)/I)**0.5
                theta=2.0*(fw*l1)/(I*(lift*l1+m2*g*l2))
                thetd=(fw*l1*wn)/(I*(lift*l1+m2*g*l2))
                maxv=thetd*l2
                thetdd=(Fw*l1*(wn**2))/(I*(lift*l1+m2*g*l2))
                maxna=(thetd**2)*l2
                maxta=(thetdd)*l2
                theta=180.0/pi*theta
```

```
                l=lt-rb
                maxna=maxna/9.81
                maxta=maxta/9.81


                write(10,15) l,theta,maxv,maxna,maxta
15              format(3x,f12.7,3x,f12.7,3x,f12.7,3x,f12.7)
                write(10,30)
30              format(20x)

20      continue


        end
```

Appendix 4.6

Balloon Descent Deployment Equations of Motion

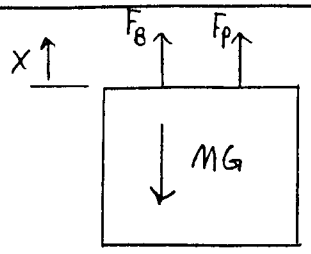

$$\Sigma F = m\ddot{x}$$

$$F_B + F_P - MG = m\ddot{x}$$

-OR-

$$\ddot{x} + G - \left(\frac{F_B + F_P}{m}\right) = 0$$

F_B IS LIFT FORCE GENERATED BY BALLOON

F_P IS DRAG FORCE GENERATED BY PARACHUTE AND BALLOON.

FIGURE 1. FBD

F_B:

BY ARCHIMEDIS PRINCIPLE,

$$F_B = V G (\rho_A - \rho_B)$$

V IS VOLUME OF BALLOON
G IS MARTIAN GRAVITY
ρ_A IS DENSITY OF ATMOSPHERE
ρ_B IS DENSITY OF BALLOON GAS

ρ_A WAS CALCULATED BY THE IDEAL GAS LAW ASSUMING

$$\text{PRESSURE, PASCALS} = 782 \exp\left(-\frac{Z+2000}{11363}\right)$$
$$\text{TEMPATURE, KELVIN} = 225.6 - .97(10^{-3})(Z+2000)$$

THIS EQUATIONS ARE CURVE FITS FROM VIKING DATA.

ρ_B WAS CALCULATED AS BEING $\left({}^{1KG\ H_2}/_{V_{BALLOON}}\right)$

AS THE BALLOON WAS BEING FILLED V & ρ_B WERE FOUND BY

$$V = V_{MAX}\left(1 - \exp\left(-{}^{t}/_{5(\text{FILL TIME})}\right)\right)$$
$$\rho_B = \left(\frac{(1KG\ H_2)\ t}{\text{FILL TIME}}\right) / V$$

F_P:

$$F_P = \tfrac{1}{2} V^2 \rho_A \left(C_{D,\text{PARACHUT}} + C_{D,\text{BALLOON}}\right)$$

-OR-

$$F_P = \tfrac{1}{2}(\dot{x})^2 \rho_A \left(C_{D,P} + C_{D,B}\right)$$

FOR ALL THE FOLLOWING GRAPHS, A DRAG COEFFICIENT FOR THE PARACHUTE OF 1 IS USED. DEPENDING ON DESIGN $0.8 < C_D < 1.2$ AND 1 IS A GOOD AVERAGE.

THE COMPUTER PROGRAM USED PROMPTED FOR TWO BALLOON DRAG COEFFICIENTS. THE FIRST WAS USED AS THE BALLOON WAS BEING FILLED, THE SECOND AFTER THE BALLOON WAS FULL. TWO SETS OF DATA ARE SHOWN BELOW, EACH WITH A DIFFERANT $C_{D,B}$.

AS THE PARACHUTE IS BEING DEPLOYED THE AREA VARIED BY:

$$\text{AREA} = A_{MAX}\left(1 - \exp\left(-\frac{t}{5(\text{DEPLOY TIME})}\right)\right)$$

WHERE DEPLOY TIME AND MAXIMUM AREA WHERE INPUTED FROM THE SCREEN.

NOTE THAT THE MASS (m) IS DISCONTINOUS WHEN THE HYDROGEN TANKS ARE DROPPED AND AGAIN WHEN THE PARACHUTE IS DROPPED.

THE COMPUTER PROGRAM:

GIVEN THE ABOVE DIFFERENTIAL EQUATION AND PARAMETERS THE PROGRAM PROMPTED FOR:

INITIAL VELOCITY
DESCENT ANGLE
INITIAL ALTITUDE
RADIUS OF BALLOON
TIME TO FILL BALLOON
TOTAL MASS OF BALLOON AND PAYLOAD → MASS OF HYDROGEN
MASS OF HYDROGEN TANK
MASS OF PARACHUTE
AREA OF PARACHUTE
PARACHUTE DEPLOYMENT TIME
PARACHUTE C_D
BALLOON C_D BEFORE FULL
BALLOON C_D AFTER FULL

INITIAL VELOCITY, ALTITUDE AND DESCENT ANGLE WERE DETERMINED BY WORK DONE BY RUSS LAHER. THE RADIUS OF BALLOON, MASS OF BALLOON, AND MASS OF HYDROGEN WERE DETERMINED BY GRANT WILLIAMS. MASS OF THE HYDROGEN TANK WAS FOUND BY JIM CANTRELL. THE REST OF THE PARAMETERS WERE FREE TO BE OPTIMIZED. WITH THE ABOVE PARAMETERS THE DIFFERENTIAL EQUATION WAS SOLVED BY IMSL DVERK, A 10TH-ORDER RUNGE-KUTTA INTEGRATION PROGRAM.

Appendix 4.7

Computer Program: Descent Deployment Model

```
**** TSO FOREGROUND HARDCOPY ****
DSNAME=STU082.FORTLIB.FORT                                    (DES      )

      PROGRAM DECENT
C
C
C     Y         = IS A 2 DIMENSIONAL ARRAY Y(1) IS ALTITUDE
C                                          Y(2) IS VELOCITY
C     TIME      = IS A ARRAY PLOTTED AGAINST POSN AND VELC (SECONDS)
C     POSN      = IS A ARRAY OF ALTITUDES AT SPECIFIC TIMES
C     VELC      = IS A ARRAY OF VELOCITIES AT SPECIFIC TIMES
C     THETA     = ANGLE OF VELOCITY AT TIME = 0 WITH RESPECT TO
C                 LOCAL HORIZON
C     MDOT      = MASS FLOW RATE OF H2 ASSUMED CONSTANT UNTIL BALLOON
C                 IS FULL
C     MH        = MASS OF HYDROGEN
C     MTNK      = MASS OF HYDROGEN TANKS
C     MPLD      = MASS OF PAYLOAD
C     MTOT      = MTNK + MPLD
C     ACHT      = PROJECTED AREA OF DEPLOYED PARACHUTE
C     TCHT      = TIME FOR PARACHUTE TO FULLY OPEN
C     CD        = DRAG COEFFICIENT ON PARACHUTE
C     FT        = BALLOON FILL TIME A INTEGER
C     ICASE     = 1 WHEN PARACHUTE AND BALLOON BOTH ARE ACTING
C     ICASE     = 2 WHEN BALLOON ONLY IS ACTING AND FILL TANKS DROPPED
C     ICASE     = 3 BALLOON FULL (TANKS DROPED) PARACHUTE STILL ACTING
C
C

      IMPLICIT REAL*8(A-H,O-Z)
      PARAMETER (PI=3.14159265400,G=3.720)
      COMMON / / FP,FB,ICASE
      INTEGER T,FT
      REAL*8 Y(2),C(24),W(2,9),TIME(900),POSN(901),VELC(900),MTNK,
     &       MPLD,MPAR,MH,MDOT
      CHARACTER DUM1,DUM2
      EXTERNAL FCN
C
C                                                    ORIGINAL PAGE IS
C                                                    OF POOR QUALITY

      ICASE = 1
      PRINT*,'ENTER INITIAL VELOCITY (IN M/S)'
      READ*,V

      PRINT*,'ENTER THE DESCENT ANGLE (IN DEGREES)'
      READ*,A
      THETA = A*PI/180.D0
      Y(2) = -V*COS(THETA)

      PRINT*,'ENTER THE INITIAL ALTITUDE (IN METERS)'
      READ*,ALT
      Y(1) = ALT

      PRINT*,'ENTER THE RADIUS OF THE FULL BALLOON (IN METERS)'
      READ*,RAD
      VMAX = 4.D0/3.D0*PI*RAD**3

      PRINT*,'ENTER THE FILL TIME (IN SECONDS)'
      READ*,FT

      PRINT*,'ENTER THE TOTAL PAYLOAD MASS (IN KG)'
      READ*,MPLD
```

```
      PRINT*,'ENTER THE MASS OF THE HYDROGEN TANKS (IN KG)'
      READ*,MTNK

      PRINT*,'ENTER THE MASS OF THE PARACHUTE (IN KG)'
      READ*,MPAR

      PRINT*,'ENTER THE MASS OF THE HYDROGEN (IN KG)'
      READ*,MH
      MDOT = MH/REAL(FT)

      PRINT*,'ENTER THE PROJECTED PARACHUTE AREA (IN M**2)'
      READ*,ACHT

      PRINT*,'ENTER THE PARACHUTE DEPLOYMENT TIME (IN SECONDS)'
      READ*,TCHT

      PRINT*,'ENTER THE PARACHUTE DRAG COEFFICIENT'
      READ*,CD

      PRINT*,'ENTER THE DRAG COEFFICIENT ON THE BALLOON AS ITS FILLING'
      READ*,CDB

      PRINT*,'ENTER THE DRAG COEFFICIENT ON THE FULL BALLOON'
      READ*,CDA
C
C
      NPTS = 901
C --------- = NUMBER OF DATA POINTS IN EACH DATA GROUP (OR LINE)
C
      NLINES = 1
C ----------  = NUMBER OF DATA GROUPS (OR THE NUMBER OF LINES TO
C              BE PLOTTED
C
      NW=2
      N=2
      X=0.D0
      TOL=.0001D0
      IND=1
C
      CALL CONPDS(11,'STU082.FORTLIB.DATA1','NEW95%','$')
      WRITE(11,1001)'TIME','POSN','VELOCITY'
 1001 FORMAT(/,5X,A,T20,A,T35,A)
 1002 FORMAT(5X,I3,T20,F8.2,T35,F8.3)

      DO 10 T=0,900
        XEND = T
        CALL FBLN(Y(1),G,VMAX,MPLD,MTNK,MPAR,T,FT)
        CALL FPAR(CD,ACHT,TCHT,Y(1),T,MPLD,MTNK,MPAR,RAD,Y(2),FT,CDB,
     &            CDA)
        CALL DVERK(N,FCN,X,Y,XEND,TOL,IND,C,NW,W,IER)
        TIME(T+1) = T
        POSN(T+1) = Y(1)
        VELC(T+1) = Y(2)
        WRITE(11,1002)T,Y(1),Y(2)
        IF(T .GT. FT )THEN
          ICASE = 2
        END IF
        IF(IER .GT. 0)THEN
          PRINT*,'IER=',IER
          STOP
```

ORIGINAL PAGE IS
OF POOR QUALITY

```
      IF(IND .NE. 3)THEN
        PRINT*,'IND=',IND
        STOP
      END IF

   10 CONTINUE
      CALL ICUPLT(TIME,POSN,NPTS,NLINES,DUM1,LHEAD,DUM2,LKEY)
      CALL ICUPLT(TIME,VELC,NPTS,NLINES,DUM1,LHEAD,DUM2,LKEY)
      END
C
C
      SUBROUTINE FCN(N,X,Y,YPRIME)
      COMMON / / FP,FB,ICASE
      REAL*8 Y(N),YPRIME(N),FP,FB
      YPRIME(1) = Y(2)
      YPRIME(2) = Y(2)*Y(2)*FP+FB-3.72D0
      END
C
C
      SUBROUTINE FBLN(Z,H,VB,PLD,TNK,PAR,IT,IF)
      IMPLICIT REAL*8(A-H,O-Z)
      COMMON / / FP,FB,ICASE

C     Z = ALTITUDE
C     H = GRAVITY
C     RC= GAS CONSTANT CARBON DIOXIDE
C     TA= TEMP OF ATMOSPHERE
C     P = PRESSURE IN BALLOON
C     S = DENSITY OF ATMOSPHERE -CALCULATED FROM IDEAL GAS USING P,TA
C     PLD= PAYLOAD MASS
C     TNK= TANK MASS
C     PAR= MASS OF PARACHUTE
C     VB= VOLUME OF FULL BALLOON
C     V = VOLUME AT TIME (T)
C     IF = FILL TIME
C     IT = TIME
C     RHOB= DENSITY OF BALLOON GAS

      RC= 187.45D0
      TA= 225.6D0-.97D-3*(Z+2.D+5)
      P = 782.D0*DEXP(-(Z+2.D+3)/11363.D0)
      S = P/(RC*TA)

C     USING A EXPONENTIAL CURVE, CALCULATE THE VOLUME OF THE BALLOON
C     AT TIME (T), BEFORE THE BALLOON IS 'FULL'

      IF(IT .EQ. 0)THEN
        V = 5.D0
      ELSE IF(IT .LE. IF)THEN
        V = VB*(1.D0-DEXP(-3.D0*DFLOAT(IT)/DFLOAT(IF)))
      ELSE
        V = VB
      END IF

C     CALCULATE THE LIFT FORCE OF THE BALLOON (IN M/S**2) BY
C     ARCHIMIDEAS PRINCIPLE

      IF(ICASE .EQ. 1)THEN
        FB = H*V*S/(PLD+TNK+PAR)
      ELSE IF(ICASE .EQ. 2)THEN
```

```
      END IF                                                            02
                                                                        02
      END                                                               02
C                                                                       02
C                                                                       02
      SUBROUTINE FPAR(DRAG,ANOT,TIM,UP,I,PLD,TNK,PAR,RD,V,IF,C1,C2)     02
      IMPLICIT REAL*8(A-H,O-Z)                                          02
      COMMON / / FP,FB,ICASE                                            02
                                                                        02
C     DRAG = PARACHUTE DRAG COEFFICIENT                                 02
C     ANOT = DEPLOYED PARACHUTE AREA                                    02
C     TIM  = TIME TO DEPLOY PARACHUTE                                   02
C     UP   = ALTITUDE                                                   02
C     I    = TIME                                                       02
C     IF   = TIME TO FILL BALLOON                                       02
C     AREA = PROJECTED CHUTE AREA AT TIME T                             02
C     R    = GAS CONSTANT                                               02
C     T    = ATMOSPHERIC TEMPATURE                                      02
C     P    = ATMOSHERIC PRESSURE                                        02
C     RHO  = ATMOSPHERIC DENSITY -FROM IDEAL GAS                        02
C     TNK  = TANK MASS                                                  02
C     PLD  = PAYLOAD MASS                                               02
C     PAR  = PARACHUTE MASS                                             02
C     RD   = RADIUS OF FULL BALLOON                                     02
C     AR   = PROJECTED BALLOON AREA AT TIME T                           02
C     SEN  = 1 OR -1 DEPEDNIG ON THE SIGN OF THE VELOCITY. FOR DRAG     02
C            FROM BALLOON                                               02
C     V    = VELOCITY                                                   02
                                                                        02
      A = 3.14159265AD0*RD**2                                           02
      Q = DFLOAT(I)                                                     02
                                                                        02
      IF(Q .LE. TIM)THEN                                                02
        AREA = ANOT*(1.D0-DEXP(-5.D0*Q/TIM))                            02
      ELSE                                                              02
        AREA = ANOT                                                     02
      END IF                                                            02
                                                                        02
      IF(Q .LE. IF)THEN                                                 02
        AR = A*(1.D0-DEXP(-5.D0*Q/DFLOAT(IF)))                          02
      ELSE                                                              02
        AR = A                                                          02
      END IF                                                            02
                                                                        02
      IF(V .LT. 0.D0)THEN                                               02
        SEN = 1.D0                                                      02
      ELSE IF(V .GT. 0.D0)THEN                                          02
        SEN = -1.D0                                                     02
      ELSE                                                              02
        SEN = 0.D0                                                      02
      END IF                                                            02
                                                                        02
      R = 187.452.0                                                     02
      T = 225.6D0-.97D-3*(Z+2.D+3)                                      02
      P = 782.D0*EXP(-(Z+2.D+3)/11363.D0)                               02
      RHO = P/(R*T)                                                     02
      IF(ICASE .EQ. 1)THEN                                              02
        FP = (.5D0*DRAG*AREA*RHO+SEN*.5D0*C1*AR*RHO)/(PLD+TNK+PAR)      02
      ELSE IF(ICASE .EQ. 2 )THEN                                        02
        FP = (SEN*.5D0*C2*AR*RHO)/PLD                                   02
```

ORIGINAL PAGE IS
OF POOR QUALITY

```
      END
C
C                                                    ORIGINAL PAGE IS
C                                                    OF POOR QUALITY
      SUBROUTINE ICUPLT(XX,YY,NPTS,NLINES,HEAD,LHEAD,KEYS,LKEY)
C
C
C
C
C --- DECLARE SOME OF THE DUMMY ARGUMENTS USING DEFAULT LENGTH SPEC.
C
      CHARACTER*(*)HEAD
      CHARACTER*(*)KEYS(*)
      REAL*8 XX(901),YY(901)
      REAL*4 X(901),Y(901)
C
C --- DECLARE CHART CONTROL VARIABLES IN THE COMMON BLOCK /PLTDAT/
C
      INTEGER
     &     LEVEL,    DISPLA,    HELP,      ISOLAT,
     &                          TIEFRE,    NGROUP,
     &     NELEMN,   LENKEY,    LENLAB,    LENHED,
     &                                     PRTCOP,
     &     PRTHED,                         PRTUNT,
     &     PCSDUM,              DIRTYP,    DIRTYQ,
     &               EXPLEV
      CHARACTER*8    FORMAT,    DATANM,    PRTDES,    DIRNAM,    DIRLIB
      REAL*4 PRTDEP,  PRTWID,    PRTOFF,    PRTHOR
C
C --- DECLARE THE COMMON BLOCK USED TO PASS THE CHART CONTROL
C     VARIABLES TO THE CHART SUBROUTINE
C
      COMMON /PLTDAT/
     &     LEVEL,    DISPLA,    HELP,      ISOLAT,
     &     FORMAT,   DATANM,    TIEFRE,    NGROUP,
     &     NELEMN,   LENKEY,    LENLAB,    LENHED,
     &     PRTDES,   PRTDEP,    PRTWID,    PRTCOP,
     &     PRTHED,   PRTOFF,    PRTHOR,    PRTUNT,
     &     PCSDUM,   DIRNAM,    DIRTYP,    DIRTYQ,
     &     DIRLIB,   EXPLEV
C
C --- INITIALIZE THE CHART CONTROL VARIABLES
C
      LEVEL = 1
C                  CHART UTILITY LEVEL IDENTIFIER
C                  1 = CHART UTILITY RELEASE 3
      DISPLA = 1
C                  CHART UTILITY FUNCTION REQUESTED
C                  1 = PRESENT HOME PANEL & BEGIN INTERACTIVE
C                      SESSION BASED ON THE FORMAT AND DATA
C                      PASSED
C                  2 = PRESENT DISPLAY PANEL & BEGIN AN
C                      INERACTIVE SESSION BASED ON THE FORMAT
C                      AND DATA PASSED
C                  3 = PRESENT DISPLAY PANEL, BUT DO NOT
C                      PERMIT AN INERACTIVE SESSION
C                  4 = PRINT THE PASSED CHART ON THE DEVICE
C                      IDENTIFIED BY THE PRTNAME PARAMETER
C                  5 = ICU WILL ADD THE PASSED CHART TO THE
C                      CURRENT PAGE
      HELP = 1
```

```
C                    PF KEY INFORMATION SWITCH
C                    1 = PF KEY INFORMATION IS DISPLAYED
C                    0 = NO PF KEY INFORMATION IS DISPLAYED
      ISOLAT = 0
C                    ISOLATION SWITCH
C                    0 = SAVE/RESTORE/DIRECTORY AVAILABLE
C                    1 = SAVE/RESTORE/DIRECTORY NOT AVAILABLE
      FORMAT = '*          '
C                    NAME OF PREVIOUSLY SAVED CHART FORMAT
C                    * = DEFAULT CHART FORMAT
C                    OR GIVE FORMAT NAME
      DATANM = '*          '
C                    NAME OF PREVIOUSLY SAVED CHART DATA
C                    * = DATA CONTAINED IN PARAMETERS
C                    OR GIVE DATA NAME
      TIEFRE = 0
C                    TIED OR FREE DATA SWITCH
C                    0 = TIED DATA, ONE SET OF X-VALUES
C                    1 = FREE DATA, SEPARATE X-VALUES
      NGROUP = NLINES
C                    NUMBER OF DATA GROUPS (I.E. # OF LINES
C                    TO BE PLOTTED)
      NELEMN = NPTS
C                    TIED DATA - NUMBER OF ELEMENTS (X VALUES)
C                    FREE DATA - MAX. # OF ELEMENTS (DATA PTS) IN A DATA
C                                GROUP
      LENKEY = LKEY
C                    NUMBER OF CHARACTERS USED TO DESCRIBE THE
C                    DATA GROUPS.              THAT IS THE DECLARED STRING
C                    LENGTH OF THE 'KEYS' ARRAY
      LENLAB = 0
C                    NUMBER OF CHARACTERES USED TO DESCRIBE THE
C                    AXES LABELS. THAT IS THE DECLARED STRING
C                    LENGTH OF THE 'LABEL' ARRAY
C                    0 = NUMERIC LABELS ARE TO USED
      LENHED = LHEAD
C                    NUMBER OF CHARACTERS IN PLOT HEADING
      PRTDES = 'EL207    '
C                    LOCAL PRINTER DESTINATION NAME.
      PRTDEP = 66
C                    PRINTER DEPTH (ROWS) OF CHART AREA
      PRTWID = 132
C                    PRINTER WIDTH (COLS) OF CHART AREA
      PRTCOP = 1
C                    NUMBER OF COPIES TO PRINT
      PRTHED = 2
C                    PRINTER HEADER PAGE CONTROL
C                    1 = HEADER PAGE PRINTED
C                    2 = NO HEADER PAGE OUTPUT
      PRTOFF = 0
C                    PRINTER VERTICAL OFFSET (ROWS)
      PRTHOR = 0
C                    PRINTER HORIZONTAL OFFSET (COLUMNS)
      PRTUNT = 4
C                    PRINTER LAYOUT PARAMETER UNITS
C                    1 = % OF PAGE
C                    2 = INCHES
C                    3 = CENTIMETERS
C                    4 = ROWS AND COLUMNS
      PCSDUM = 0
C                    NOT USED
```

```
      DIRNAM = '        '
C                     DIRECTORY LISTING OBJECT NAME
      DIRTYP = 0
C                     DIRECTORY LISTING OBJECT TYPE
C                     0 = DEFAULT, NO INITIAL LIST
      DIRTYQ = 0
C                     DIRECTORY LISTING OBJECT SUBTYPE
C                     0 = DEFAULT
      DIRLIB = '        '
C                     DIRECTORY LISTING OBJECT LIBRARY
      EXPLEV = 1
C                     INITIAL EXPERIENCE LEVEL VALUE
C                     1 = DEFAULT, STANDARD LEVEL
C                     2 = ADVANCED LEVEL
C
C
C --- CHECK FOR FORMAT
C
      DO 11 I=1,NPTS+1
        X(I)=XX(I)
        Y(I)=YY(I)
 11   CONTINUE

      PRINT*,'IF A PREVIOUSLY STORED ICU FORMAT IS TO BE USED'
      PRINT*,'ENTER THE NAME OF THE FORMAT'
      PRINT*,'FOR DEFAULT FORMAT ENTER BLANK'
      READ(5,'(A)')FORMAT
      IF(FORMAT.EQ.' ') FORMAT='*'
C
C*************************************************************************
C**        INITIALISE GDDM AND CALL THE CHART UTILITY                   **
C*************************************************************************
C
      CALL FSINIT
      CALL CHART(LEVEL, DCONTL, X, Y, KEYS, LABEL, HEAD)
C
C --- LEVEL  = FIRST VARIABLE IN COMMON BLOCK OF THE CHART CONTROL VAR.
C --- DCONTL = AN INTEGER ARRAY THAT STORES THE NUMBER OF DATA POINTS.
C              FOR FREE DATA ONLY. FOR EXAMPLE
C              IF DCONTL(1) = 5  THE FIRST 5 X & Y VALUES MAKE UP THE
C                                FIRST DATA GROUP
C              IF DCONTL(2) = 20 THE NEXT 20 X & Y VALUES MAKE UP THE
C                                SECOND DATA GROUP
C              IF TIED DATA USED, DCONTL BECOMES A DUMMY VARIABLE
C --- X = REAL ARRAY OF X VALUES
C --- Y = REAL ARRAY OF Y VALUES
C --- KEYS = CHARACTER ARRAY HOLDING DESCRIPTIONS OF THE DATA GROUPS
C --- LABEL = CHARACTER ARRAY HOLDING LABELS FOR THE AXES
C             IF NUMERIC LABELS ARE USED, LABEL IS A DUMMY VARIABLE
C --- HEAD = CHARACTER VARIABLE HOLDING THE PLOT HEADING
C
C
C --- TERMINATE THE GDDM SESSION
C
      CALL FSTERM
      RETURN
      END
```

ORIGINAL PAGE IS
OF POOR QUALITY

Appendix 4.8

Mass Flow Calculations

MASS FLOW CALCULATIONS

The entire mass flow calculations is based on the assumption that the hydrogen behaves as a ideal gas, therefore a few words need to be said in that regard. A gas is said to behave ideally if it is 'substantially' above it's critical tempature and below it's critical pressure. For hydrogen those numbers are 32.94 K and 1.294 Mpa. The maximum pressure that the hydrogen will experiance will be about 28 Mpa, or 22 times greater than critical. It is also known that for a ideal gas enthalpy is independant of pressure and a function of tempature only. Knowing this and checking values of enthalpy in the region in question it is found that enthalpy changes only slighly with pressure at this tempature. Also if we look at a t-s diagram we can see that for the region in question we are on a 'nearly' constant enthalpy line. See figures 1 and 2. From here values of pressure were calculated using ideal gas and Redlich-Kwong and compared it was found that they differ by only 15%. See equation 1. From this it was decided that the ideal gas assumption would be adequate, bearing in mind that our calculations may be off by 15 to 20 percent.

$$P_{IDEAL} = \frac{nRT}{V} = 22.86\ MPA$$

1

$$P_{R-K} = \frac{RT}{\nu - b} - \frac{A}{\sqrt{\nu}(\nu + b)T^{1/2}} = 28.23 MPA$$

$$A = 4.934\, B\, L_N\, RT_c^{1.5}$$

$$B = .0867\ \frac{RT_c}{P_c}$$

After the ideal gas assumption has been made calculating mass flow rates becomes much simplier.

UME FANNO LINE FLOW

$$= \frac{.02(15)}{.0254} = 11.81$$

APP E GAS DYNAMICS JAME E.A. JOHN

$= .22$

$T^* = 1.1885$

$P^* = 4.9554$

APP A FOR $M_I = .22$

$P_T = .9668$

$T_T = .9904$

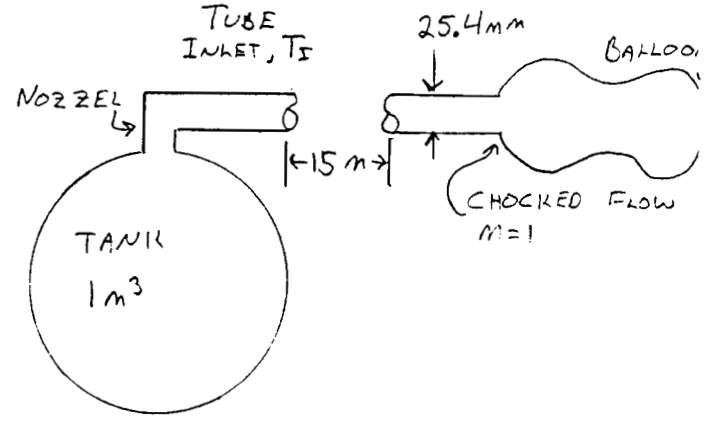

INITIAL CONDITIONS

25 KG H_2

220°K

28.23 MPA

ff = .02

P_{BAL} = CONSTANT

$C_P/C_V = 1.4$

BALLOON REQUIRMENT 22 KG

FIGURE 3 MASS FLOW MODEL

FLOW WILL REMAIN CHOCKED UNTIL

$$P_{TANK} = P_{BALLOON}\left(\frac{4.9554}{.9668}\right)$$

$\simeq 3$ KPA IF $P_{BALLOON}$ IS EQUAL TO ATMOSPHERIC PRESSURE.

SINCE FLOW IS CHOKED, WE HAVE FANNO LINE FLOW. NOW WE ASSUME ISENTROPIC FLOW THROUGH THE TANK NOZZEL INTO THE TUBE INLET, AND THE TEMPATURE IN THE TANK CAN BE FOUND BY:

$$T_2 = T_1\left(\frac{P_2}{P_1}\right)^{\frac{K-1}{K}} \qquad \text{EQ 2}$$

THE TEMPATURE AT THE TUBE INLET IS,

$$T_I = T_T (.9904)$$ Eq 3

THE PRESSURE AT THE TUBE INLET IS,

$$P_I = P_T (.9668)$$ Eq 4

THE VELOCITY AT THE TUBE INLET IS,

$$V = M_I \sqrt{KRT}, \quad M_I = .22$$ Eq 5

THE MASS FLOW RATE AT THE TUBE INLET IS,

$$\dot{m} = \rho_I A V$$ Eq 6

WHERE ρ_I IS FOUND AT P_I AND T_I BY THE REDLICH-KWONG EQUATION.

AT $t = 0^+$

$M_{TANK} = 25$ KG
$P_T = 28.23$ MPA
$T_T = 220°K$

$P_{INLET} = 27.29$ MPA Eq 4
$T_I = 217.89°K$ Eq 3
$\rho_I = 24.55$ KG/M³ (REDLICH-KWONG)
$V_I = 246.8$ M/S Eq 5
$\dot{m}_I = 3.07$ KG/S Eq 6

AT $P_T = 23$ MPA
$T_T = 209.5°K$ Eq 2
$M_T = 22.13$ KG R-K

$P_I = 22.24$ MPA Eq 4
$T_I = 207.5°K$ Eq 3
$\rho_I = 21.71$ KG/M³ R-K
$V_I = 240.8$ M/S Eq 5
$\dot{m}_I = 2.4$ KG/S Eq 6

$$\dot{m}_{AVE,\ 0^+ \to 23} = 2.86 \text{ KG/S}, \quad \Delta t = \frac{25 - 22.13}{2.86} = 1.004 \text{ S}$$

ONTINUING UNTIL THE REQUIRED 22 KG HAVE BEEN EXHAUSTED YEILDS:

$\Delta t = 22.6$ SEC
$T_{T,FINAL} = 87.85°K$
$T_{I,FINAL} = 87.004°K$
$P_{T,FINAL} = 1.1$ MPA

INE CONCERN IS THAT THE FINAL EXIT TEMPATURES ARE GETTING RATHER W. REMBER THAT T_I IS AT THE TUBE INLET, AND THAT $T/T^* = 1.1885$. A NAL AVERAGE TEMPATURE OF THE GAS IN THE BALLOON MAY BE FOUND BY LASSICAL THERMODYNAMICS. HOWEVER, ACCURATE DATA AT SUCH HIGH PRESSURES

HAD BY :

$$T_{AVE,FINAL} = 1.1885\left(\frac{217.89 + 87.004}{2}\right) = 181.2°K$$

BY PRESENTING THESE FIGURES IT SHOULD NOT BE CONSTRUED THAT WE ARE RECOMENDING SUCH A HIGH MASS FLOW RATE. RATHER THAT SUCH IS POSSIBLE, SINCE IT IS TO YOUR ADVANTANGE TO FILL THE BALLOON AS RAPIDLY AS POSSIBLE.

CONCERNING WHY 3KG OF HYDROGEN IS LEFT IN TANK. SINCE THE TEMPATURE IN THE TANK IS :

$$T_2 = T_1\left(P_2/P_1\right)^{\frac{K-1}{K}}$$

WHEN P_2/P_1 GETS TO BE A SMALL NUMBER, T_2 BEGINS TO DROP OFF MORE AND MORE QUICKLY. THEREFORE TO KEEP THE FINAL TEMPATURE UP AS MUCH AS POSSIBLE, WE NEED TO KEEP THE PRESSURE DROP AS LOW AS POSSIBLE. ONE WAY TO DO THIS IS TO KEEP SOME MASS IN THE TANK. ANOTHER WAY COULD BE A VARIBLE VOLUME TANK THAT KEPT THE GAS COMPRESSED. THIS WAS NOT CONSIDERED AS IT WOULD ADD MASS TO A ALREADY MASSIVE TANK

IN CONCLUSION, WE WOULD LIKE TO STATE THAT THE LIMITING FACTOR IN THE MASS FLOW IS THE BALLOON. FURTHER STUDY IS NEEDED TO DETERMINE HOW RAPIDLY THE BALLOON CAN BE FILLED WITHOUT DAMAGE TO THE BALLOON FABRIC.

Appendix 4.9

H_2 Storage for the Balloon Rover

H_2 STORAGE FOR BALLOON ROVER

Mass of H_2: 22 Kg

Method of Storage: conventional high pressure

volume: 1 m^3

Temperature range: 200K - 300K

COMPUTATIONS:

since the volume constraint, mass of H_2, and the temp. range force the storage pressure well above the critical pressure of 1.3 MPa, the reidlich-kwong equation of state is used:

$$P = \frac{\bar{R}T}{\bar{v}-b} - \frac{a}{\bar{v}(\bar{v}+b)T^{\frac{1}{2}}} \qquad [1]$$

where P is the storage pressure (Pa)

using this and the afforementioned parameters yeilds a storage p=28 MPa

now consider the vessel itself, a spherical thin wall pressure vessel:

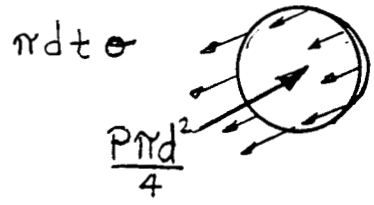

now equating stress with the resultant pressure force:

$$\sigma = \frac{P\,d}{4\,t}$$

d= diameter of vessel
t= thickness of the wall

the use of conventional metals in the vessel construction results in high mass figures (225 Kg for Titanium) for the vessel. Thus, other conventional materials was sought, in this case carbon fiber reinforced laminates. From a computer program developed by Professor Steve Folkman at Utah State University for composites, the following specifications were developed:

Laminate type: 4 ply quasi isotropic
Fiber type: carbon
Matrix: grey epoxy
Failure at specified stress: 1 ply matrix seperation
Stress at failure: 910 MPa
Approximate density: 1378 Kg/m^3

Using these figures for the vessel design yeilds the following:

size: 1.241 m inside diameter
10 mm wall thickness

mass: 68.75 Kg (less H_2 contents)

Laminate configuration:

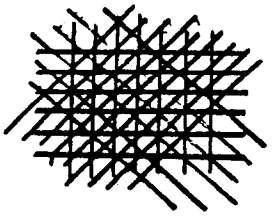

0° - -45° - 45° - -90°

REFERENCES:

[1] Black, W. and Hartley, J. , Thermodynamics, Harper and Row, 1985.

```
ccccccccccccccccccccccccccccccccccccccccccccccccccccccccccccccccccccccc
c                                                                       c
c  PROGRAM WRITTEN BY JAMES CANTRELL FOR UTAH STATE UNIVERSITY          c
c  ADVANCED SPACE DESIGN PROGRAM. THIS COMPUTES THE SIZE AND MASS       c
c  OF A COMPOSITE HYDROGEN VESSEL FOR THE STORAGE OF 22 Kg.  ALL        c
c  FIGURES AND ASSUMPTIONS ARE COVERED IN THE SPRING QUARTER TEXT       c
c                                                                       c
ccccccccccccccccccccccccccccccccccccccccccccccccccccccccccccccccccccccc

c       declare variables

        real press, t, rho, r, z, rconst, Temp, mass,masst,pi,sigma

        open(unit=10,file='comp.out',status='new')
        open(unit=11, file='comp2.out',status='new')

c       define operational parameters

        Temp=250.0
        Rconst=4124.0
        mass=19.0
c       compressibility factor z
c       based on the reidlich-kwong equation of state
        z=1.3
c       composite density (Kg/m^3)
        rho=1503.0
        sigma=870000000.0
        pi=3.1415

c      vary radius and compute volume and mass of the tank

        do 20 r=.3,.62,.0005

                volume=4.0/3.0*pi*(r**3)
                press=z*mass*rconst*temp/volume
                t=(press*r)/(2.0*sigma)
                masst=rho*1.33*pi*((r+t)**3-(r**3))
c               write to output files
                write(10,15) r,volume
                write(11,15) r,masst
15              format(1x,f10.3,1x,f10.3)

20      continue



        end
```

Appendix 4.10

Payload Structural Analysis (Preliminary)

PAYLOAD STRUCTURE ANALYSIS (PRELIMINARY):

Consider the general payload structure shown below:

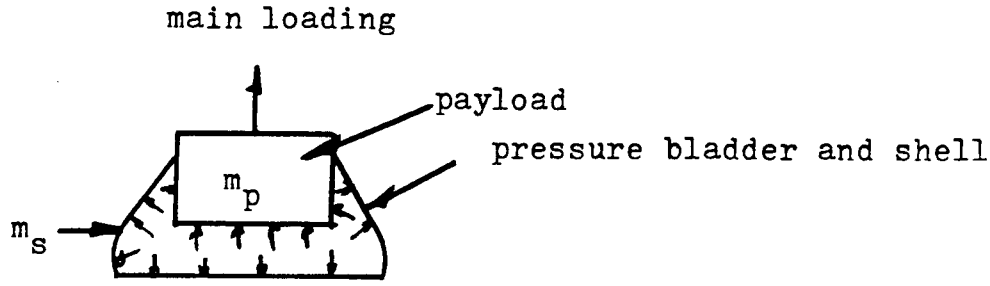

Two distinctly different regimes of loading occur on the shell, the impact loading on the bottom and the lander bladder pressure on the sides of the shell. The payload similarly experiences similar loadings but the main source of stress is due to the tether on the top ofthe payload and the dynamic loading on the bottom due to the payload mass. The following is a simplified analysis of the overall structure performed in order to obtain a rough estimate of the mass required.

LANDER SHELL:

consider the descent of the lander as it is approaching the surface. Speeds of up to 15 m/s have been predicted [1] . based on this, the loading on the shell was based on the peak bladder pressures [1] , and the dynamic loading of the shell itself. The dynamic loading on the shell is computed as follows:

assume: shell is dynamically isolated from the payload by virtue of the pressure bladder

system:

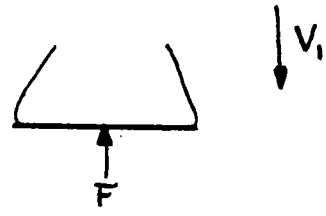

momentum exchange:

$$m_1 v_1 + \int_0^{\tau} F\,dt = m_2 v_2$$

$$m_1 = m_2 = m_s \quad : \quad \tau = 0.1 \quad [2] \quad : \quad v_2 = 0$$

solving: $F = m_s v/\tau$

PAYLOAD STRUCTURE ANALYSIS CON'T :

for the purposes of iteration and the general factor of safety:

assume m_s = 20 Kg and this yeilds: F=3000 N

now we assume the circular flat plate analysis developed in [3], where the general formula for the stresses in the plate are:

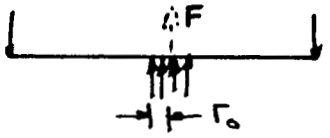

simply supported plate (end rotation) with a distributed center load for max. stress (ie landing on a rock)

$$M_{max} = \frac{w}{4\pi}\left[(1+\nu)\ln a/r_o + 1\right]$$ (maximum moment on plate)

$$\sigma_{max} = \frac{M_{max} c}{I}$$ (maximum stress in the plate)

ν = poisson's ratio = 0.385

$w = F/(\pi r_o^2)$ (distributed loading)

$I = t^3 d/12$ (moment of inertia @ max. stress moment ie @ center)

solving for t yeilds: t= 12mm and a mass of 13.06 Kg (composite construction)

PRESSURE BLADDER LOADING ON THE SIDES OF THE SHELL:

From [1] , the peak bladder pressure is 17.85 KPa based on Pi=2100 Pa Vi=0.079 cubic meters and V=0.066 cubic meters. Solving for the max. normal stress in the shell walls at the top of the shell:

t= 2mm (greatly oversized S.F. = 5)

mass = 6.5 Kg

PAYLOAD TOPPLATE LOADING:

system:

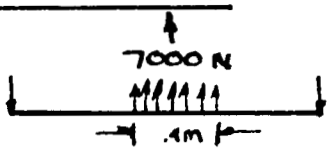

where the loading is based on 2 g's maximum dynamic loading [1], and using the above mentioned flat plate analysis yeilds:

t = 13 mm : mass= 8 Kg (TOP PLATE)

STRUCTURAL ANALYSIS CON'T:

since the dynamic loading is due to the deceleration of the balloon during flight and the loading on the bottom peaks during the landing, a different analysis was performed with the load nuiformily distributed on the bottom of the payload cannister. Here 30 g's was used as the max. loading. Note also that the loading on the top plate of the payload cannister is not affected upon landing as the balloon is no longer attached at this point. Using the flat plate analysis for the bottom plate yeilds:

t= 12 mm : mass = 7.5 Kg (composite construction)

Additionally, the cannister walls are loaded dy the balloon in flight and the stresses here are analyzed as follows:

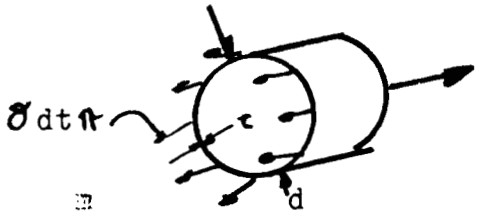

F= 7000 N (2g's loading by balloon)

solving for the stress yeilds: t= 1mm (greatly oversized)
mass = 1.95 Kg

In final view the overall mass of the payload structure is 30 Kg.

REFERENCES:

[1] Mars Lander/Rover Vehicle Development, Utah State University winter quarter report, 1987.

[2] computer program developed by Steve Folkman, Utah State University

[3] Roark, R. J., and Young, W. C., Formulas For Stress and Strain, McGraw Hill, Fifth edition.

Appendix 6

Payload Power Systems

SOLAR CELLS

STRUCTURE

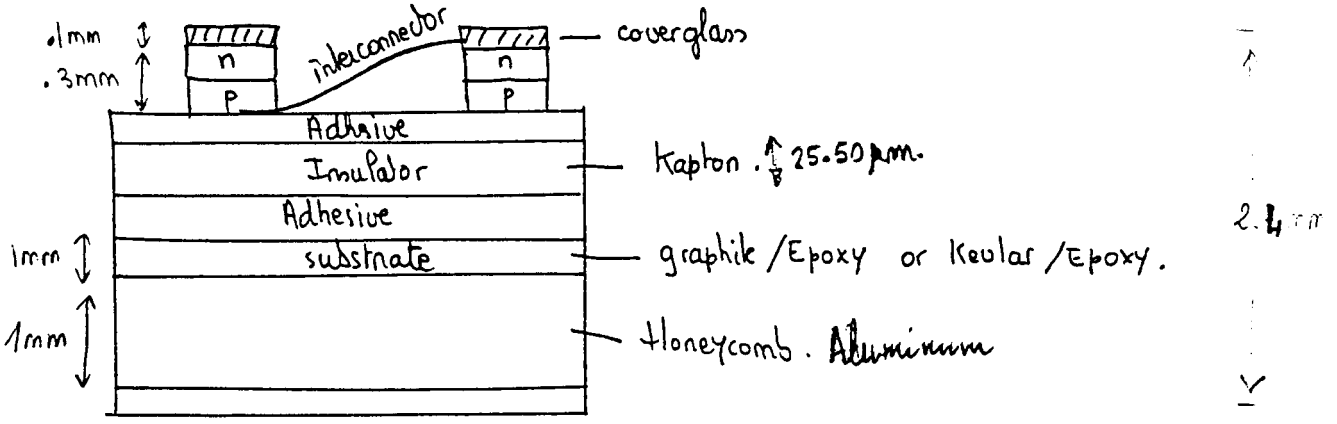

Solar Array Structure.

Total Solar Array Mass (less support structure) : 9.889 kg/m²

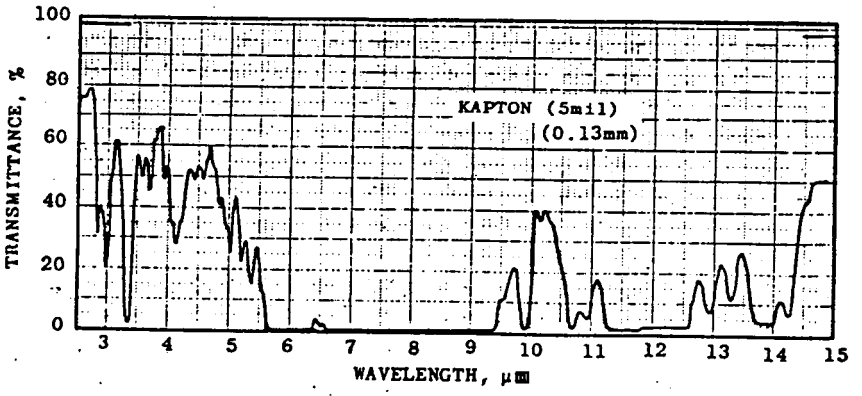

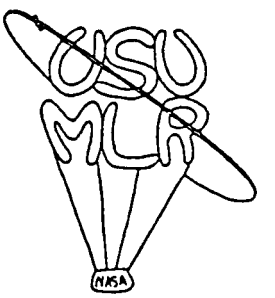

CHOICE OF SOLAR CELLS

EFFICIENCY :	SILICON	VIOLET CELLS	BLACK CELLS	GaAs
	10%	14%	15.5%	21%

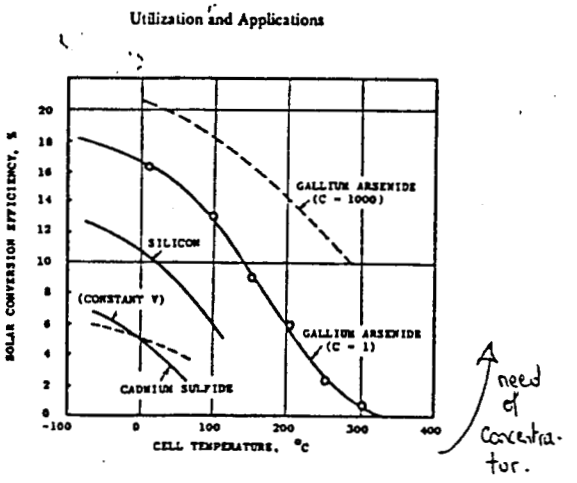

Variation of efficiency with cell temperature for the major types of solar cells.

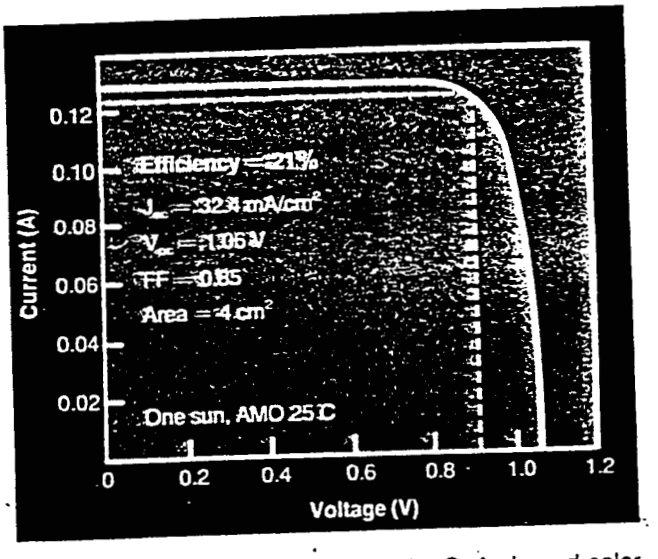

MOCVD RESEARCH has produced a GaAs-based solar cell that has a 21% conversion efficiency. Graph shows the current-voltage characteristics of the cell design.

SOLAR ARRAY TEMPERATURE

Effective solar absorptance : $\alpha se = \alpha s - Fp * \eta$

s: average solar cell array absorptance

Fp: Total active area / Total area = 0.9 (10% margin)

η : efficiency = 21%

-> $\alpha s = .8$ -> $\alpha se = .611$

Steady state operating temperature of the solar array :

$$Top = \left| \frac{\alpha se * Af * S * \cos\alpha}{(\varepsilon f * Af + \varepsilon b * Ab)\,\sigma} \right|^{1/4}$$

Af : array front side area

Ab : array back side area

f : emittance of the array front side

b : emittance of the array back side

S : solar constant = 540 W/m2

σ : Stefan Bolzmann cste = 5.67 10E-8

α : angle of incidence of sunlight

Af = Ab = .786 m2 $\alpha s = .8$ $\varepsilon f = .8$ $\varepsilon b = .7$

Angle	0	10	20	30	50	70	80
temperature (K)	249.5					190.85	161.1

Mars : 151 K -> 242 K

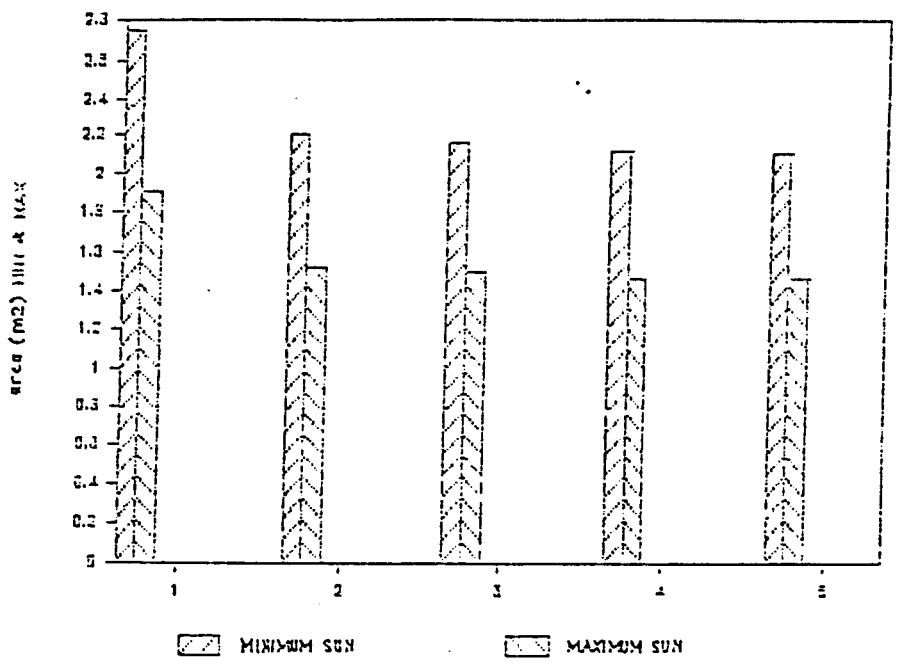

MIN : .79 M2 10.65 KG

MAX : 2.92 M2 39.53 KG

FOR 85W

wire length depending on sun declination

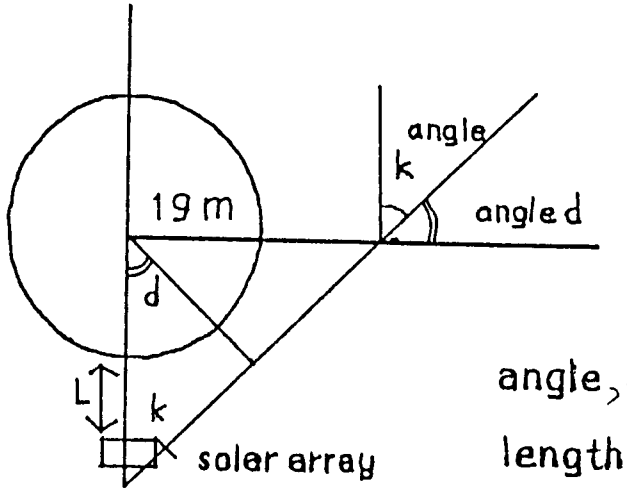

angle, d	40	60	80
length	6.6	19.6	90

Appendix 7.1

Payload Mass and Power Sizing

CANDIDATE BALLOON ROVER SUBSYSTEMS

# OF CODE (mass power volume)	Kg	W	M3
1 Aerial photography (9kg)			
a In flight (3kg)			
Cameras (2)	3.0	4.0	.006
w/ stereoscopic camera enclosure			
b Ground (6kg)			
Cameras (2)	3.0	4.0	.006
w/ stereoscopic camera enclosure			
camera boom w/ actuators	3.0	8.0	-
2 Metereology Transducers (3.7kg)			
Irradiance			
wind speed			
wind direction			
humidity	2.5	1.0	-
temperature			
pressure	1.2	-	-
3 Composition (9.8kg)			
atm. mass spectrometer	6.8	14.0	.02
neutron backscatter	2.0	1.0	.006
volatile detector	1.0	5.0	.003
4 Computers/Communications (12kg)			
large memory dataloggers	2.0	15.0	-
vision	3.0	25.0	-
communication telemetry, data transfer	5.0	30.0	-
sequencing/crunching (programmable)	2.0	10.0	-
5 Balloon Position (7kg)			
altimeter radar	2.0		
internal ref. unit (FORS)	5.0	10.0	-
6 Seismommetry (7.5kg)			
seismometer	2.5	10	-
active seismic thumper	5.0	bat	-
7 Power (21.8kg)			
RTG (Viking type-8W/kg)	15.0	120 W	
RTG supports	0.8	-	
power distribution unit	5.0	4	
Radioisotope heating unit	1.0	-	-

BALLOON ROVER SUBSYSTEMS

SUBSYSTEM	MASS (kg)
1 Aerial photography	9.0
2 Meteorology Transducers	3.7
3 Composition	9.8
4 Computers/Communications	12.0
5 Balloon Position	7.0
6 Seismometry	7.5
7 Power	17.4 to 21.8

INSTRUMENT LIST

	MASS	POWER
SURFACE SCIENCE		
2 Facsimile Cameras	2.0	.2
1 Neutron Backscatter Dev.	2.0	1.0
1 Volatile Detector	1.0	5.0
1 Proximity Sensor	3.0	2.0
5 Sun Sensors	0.4	-
1 Gyrocompass	4.5	-
1 Inclinometer	0.8	-
1 Metereology Boom	5.5	10.0
1 Seismometer	2.5	10.0
1 Active Seismic Thumper	5.0	bat
COMPUTER/DATA STORAGE		
1 Vision	3.0	25.0
1 Sampling System	3.0	15.0
1 Science	3.0	15.0
1 Common Data Storage	10.0	8.0
1 Data Handling	27.0	12.0
2 Digital Tape Recorder	17.8	18.0
1 Sampling Processing Electronics	4.0	2.0
HARDWARE		
1 Camera Pointing Platform	4.0	2.0
1 Stereoscopic Camera Enclosure	3.0	-
1 Stereo Tilt/Pan Actrs.	4.0	8.0
1 Fiber Optics Rotation Sensor (FORS)	5.0	10.0
1 Pendulous Sensor	1.2	0.8
1 Radioisotope Heating Unit	2.0	-
1 Power Control Unit	5.0	4.0
1 Power Distribution Unit	5.0	4.0
1 Scan Platform/ Gimball	3.0	-
1 Camera Boom w/ Actuators	3.2	bat
1 RTG Radiator Plate	3.0	-

BALLOON ROVER MASS BUDGET

BALLOON FABRIC + HYDROGEN GAS	254 KG
SCIENTIFIC PAYLOAD	62 KG
TETHERING	23 KG
PAYLOAD CANNISTER	15 KG
LANDER SHELL + PRESSURE BLADDER	16 KG
TOTAL MASS	370 KG

Balloon PLYD CANNISTER (Shapes - Sizes)

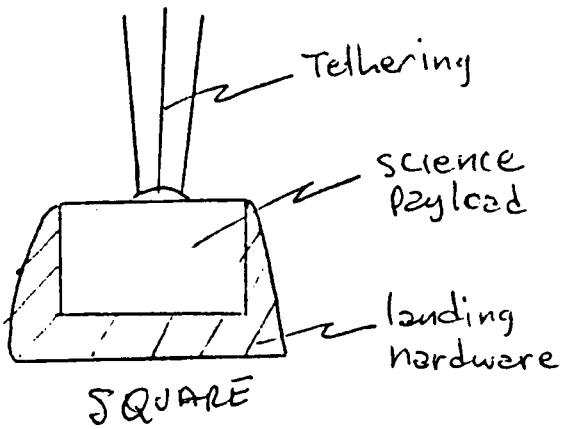

SQUARE

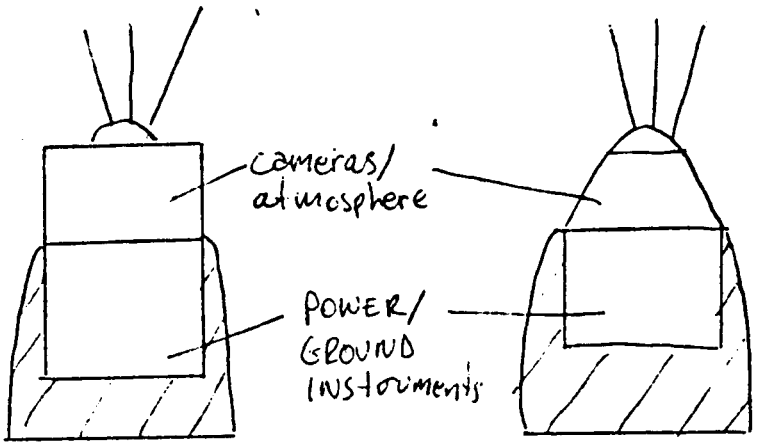

cylinder

Cylinder + cone

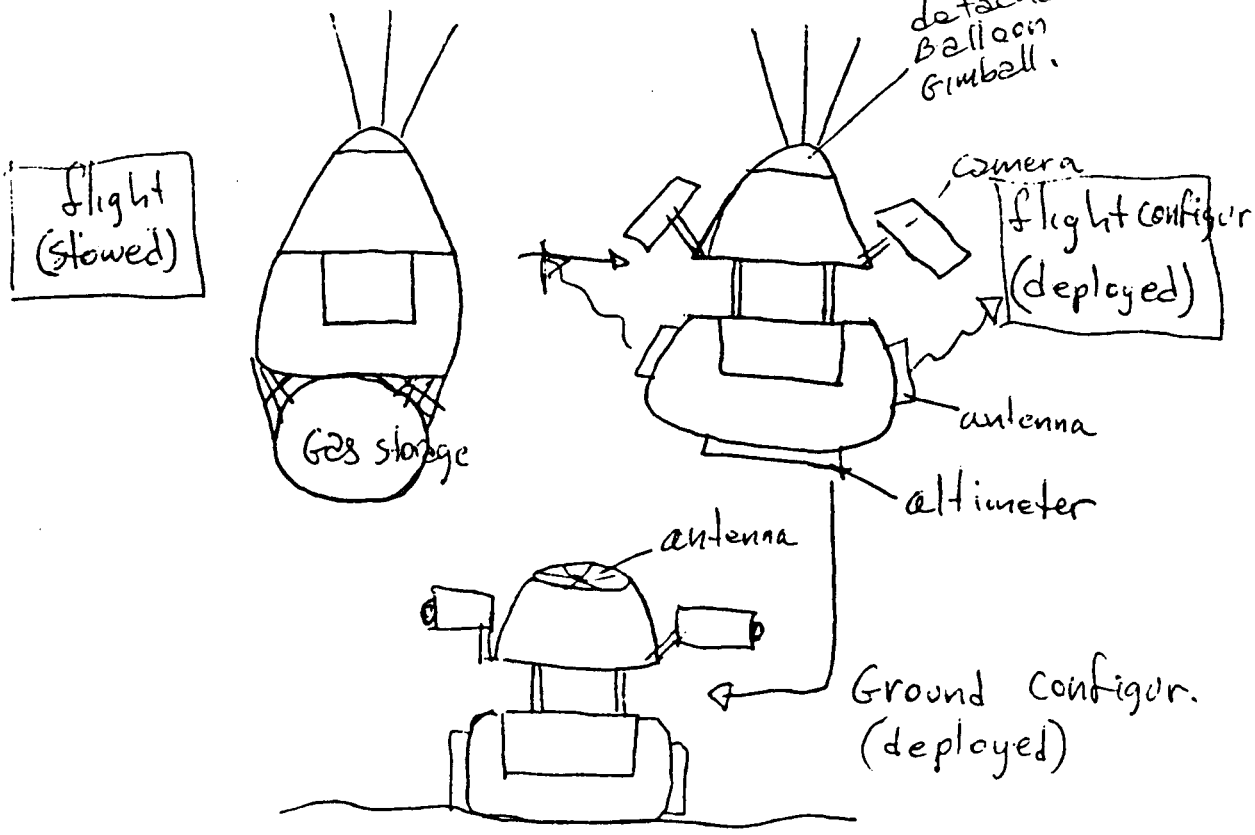

Camera Arrangements

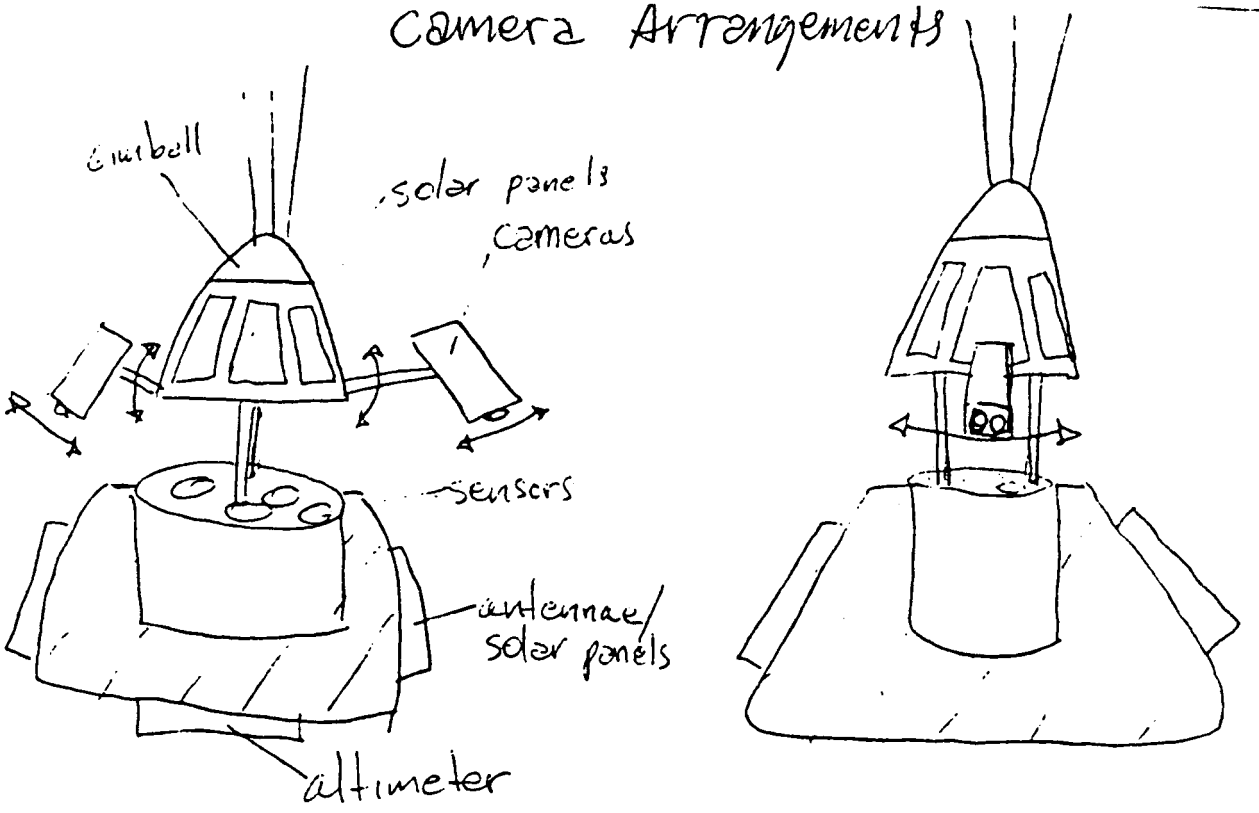

Type 1

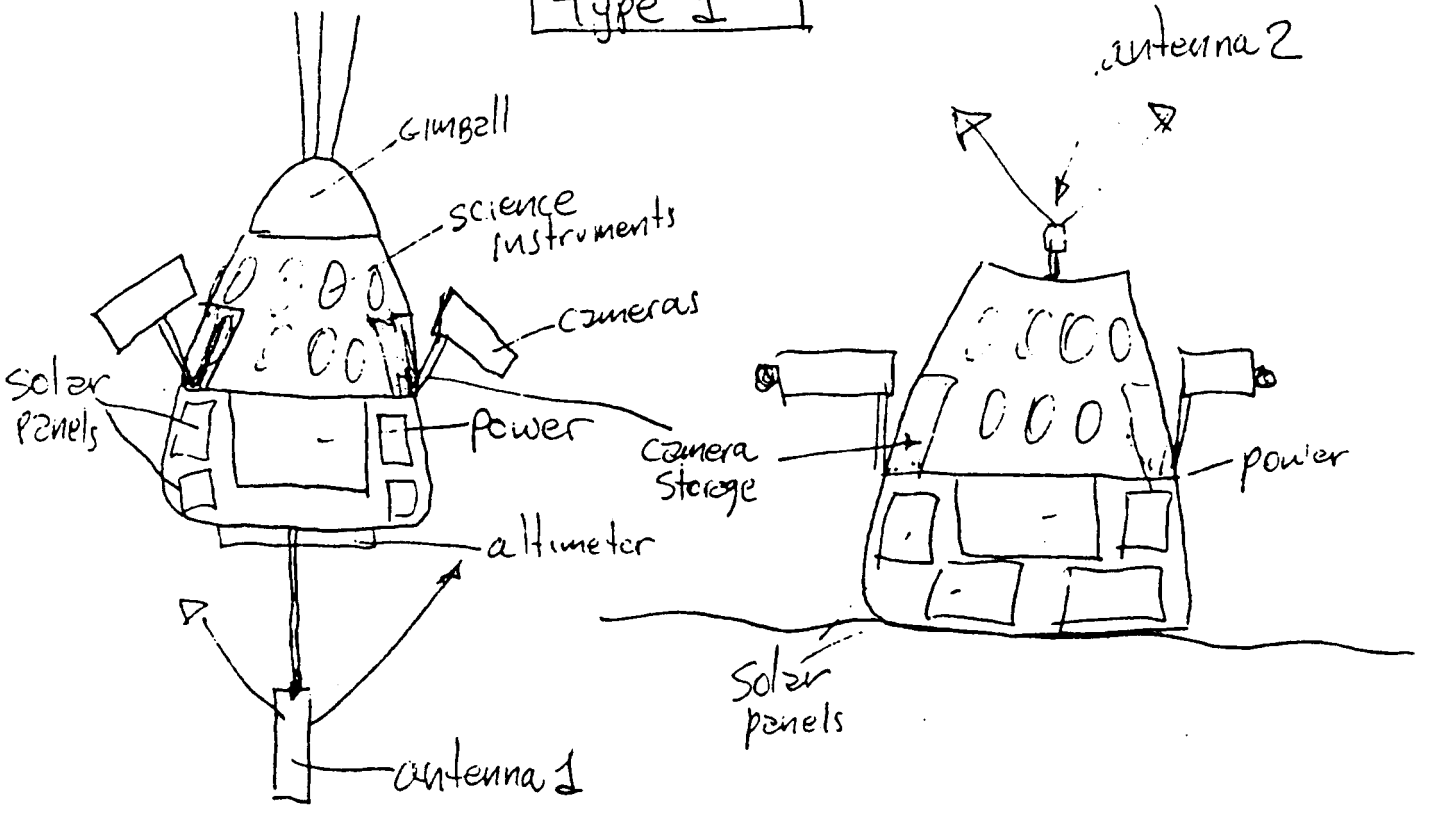

in flight

Type 2

Appendix 7.2

Payload Oscillations (Tethering)

The payload tethering oscillations equations were derived from mechanical vibrations. They are as follows:

For pendulum oscillations:

Sum of Moments about Center of Mass=I_{CM}Angular Acc.

$$F_D L_2 \cos(\text{theta}) - gL_{NET} L_2 \sin(\text{theta}) - M_1 g L_1 \sin(\text{theta}) = I_{CM}\text{Angular Ac}$$

which reduces to

$$W_N = \frac{\text{Sqrt}(gL_{NET}L_2 - TL_T \pm M_1 g L_1)}{\text{Sqrt}(I_{CM})}$$

For Torsional oscillations:

$$4T_Y D = I(\text{Angular Acceleration Beta})$$

which reduces to

$$W_N = \frac{\text{Sqrt}(4TD\cos(\text{theta}))}{\text{Sqrt}(I_{CM})}$$

where

I_{CM}=Moment of Inertia about the Center of Mass
W_N=Natural Angular Acceleration

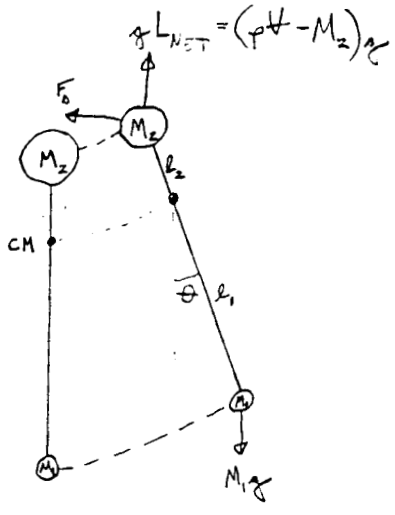

PENDULUM OSCILLATIONS

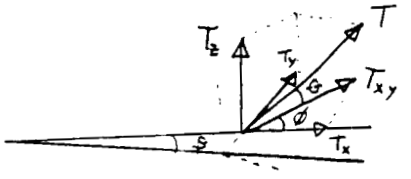

$$\beta = \sin^{-1}(\cot\phi)$$
$$T_y = T\cos\theta\sin\phi$$
$$\phi = \frac{\pi}{2} - \tan^{-1}\beta$$

TORSIONAL OSCILLATIONS

Appendix 8.1

Payload Thermal Control

Payload Heat Transfer

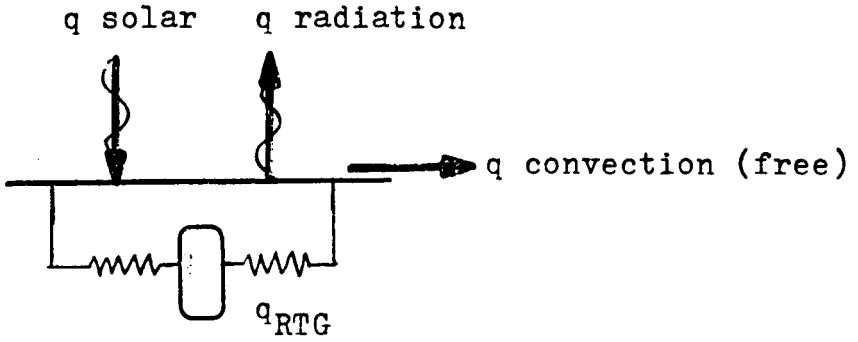

Figure 1. payload heat control

free convection environment:

from reference , the following equations were obtained:

$$Ra_x = Gr_x Pr = \frac{\rho_\infty^2 c_p g \beta (T_w - T_\infty) x^3}{ku}$$

$$\overline{Nu} \cong 0.54\ Ra^{\frac{1}{4}} = \bar{h}L/k$$

so the free convection coefficient $\bar{h}$ becomes:

$$\bar{h} = \frac{0.54\ Ra^{\frac{1}{4}} K}{L} = \frac{.252\ W}{m^2 K} \text{ for the martian atmosphere @ 220 K}$$

so from this, free convection on the plate was neglected in the analysis and radiation heat transport was the main form of heat transfer out of the RTG.

the total heat flux out of the RTG is approximately 1000 W for the 50 w power output, the base operating temperature is 170 C , and the solar flux on the martian surface is 400 W/m^2

ENERGY BALANCE :

$$\boxed{q_{out} = q_{in}}$$

σ = Stephan-Boltzmann constant
T_s = plate surface temp. (K)
T_a = atmosphere temperature (K)
A_s = plate surface area (m^2)

$$\sigma \epsilon_p T_s^4 A_s = 400\ (A_s) + 1000\ W + \sigma \epsilon_a T_a^4 A_s$$

here the emmisivity of the martian atmosphere is 0.02, and since the plate would thus be radiating into deep space for the most part, the view factor was assumed to be equal to 1, and the emmisivity of the plate = 0.8

Payload Heat con't.

solving for the surface temperature:

$$T_s = \left[\frac{1000 + 400(0.8)(0.944)}{5.67 \times 10^{-8}(0.8)(0.944)} \right]^{\frac{1}{4}} \qquad \boxed{= 417.6 \text{ K} = 144 \text{ C}}$$

and solving for the thermal resistance between the RTG and the fin using six thermal strips:

$$Q = dT/R_{th} = \frac{171-144}{R_{th}} = 1000 \qquad \boxed{R_{th} = 37.4 \text{ K/W}}$$

but using six thermal strips, the individual resistance R_i becomes:

$$\boxed{R_i = 6 * R_{th} = 244 \text{ K/W}}$$

and using aluminum, insulated for radiation on the boundries, we obtain the size and mass:

length each @ 37cm
diameter each @ 3mm
mass total @ 0.037 Kg

Appendix 8.2

Tethering Analysis

PAYLOAD TEHTHERING FORCE ANALYSIS

consider the balloon and tethering shown with a payload force loading as shown:

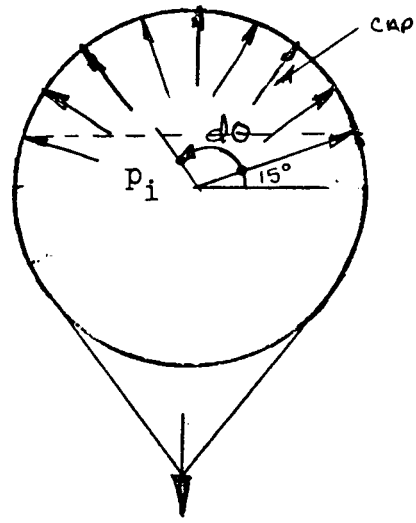

CONSIDER THE PRESSURE UNDER THE CAP:

$$F = m(g_m + 2(9.81)\,M/S^2)$$

equating $\sum F = ma$ we obtain:

$$m(g_m + 2(9.81)) = F = \int_{15^\circ}^{165^\circ} p_i \sin\theta \; A_x \, d\theta$$

since:

$$A_x = 2\pi(19)(19-R \qquad = 4.48$$

the integral becomes:

$$m(g_m + 2(9.81)) = 4.48 \int_{15^\circ}^{165^\circ} p_i \sin\theta \; d\theta$$

solving for p_i: the stress cube becomes

$dP - p_i = 91.19$ Mpa $- .27$ Mpa $= 90.92$ MPa